

**DATA-DRIVEN HEALTHCARE MANAGEMENT: AN ANALYTICS
APPROACH TO BLOOD PRESSURE CONTROL AND
CARDIOVASCULAR DISEASE PREVENTION**

A Dissertation
Presented to
The Academic Faculty

By

Anthony J. Bonifonte

In Partial Fulfillment
of the Requirements for the Degree
Doctor of Philosophy in the
H. Stewart Milton School of Industrial and Systems Engineering

Georgia Institute of Technology

May 2018

Copyright © Anthony J. Bonifonte 2018

**DATA-DRIVEN HEALTHCARE MANAGEMENT: AN ANALYTICS
APPROACH TO BLOOD PRESSURE CONTROL AND
CARDIOVASCULAR DISEASE PREVENTION**

Approved by:

Dr. Turgay Ayer, Advisor
H. Stewart Milton School of Industrial and Systems Engineering
Georgia Institute of Technology

Dr. Benjamin Haaland
H. Stewart Milton School of Industrial and Systems Engineering
Georgia Institute of Technology

Dr. Kamran Paynabar
H. Stewart Milton School of Industrial and Systems Engineering
Georgia Institute of Technology

Dr. Julie Swann
H. Stewart Milton School of Industrial and Systems Engineering
Georgia Institute of Technology

Dr. Emir Veledar
Division of Cardiology
Emory University School of Medicine

Dr. Yao Xie
H. Stewart Milton School of Industrial and Systems Engineering
Georgia Institute of Technology

Date Approved: March 12, 2018

It was 3% of extra order snatched out of the grasp of entropy.

Francis Spufford, Red Plenty

If you want to build a ship, don't drum up the men and women to gather wood,
divide the work, and give orders. Instead, teach them to yearn for the vast and
endless sea.

Antoine de Saint-Exupéry

To Ondrea - you are the Hobbes to my Calvin

ACKNOWLEDGEMENTS

This thesis would not have been possible without the support of a great many people. First, I would like to thank my advisor Turgay Ayer. From him I learned how to approach a problem from many angles, how to be critical of your work to improve it, and how to convince others of the value of your work. I would also like to thank my committee, Dr. Swann and Dr. Paynabar for their helpful feedback in shaping and improving the work, and especially Dr. Veledar, Dr. Haaland, and Dr. Xie, who helped guide development of chapters II, III, and IV, respectively.

I would like to thank other ISyE faculty who have helped my professional career. Dr. Chen Zhou offered me opportunities to teach courses in the department and was a wonderful resource. Dr. Ron Johnson was a fantastic teaching mentor and instilled in me the confidence to stay true to myself in the classroom and the courage to confront difficult situations. Dr. Dave Goldberg modeled how to teach difficult technical topics and taught me obviously (to use his word) you can be both an outstanding teacher and researcher at the same time. Dr. Peter Wilson at Emory University helped guide the clinical aspects of my research and was invaluable in teaching me to think from the user's perspective.

Other Georgia Tech professionals have also supported and guided me along my path. My mentor Dr. Tris Utschig in the Center for the Enhancement of Teaching and Learning showed me you can have a work/life balance and displayed a constant patience and compassion. Dr. Dia Sekayi, Dr. Carol Sullivan, and Dr. Kate Williams in the center taught me everything I know about teaching and provided wonderful opportunities to grow as a teacher. I would be remiss in not thanking Ms. Pam Morrison and Ms. Amanda Ford as graduate program managers for creating the administrative support all this work could be built on.

Our research group of Jan Valachy, Qiushi Chen, Can Zhang, Caglar Caglayan,

Jia Yan, and Zhaowei Shi were as great a coalition as could be wished for. Thank you for all the insightful research feedback, moral support, and camaraderie. Our dinners will be missed.

Many friends at Georgia Tech supported me along the way and deserve my gratitude. Erin Garcia shared my career dreams and always had wonderful teaching advice to offer. Carl Morris always had time to share and enlightening intellectual conversation to fill it. Greyson Daugherty is the most extraordinary person I have ever known, and kept me intellectually stimulated. Brian Kues, Jeff Pavelka, and Ben Johnson shared many great conversations and made my time in Atlanta enjoyable. Thank you all for the companionship.

Finally, I owe a debt of gratitude to my family. My mother pushed me from a young age, teaching me to never accept anything less than my best. The biggest thanks go to my wife Ondrea. Her love, sacrifice, suggestions, and support made this thesis possible. Thank you for believing in me even when I didn't believe in myself.

TABLE OF CONTENTS

Acknowledgments	v
List of Tables	xi
List of Figures	xiii
Chapter 1: Introduction and Background	1
1.1 Background	1
1.1.1 Cardiovascular Disease	1
1.1.2 Framingham Heart Study	2
1.1.3 J-Curve Effect	4
1.1.4 Antihypertensive treatment	6
1.1.5 Blood Pressure Monitoring	8
1.2 Chapter II: Antecedent Blood Pressure as Predictor of Cardiovascular Disease	9
1.2.1 Objectives	9
1.2.2 Methodology	9
1.2.3 Contribution	10
1.3 Chapter III: Analytics Approach to Blood Pressure Control	10
1.3.1 Objectives	10

1.3.2	Methodology	11
1.3.3	Contribution	11
1.4	Chapter IV: Personalized Blood Pressure Management	12
1.4.1	Objectives	13
1.4.2	Methodology	13
1.4.3	Contribution	13
Chapter 2: Antecedent Blood Pressure as Predictor of Cardiovascular Disease		15
2.1	Introduction	15
2.2	Methods	16
2.2.1	Population Sample	16
2.2.2	Study Inclusion	16
2.2.3	Clinical Measurements	17
2.2.4	Follow Up for Cardiovascular Disease Outcomes	18
2.2.5	Statistical Methods	18
2.2.6	Secondary Analyses	19
2.3	Results	20
2.3.1	Study Sample Characteristics	20
2.3.2	Age and Sex Adjusted Simple Cox Models	21
2.3.3	Multivariate Models	22
2.3.4	Hypertensive History	24
2.3.5	Secondary Analyses	24
2.4	Discussion	26

Chapter 3: Analytics approach to Blood Pressure Control	29
3.1 Introduction	29
3.2 Literature Review	32
3.3 Model and Analysis	37
3.3.1 A Model for Blood Pressure Progression	39
3.3.2 Anti-hypertensive Treatment	43
3.3.3 Characterization of the Hazard Ratios	43
3.3.4 Minimum Risk-Adjusted Hazard Ratio	44
3.3.5 Approximate Confidence Intervals for Hazard Ratio	55
3.4 Data and Parameter Estimations	57
3.4.1 Blood Pressure Change: Gaussian Mixture Models	57
3.4.2 Antihypertensive Treatment	58
3.4.3 Hazard Ratio	62
3.4.4 External Validation	63
3.5 Numerical Results	65
3.5.1 Treatment Initiation Thresholds	66
3.5.2 Treatment Intensification Thresholds	68
3.5.3 Results for Patients Currently on Treatment	69
3.5.4 Simulation Model	70
3.5.5 Approximate Confidence Intervals for Hazard Ratio	72
3.6 Sensitivity Analysis	73
3.6.1 Sensitivity to Hazard Ratio	74
3.6.2 Sensitivity to BP Progression	76

3.6.3	Sensitivity to the Risk Behavior	79
3.6.4	Sensitivity to Blood Pressure Measurements	80
3.6.5	Sensitivity to Treatment Effect	81
3.6.6	Sensitivity to Length of Time to Achieve Treatment Benefit	81
3.6.7	Sensitivity to Planning Horizon T	83
3.7	Discussion and Conclusion	84
3.7.1	Limitations	85
3.7.2	Future Work and Conclusion	87
Chapter 4: Personalized Blood Pressure Management		89
4.1	Introduction	89
4.2	Literature Review	91
4.3	Method	93
4.3.1	Bayesian Belief Changepoint Detection	95
4.3.2	Naive CUSUM Changepoint	100
4.3.3	Performance Evaluation	106
4.4	Numerical Results	107
4.5	Discussion and Conclusion	113
Chapter 5: Conclusion		117
5.1	Summary	117
References		137
Vita		138

LIST OF TABLES

1.1	Comparison of Framingham Heart Study and Offspring Study	5
2.1	Summary Statistics, Framingham Offspring Exam 3	20
2.2	Age and Sex Adjusted Cox Models	21
2.3	Multivariate Cox Models	22
2.4	Antecedent Hypertension Models	23
2.5	Antecedent Diastolic Pressure Models	25
2.6	Mean Arterial Pulse Models	25
3.1	Gaussian Mixture Model for Systolic and Diastolic BP	58
3.2	Fitted BP Gaussian 4-mixture model	58
3.3	Expected BP reductions for initiating treatment	60
3.4	Expected BP gain for removing all treatment	61
3.5	Expected systolic BP reduction from antihypertensive treatment	62
3.6	Expected diastolic BP reduction from antihypertensive treatment	62
3.7	CVD Risk Hazard Ratio	63
3.8	BP progression model validation	67
3.9	Confidence interval relative error	73
3.10	CKD patient hazard ratio	76

4.1	Chapter 4 Notation	94
4.2	BP Changepoint Detection Performance Statistics	113

LIST OF FIGURES

1.1	J-curve effect	6
3.1	Fitted Hazard Ratio Surface	64
3.2	BP progression model validation	65
3.3	BP progression model validation	66
3.4	Optimal thresholds for initiation of treatment	68
3.5	Optimal dosage intensification thresholds	69
3.6	Dosage intensification for 1 drug standard dose	70
3.7	Histogram of simulated hazard ratios, initial BP 150/100	73
3.8	QQ plot of simulated hazard ratios, initial BP 150/100	74
3.9	Simulated and exact confidence intervals	75
3.10	Fitted hazard ratio surface for Kovesdy study	77
3.11	Optimal treatment decisions for Kovesdy study	78
3.12	Optimal intensification with 25% misspecified BP progression	78
3.13	Optimal intensification thresholds with $\lambda = 1$	80
3.14	Optimal treatment decisions, treatment effect + 25%	81
3.15	Optimal treatment decisions, treatment effect - 25%	81
3.16	Optimal treatment decisions, treatment occurring in 3 months	82

3.17	Optimal treatment decisions, treatment occurring in 5 years	82
3.18	Optimal treatment decisions, $T=1$	83
3.19	Optimal treatment decisions. $T=5$	83
4.1	Bayesian filtering	98
4.2	Bayesian Changepoint Detection Procedure	100
4.3	Naive test statistic example sample path	102
4.4	Naive Changepoint Procedure ARL	105
4.5	Naive Changepoint Procedure DD	106
4.6	Naive test statistic example on real pressure	107
4.7	ROC Changepoint Detection Performance, $m = 90$	110
4.8	ROC Changepoint Detection Performance, $m = 182$	111
4.9	ROC Changepoint Detection Performance, $m = 365$	112

SUMMARY

This thesis develops analytics based tools using operations research and statistical methodologies to address problems in the domain of cardiovascular disease and blood pressure management. Cardiovascular disease is the leading cause of death in the United States and worldwide, and a major component of healthcare costs. Elevated blood pressure (hypertension) has been shown as a significant risk factor for cardiovascular disease. Antihypertensive treatment can effectively lower cardiovascular disease risk by reducing elevated pressure, but over-aggressive treatment can increase risk. Current guidelines for administering antihypertensive treatment are based on randomized control trials which are limited by resource constraints in what they can examine. We develop data-driven mathematical models to optimize treatment decisions, monitor blood pressure from mobile health technologies, and maximize population health.

In chapter I, we introduce background knowledge on the clinical characteristics of cardiovascular disease and blood pressure. This introduction frames the context of the thesis and justifies assumptions we make about the disease progression and treatment. We proceed to offer a summary of the remaining chapters, detailing the objectives, methodologies, and contributions of each chapter.

In chapter II, we show that history of a patient's blood pressure is an important predictor of future cardiovascular risk. Standard risk prediction models consider only a patient's current blood pressure and ignore history. Using Cox model survival analysis and the Framingham Heart Study data set, we demonstrate antecedent blood pressure is a more significant predictor of cardiovascular disease than current pressure. The model's predictive ability is significantly improved by the addition of antecedent pressure, demonstrating the predictive value of historical measurements. We confirm these findings in other data sets and with different baselines, lengths of history, and

follow-up intervals. The results of this chapter motivate the following chapters by emphasizing the importance of a time integrated measure of blood pressure as a risk for cardiovascular disease.

In chapter III, we develop a population level optimal antihypertensive treatment policy. We model blood pressure as a continuous time, continuous state stochastic process, specifically a geometric Brownian motion mixture model, which we demonstrate is a good statistical fit. Using published parameters of cardiovascular disease risk as a function of blood pressure, we create a closed form analytical expression for the expectation and variance of hazard a patient experiences over the following T years as a function of their current blood pressure and drift and covariance of change over time. Using meta-analyses of randomized control trials, we estimate the effects of different dosages of antihypertensive treatment and optimize over treatment decisions. We create a threshold based population level optimal treatment policy for initiation and intensification of antihypertensive treatment, and show significant improvement over current guidelines in a large scale simulation model.

In chapter IV, we develop two changepoint detection-based algorithms for screening blood pressure from wearables and other mobile health technologies. Such devices are becoming more ubiquitous and can gather many more measurements than traditional clinical measurements. The first algorithm uses knowledge of the disease progression to maintain a Bayesian belief of the true state. This method is highly accurate, but may be difficult to implement in practice due to the parameter estimation and necessity of simulation to calibrate the algorithm. We subsequently develop a Naive changepoint detection algorithm that is simple and generalizable to other continuous health characteristics such as cholesterol, glucose level, and pulse.

CHAPTER 1

INTRODUCTION AND BACKGROUND

1.1 Background

1.1.1 Cardiovascular Disease

Cardiovascular disease (CVD) is the leading cause of death worldwide and within the United States [1, 2]. The American Heart Association reports that approximately 800,000 deaths in the United States are attributable to CVD every year and financial burden exceeds 300 billion dollars in healthcare and lost productivity [3]. Many of the causes of CVD are controllable through medication or lifestyle change, so improving our knowledge of risk factors over time and how they may affect CVD risk is worthy of investigation.

CVD is a group of disorders of the heart and blood vessels including coronary heart disease, cerebrovascular disease, peripheral arterial disease, and others [4]. The acute events most associated with CVD are heart attack, which occurs when the blood flow to the heart is blocked by a blood clot, and ischemic stroke, which is when a blood vessel to the brain is blocked [5]. Other associated events are heart failure, which is when the heart isn't pumping blood as strong as it should, and arrhythmia, abnormal rhythms of the heart [5].

There are many known risk factors for CVD. Age, sex, diabetes, and certain genetic markers are uncontrollable risk factors. Controllable factors include cholesterol, smoking, body mass index, and elevated blood pressure (BP). Of particular interest, and the central focus of this thesis, is blood pressure. Blood pressure comprises two measurements, systolic (SBP) and diastolic (DBP), both measured in millimeters of mercury (mm Hg); elevated BP is referred to as hypertension. BP is typically reported

as systolic and diastolic with a ‘/’ character between, and for example BP 120/80 is pronounced ‘120 over 80’. BP is a ubiquitous measure, and is taken virtually anytime meeting a physician [6, 7]. Typically it is recorded with a mercury sphygmometer by a trained health professional, but automatic measurement is an option that reduces human effort but is less accurate [8, 9, 10].

Behavior interventions such as healthier diet, salt reduction, smoking cessation, and increased physical activity have been demonstrated as effective for reducing BP, improving health, and reducing the risk of CVD [11, 12]. Since these behavioral modifications promote overall health and are costless, they are universally recommended by physicians [13]. For patients whose BP remains elevated, they can begin an oral regimen of drugs designed to reduce BP, called antihypertensive drugs, detailed in § 1.1.4.

1.1.2 Framingham Heart Study

The Framingham Heart Study was the first study of its kind to investigate cardiovascular risk factors in a longitudinal cohort [14]. It was instrumental in establishing that blood pressure and other risk factors preceded the development of cardiovascular disease, and were not unavoidable side effects, as previously believed [15]. It was one of the key studies to identify the health risks of smoking [16]. To this day the Framingham Heart Study remains the largest, longest tracked longitudinal cohort for cardiovascular disease and has funding from the National Heart, Lung, and Blood Institute (NHLBI). The Framingham Risk Score which predicts the risk of cardiovascular disease is still used as the gold standard today [17, 18] and recommended by the NHLBI. [19].

The Framingham Heart Study contains two major sub-studies, the Original Cohort (FHS) and the Offspring Cohort (FOS). Both studies contain major advantages and disadvantages, which we detail presently. We will make extensive use of both studies

throughout this thesis. Both studies are still to this day tracking patients.

The Original Cohort consisted of 5,209 men and women who were free of CVD between the ages of 30 and 62 recruited beginning in 1948 in Framingham Massachusetts [20]. Beginning at their initial examination, patients attended a follow-up exam every 2 years. A variety of clinical and behavioral characteristics were recorded at each examination, including age, blood pressure, diabetes status, smoking status, and what medications each patient was taking. Exam 32 of the Original Cohort, the most recent as of this publication, concluded in April 2014.

The Offspring Cohort began in 1971 with 5,124 men and women, consisting of the offspring of the Original Cohort and their spouses [21]. Eight years passed between the first and second examination, and four years between every subsequent examination. Measurements at each exam were similar to those taken in the Original Cohort, with added information regarding genetic markers and the inclusion of cholesterol measurements. Exam 9 of the Offspring Cohort, the most recent as of this publication, concluded in April 2014.

From a modeling perspective, the advantages of the Original Cohort are more frequent observations, a longer history, and a very small percentage of patients taking antihypertensive medication. Antihypertensive medication was less widespread because they had not yet been demonstrated as effective in reducing risk of cardiovascular disease. Patients taking antihypertensive medication complicate modeling, since their pressures will be lowered to various extents depending on how long they have been taking the medications. The disadvantage of the Original Cohort is lack of cholesterol measurements. Cholesterol measurements are frequently not recorded at examinations, and when they are, low-density lipoproteins (LDL), or “bad cholesterol” is merged together with high-density lipoproteins (HDL), or “good cholesterol”. This blend of good and bad cholesterol makes any measurements useless in predictive ability. Another disadvantage is the demographics and behavioral characteristics are

not representative of today because of the age of the data. We will make use of the data from this study in chapters III and IV of the thesis for modeling change in blood pressure over time because of the more abundant measurements, less time between measurements, and lack of complications from antihypertensive medication. While the distribution of blood pressure values in the population may have changed in recent history, it is reasonable to believe that the physiology of blood pressure progression has not changed appreciably since these studies, so the older data is not problematic.

The advantages of the Offspring Cohort are more measurements per exam and a more modern data closer indicative of the demographics and behavioral characteristics of today. Scientific advances permit the collection of LDL and HDL cholesterol values separately at each exam, adding them as useful risk factors for prediction. The downsides are fewer examinations due to the more recent start date, less length of followup, and longer intervals between observations. We will make use of the data from this study in chapter II for developing risk prediction models of cardiovascular disease. All modern risk equations are built on the Offspring Cohort owing to a more modern data set with more predictor variables. The characteristics of each study and how we make use of them in this thesis are presented in table 1.1.

1.1.3 J-Curve Effect

In the 1960's, the first studies from the Framingham Heart Study identified elevated BP as a risk factor for cardiovascular disease and all-cause mortality [22]. In 1979, Stewart reported increased risk for patients with $SBP < 130$ or $DBP < 85 - 90$ [23]. This was referred to as the J-Curve effect, so named because risk is lowest at an intermediate pressure, with increasing risk on either side of optimal [24]. See Figure 1.1 for a visualization of this phenomenon. While a few earlier trials have found no support [25, 26], there exists strong evidence for the existence of this effect [27]. Several recent clinical trials have validated the J-Curve effect in the general population

Table 1.1: Comparison of Framingham Heart Study and Offspring Study

	Framingham Heart Study (FHS)	Framingham Offspring Study (FOS)
Year Began	1948	1971
Number of participants	5,209	5,124
Years between examinations	2	8 between first and second, 4 between subsequent
Number of examinations by 2016?	32	9
Dominant use of antihypertensives?	No	Yes
Cholesterol measurements?	No	Yes
Used in this thesis	Chapters III and IV - parametrizing BP progression model	Chapter II - risk prediction models

[28, 29] or in specific subpopulations [30, 31, 32]. Other studies have demonstrated no value in initiating antihypertensive treatment in patients with intermediate risk and moderate-low pressures [33], and an increase in cardiovascular risk in patients with low pressure placed on antihypertensive treatment [34].

The existence of the J-curve effect has important clinical implications, imposing fundamental tradeoffs in BP management. Aggressive treatment may lower BP below optimal, thereby increasing risk. The tradeoffs are further complicated when considering systolic and diastolic BP jointly. For example, consider a patient with high SBP and moderate-low DBP (referred to as isolated systolic hypertension). Placing this patient on treatment will lower their SBP and subsequently lower risk, but concurrently lower DBP and, due to the J-curve effect, increase risk. The decision of whether to initiate treatment must weigh the benefits of SBP reduction against the penalty of DBP reduction.

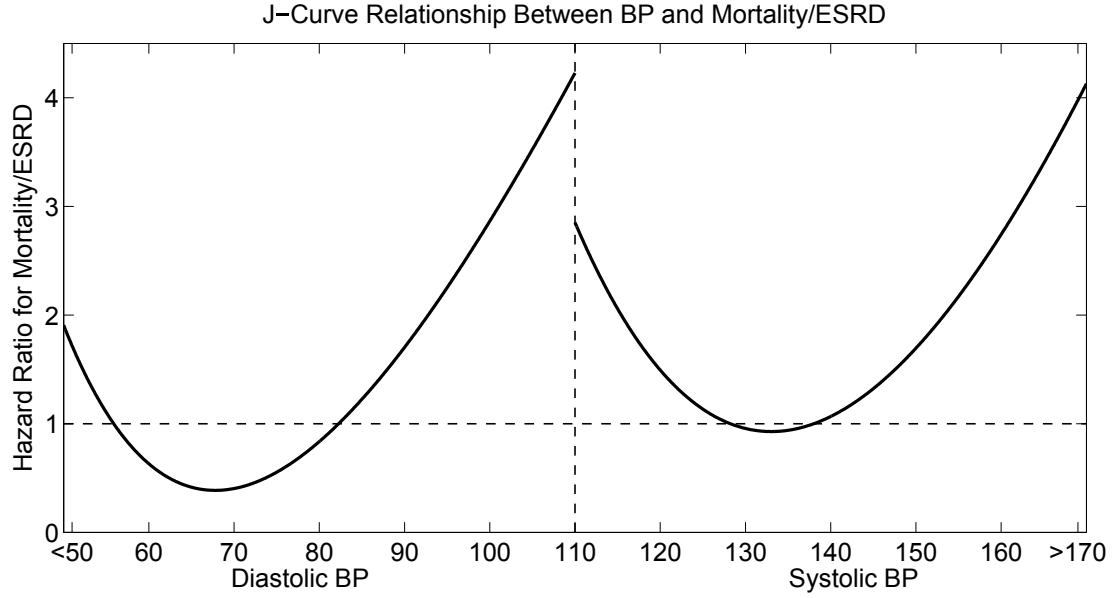


Figure 1.1: J-curve effect of diastolic and systolic blood pressure on mortality and end-stage liver disease. Figure adapted from [35].

1.1.4 Antihypertensive treatment

Antihypertensive drugs have been instrumental in improving public health [36, 37]. The drugs are widely effective, cheap, and with minimal side effects. [38] estimate that use of antihypertensives prevented 86,000 premature deaths from cardiovascular disease in 2001. They are extremely cheap, estimated at \$212 for one year of generic BP treatment [39, 40].

There are 5 primary classes of hypertension drugs: thiazides, β blockers, angiotensin converting enzymes (ACE) inhibitors, angiotensin II receptor antagonists, and calcium channel blockers [41]. In a review of 354 randomised trials, Law et. al. 2003 [42] found that all five categories of drug produced similar reductions in blood pressure. They found that within a given dose, few statistically significant differences existed, and no category of drug was overall more effective than another. We will therefore ignore categories of drugs, and consider only dosage and pre-treatment pressure.

In a meta-analysis of randomized control trials, Law et. al. [43] explored the

cause of CVD risk reduction from antihypertensive treatment. They report there was a 31.5% reduction in CVD events for a blood pressure reduction of 10 mm Hg systolic or 5 mm Hg diastolic, similar to the 30.5% expected reduction from the blood pressure reduction owing to antihypertensive treatment, indicating the benefit of antihypertensive treatment is explained by the blood pressure reduction itself. That is, the reduction in CVD from antihypertensive treatment is explained entirely by the blood pressure lowering, with no additional CVD reduction beyond that predicted by the blood pressure reduction. We are therefore justified in assuming all the value of antihypertensive treatment comes from the blood pressure reduction. They also find that the almost full potential effect of blood pressure reduction from treatment is achieved within a year, so we will model treatment accordingly.

It is generally accepted in clinical practice that the adverse effects of hypertensive treatment are small or negligible [44]. [43] verify this assumption by performing a meta-analysis of randomized control trials. The most common symptoms attributable to each class of drug are: thiazides - dizziness, impotence, nausea, muscle cramps; β blockers - cold extremities, fatigue, nausea; ACE inhibitors - cough; calcium channel blockers - flushing, ankle oedema, dizziness. [42] find that at standard dose, 9.9% more patients taking thiazides report symptoms (compared to placebo), 8.3% of those taking calcium channel blockers, 7.5% of those taking β blockers, and 3.9% of those taking ACE inhibitors. Considering higher dosages, they find adverse effects are less than additive in dosage. They find the prevalence of symptoms sufficiently severe to stop treatment was under 1% across all drug categories. These adverse effects are minor enough that we will examine blood pressure treatment decisions solely based on reduction in cardiovascular events.

1.1.5 Blood Pressure Monitoring

Traditionally, BP was measured at annual clinical examinations or other office visits. These measurements are quite accurate, being taken by trained health professionals following guidelines for proper BP measurement [45]. Individuals suspected of having hypertension were given home or ambulatory BP monitors, recorded frequently for a length of time (typically one week to one month), and the average BP was calculated. Patients with average BP above a threshold value, typically systolic 140 mm Hg or diastolic 90 mm Hg, initiated antihypertensive treatment [36].

Wearables and other devices associated with the Internet of Things, collectively known as mobile health (mHealth), have the potential to revolutionize the management of chronic disease. Specifically, mHealth provides new opportunities for screening and monitoring BP in non-clinical settings [46]. As of August 2017, the Consumer Technology Association forecasted the sale of wearables would reach 48 million units and earn \$5.5 billion in revenue in 2017 [47]. The largest categories in these sales are fitness trackers and smart watches, which measure and record vital measurements (VMs) such as pulse, heart rate variability, blood oxygenation, and blood sugar. In addition to these existing technologies, innovative new ones have the potential to make health measurements even more ubiquitous, such as the Ford Motor Company exploring the integration of blood pressure sensors in their vehicles [48] and the Microsoft Kinect video game console measuring heart rate with infrared cameras [49]. In January 2018, Omron Healthcare debuted a wearable BP monitor that will enter the marketplace fall 2018 [50]. These devices offer access to unprecedented amounts of individual, patient-level data that are recorded at short intervals. It is anticipated that by 2020, even more wearables may be capable of blood pressure monitoring [51]. Many of these technologies integrate with smartphones to provide data tracking and visualization. However, the data analytics potential of these measurements remains largely unexplored [52]. Statistical and mathematical models can analyze the data

from these technologies and improve patient level health outcomes.

1.2 Chapter II: Antecedent Blood Pressure as Predictor of Cardiovascular Disease

Cardiovascular disease risk prediction equations input the risk factors of an individual and output that individual's likelihood of developing CVD in some future time window. Risk prediction models built on the Framingham Offspring data set are common in clinical practice, and regarded as the gold standard. This study aims to improve the prediction model by incorporating a novel risk factor, antecedent blood pressure. Current risk prediction models are based on only current pressure, and do not consider the blood pressure history of patients.

1.2.1 Objectives

Our objectives in this study are to improve the predictive ability of CVD risk equations and demonstrate history of blood pressure is a significant predictor of CVD. We wish to demonstrate history of a patient's blood pressure matters, and risk is not solely determined by current pressure. This motivates further chapters by necessitating a time integrated measure of risk.

1.2.2 Methodology

We develop risk equations using Cox proportional hazard survival models built on the Framingham Offspring data, considering exam 3 as the baseline. We consider both simple age and sex adjusted models, and full models with a complement of risk factors. To each we examine model improvement when adding simple average of patients' BP at exams 1 and 2. To compare the predictive power of these models and explore if the differences are significant, we utilize C-statistic (concordance) tests, net reclassification (NRI), and integrated discrimination improvement (IDI).

1.2.3 Contribution

We find that antecedent systolic blood pressure is a statistically significant predictor of CVD. When antecedent pressure is added to a traditional risk factor model, current BP becomes not statistically significant. A reasonable conclusion is that long-term information related to blood pressure continues to be relevant and higher BP levels in the past may exert long term effects on CVD risk. This finding motivates the following chapter by demonstrating the importance of a time integrated risk of CVD.

1.3 Chapter III: Analytics Approach to Blood Pressure Control

The current widely adopted guidelines for initiating antihypertensive treatment [36] suggest initiating treatment in patients < 60 years old with SBP ≥ 140 mm Hg or DBP ≥ 90 mm Hg. However, these guidelines are based on randomized control trials which are limited in the thresholds they can examine. Recent evidence from a significant clinical trial [53] suggest the thresholds should be lowered, but there is no consensus and no data exist to suggest what the optimal thresholds should be. This study aims to develop a longitudinal model of blood pressure progression in the population and use that model to determine optimal treatment initiation thresholds.

1.3.1 Objectives

The first objective of this study is to find optimal antihypertensive treatment initiation and dosage thresholds, which can both recommend future RCT design and serve as a decision support tool. This can improve public health by defining data-driven guidelines for antihypertensive treatment and exploring potential improvements in hypertension management by recommending promising options for exploration in RCTs. A secondary objective of this study is to develop a continuous time, continuous space model of systolic and diastolic blood pressure progression. Existing models of

blood pressure are Markovian and typically have a small state space corresponding to definitions of hypertension. Such an approach may also be useful for modeling other continuous health measurements such as cholesterol, blood glucose, and body mass index.

1.3.2 Methodology

We model systolic and diastolic blood pressure as a continuous time stochastic process, specifically a geometric Brownian motion mixture model. We parametrize the BP progression model using Framingham Original data. We fit a model of CVD risk of blood pressure, parametrized by a large population level study. We model the blood pressure lowering effects of antihypertensive treatments and parametrize from a large meta-analysis of clinical trials. By integrating the risk of blood pressure over time using the fitted progression model, we derive an analytical expression of the expectation and variance of hazard experienced by a patient over the following T years as a function of current pressure. We solve a mean-variance optimization model to find the optimal treatment initiation and dosage intensification thresholds. This model allows us to capture different attitudes towards risk, for example risk-neutral or risk-averse. We show the distribution of incurred hazard ratio does not follow a simple form, yet we construct approximate confidence intervals using radial basis functions. We conduct a simulation study to compare our policy to existing guidelines.

1.3.3 Contribution

This work makes contributions in both the methodological and clinical domains. From the methodological perspective, we provide a novel mixture-based continuous time, continuous space model of disease progression. The model is robust to distributional forms owing to the flexibility of Gaussian mixtures. Such a model can be used for other health care measurements such as cholesterol, blood glucose in diabetics, and

body mass index. Our analytical solution of the expected value and variance of the hazard ratio is a novel theoretical contribution, as most models in the health domain derive solutions from iterative numerical approaches. From a clinical perspective, our findings have several policy implications which may guide RCT designs and merit further testing in future clinical trials: 1) while the current guidelines consider systolic and diastolic pressure treatment thresholds independently, thresholds that jointly depend on both measurements may substantially improve health outcomes, 2) similar to treatment initiation decisions, there exist optimal treatment intensification threshold levels, that are likely to improve clinical outcomes, 3) while current guidelines suggest treating both cases of isolated hypertension, there may be tradeoffs associated with treating mild isolated diastolic hypertension. Our simulation model demonstrates significant improvement of our policy over current guidelines, saving an estimated additional 15 thousand premature deaths from hypertension annually. An advantage of our approach as a decision support tool is the construction of confidence intervals on hazard ratio experienced by a patient taking various treatments. This allows users to weigh the relative benefit of treatments with exogeneous factors such as patient preference, cost, and potential side effects.

1.4 Chapter IV: Personalized Blood Pressure Management

Wearables and other mobile health technologies have the potential to revolutionize the management of chronic disease. Fitness trackers and smart watches can measure and record vital measurements such as pulse, heart rate variability, blood oxygenation, blood sugar, and blood pressure. These devices offer access to unprecedented amounts of individual, patient-level data that are recorded frequently. Statistical and mathematical models can analyze the data from these technologies and design effective disease monitoring tools.

1.4.1 Objectives

The objective of this chapter is to design statistical and mathematical methods that use measurements from wearables or other technologies to make screening decisions for chronic diseases. We aim to develop a changepoint detection algorithm that signals the user when the likelihood the vital measurement has exceeded some threshold value is high. Such a signal may suggest the user follow up with a clinician for diagnosis and treatment options (for example, in the case of blood pressure or cholesterol) or take immediate action (for example, an elevated heart rate or low blood glucose level). The proposed algorithms are able to incorporate sporadically timed observations to reflect the usage of mobile health technologies.

1.4.2 Methodology

We first design a Bayesian belief-based changepoint method that uses knowledge of the disease progression and measurement error in the mobile technology. Our analyses find this method performs quite well, but remark the difficulty in implementation of such a procedure. Specifically, the exact disease progression distribution is required, and simulations must be conducted to estimate the desired sensitivity and specificity. Motivated by the implementation difficulties of this procedure, we next develop a Naive changepoint procedure that makes few assumptions and is applicable to a wide variety of health measurements. Finally, we demonstrate the effectiveness of our algorithms on simulated blood pressure data and show the improvement in our algorithms over benchmark policies.

1.4.3 Contribution

This work provides two algorithms that use frequent, highly noisy observations of blood pressure or other vital measurements to decide if the measurement has risen above a specified threshold. If the disease progression is known and calculations can

be performed to calibrate algorithm performance, the Bayesian changepoint approach has good performance. On the other hand, this may face challenges in practice, and if the disease progression is unknown or simulations are not possible, the Naive changepoint provides a simple way of analyzing the measurements at the price of slightly worsened performance. Methodologically, our work develops changepoint detection algorithms that operate on temporally correlated observations, unlike most existing algorithms.

CHAPTER 2

ANTECEDENT BLOOD PRESSURE AS PREDICTOR OF CARDIOVASCULAR DISEASE

2.1 Introduction

As discussed in chapter I, prior research has identified many risk factors for CVD, including age, sex, cholesterol, smoking, diabetes, and elevated levels of BP [54]. Many of the causes of CVD are controllable through medication or lifestyle change, so improving our knowledge of risk factors over time and how they may affect CVD risk is worthy of investigation. Most risk estimate models use a patient's current blood pressure and ignore history of BP [55]. Clinical studies have indicated that a patient's BP history may be an important factor [56, 57, 58]. Many patients exhibit high BP variability over time [59, 60], and the most recent point estimate may not capture this information. Furthermore, long-term exposure to elevated BP levels may have important effects on CVD risk. Antecedent BP includes some of this information, and may have meaningful effects on a patient's CVD risk status.

In this chapter we examine the potential effects of incorporating antecedent BP into modern CVD risk prediction models. Previous studies examining antecedent BP as a risk factor [57] have examined an older cohort in the Framingham Original study. Anti-hypertensive treatment has improved since the data examined in that study, and more detailed cholesterol information is available. Other CVD risk studies examining changes in BP over time only classify individuals by stage of hypertension [58]. Studies that incorporate antecedent pressures report current, recent, and remote measures, without considering trends within an individual [61]. In this chapter we consider the improvement in risk prediction from adding additional BP measurements over time.

We further consider whether stage of antecedent hypertension is sufficient to improve risk prediction, or if exact antecedent pressures are necessary. This study motivates further questions regarding how much BP history is relevant to CVD prediction, and how best to weigh past measurements.

2.2 Methods

2.2.1 Population Sample

As discussed in § 1.1.2, the Framingham Heart Study is a longitudinal observational study that began in 1948. The Offspring Cohort began in 1971 with approximately 5000 participants and was used to undertake the data analyses. Exam 1 collected data from 1971-1975, exam 2 from 1979-1983, and exam 3 from 1983-1987. This work was approved by the Emory Institutional Review Board and public-use data were accessed through the National Institutes of Health.

2.2.2 Study Inclusion

We included data from Offspring Study participants who attended Exam 3 if they met the following criteria: (1) individuals must not have had any cardiovascular event (myocardial infarction, angina pectoris, stroke, intermittent claudication, or cardiac failure) at the time of exam 3 or prior to that date, (2) participants had a systolic blood pressure measurement from exam 1 and potentially from exam 2, (3) all other CVD predictors were recorded at exam 3, and (4) study subjects must have either a recorded death time or last known time alive. Out of 3765 participants who attended exam 3, a total of 3344 met these selection criteria (1604 men, 1740 women). Persons with missing data values were omitted, and no interpolation was performed. There was an 8 year interval between exams 1 and 2, and 4 years between exams 2 and 3.

2.2.3 Clinical Measurements

There were 3344 participants who satisfied the selection inclusion criteria. Blood pressure was measured at the FHS with the subject sitting for at least five minutes using an appropriate cuff size. The BP measurements for this project were performed using a mercury column sphygmomanometer with quality control evaluations of the staff who made the measurements. BP was measured twice by a clinician for each participant at each exam, and the average of these determinations was used as the BP in the analyses. Antecedent systolic BP was defined as the simple average of the BP measurements at exams 1 and 2. For the 416 participants missing BP measurements at exam 2, the exam 1 measurement was used as the antecedent. A study subject was considered on treatment for hypertension if the participant either reported currently taking one of a number of drugs designed to lower blood pressure, or if the offspring exam records indicated that the person was being treated for hypertension. The specific drugs included at exam 1: diuretics for fluid retention or BP and hypotensive medications; exam 2: propranolol, hypotensive medications, aldomet, spironolactone, and diuretics for hypertension or other; exam 3: calcium channel blockers, beta blockers, peripheral vasodilators, diuretics, potassium sparing diuretics, reserpine derivatives, methyldopa, clonidine, wytensin, ganglionic blockers, renin angiotensin blockers, and other anti-hypertensive drugs. Cigarette smoking was assessed by questionnaire based on regular smoking over the past year.

Cholesterol was determined using enzymatic methods and HDL cholesterol was measured after precipitation of plasma with dextran sulfate. Diabetes was considered present if the subject took glucose lowering medication or if fasting glucose was greater than 126 mg/dl.

2.2.4 Follow Up for Cardiovascular Disease Outcomes

Participants were followed until they first experienced a CVD event or until 20 years after the exam 3. We defined a CVD event as death by CVD, myocardial infarction, coronary insufficiency, cerebrovascular disease, intermittent claudication, or congestive heart failure. Cardiovascular events were adjudicated by a panel of 3 Framingham clinicians using endpoint criteria that have in place since the start of the study and have been published in official documentation [62]. Participants not experiencing an event were censored at the time of their death or at the time they were last known to be alive.

2.2.5 Statistical Methods

Survival analysis is concerned with analyzing the duration of time until events occur, such as a CVD event. There are two components to a survival model, the baseline hazard function $\lambda_0(t)$ and a function $h(t)$. The underlying baseline hazard function $\lambda_0(t)$ describes the baseline hazard for an average individual with baseline values of the predictor variables. The function $h(t)$ describes how the hazard varies with the predictor variables. The Cox proportional hazards model assumes these functions are multiplicative in describing the hazard $\lambda(t)$ for an individual [63]. The hazard for a particular individual $\lambda(t)$ is thus described as

$$\lambda(t) = h(t)\lambda_0(t) = \lambda_0(t) \exp(\beta_1 X_1 + \cdots + \beta_n X_n),$$

where β_i are fitted coefficients and X_i are the predictor variables. Under this model, the hazard ratio (HR) of a predictor X_v is given by $\exp(\beta_v)$, meaning a one unit increase in X_v corresponds to a multiplicative increase in hazard of $\exp(\beta_v)$.

Cox proportional hazards models were used to evaluate the strength of various variables in predicting CVD risk. We first created simple age- and sex- adjusted risk

models using current systolic BP, antecedent systolic BP, and both BP measures. We next created multivariable Cox models. The conventional model used age, cholesterol, HDL cholesterol, and systolic BP at exam 3 as continuous variables. Sex, smoking, diabetes, and BP treatment were used as categorical variables. The antecedent model included all of these variables, except antecedent BP was used in place of systolic BP. Finally, a full model contained all of these variables and both BP measurements. We also created models examining history of hypertension (exam 1 or 2 BP measurement < 140 or on BP treatment) as a predictor instead of the exact antecedent BP.

To compare the predictive power of these models and explore if the differences were significant, we utilized C-statistic (concordance) tests [64], net reclassification (NRI) [65], and integrated discrimination improvement (IDI)[65]. The IDI test is a measure of the new model's improvement in average sensitivity without reduction in average specificity, and the NRI test examines the upward and downward movement of predicted risk in those with and without events. We performed two versions of the NRI test, continuous and categorical. The former tests the incremental differences in predicted probabilities, and the categorical test considers movement between pre-defined ranges of risk. We used CVD risk category boundaries derived from tertiles of risk. The net estimate for the percentage reclassified is calculated separately for those experiencing events and not. For those with events, it is defined as the number of individuals reclassified upwards minus the number of individuals reclassified downwards, divided by the total number of individuals with events, and for those without events it is the number reclassified downwards minus the number reclassified upwards divided by the number of individuals without events.

2.2.6 Secondary Analyses

To assess the robustness of our findings, we considered secondary analyses. The models described above were run with diastolic BP instead of systolic. Further models

Table 2.1: Summary Statistics, Framingham Offspring Exam 3

Predictor	Overall	Men		Women	
		Case	NonCase	Case	NonCase
# Participants	3344	414	1190	229	1511
# CVD Events	643				
Age	47.8 ± 10.0	52.5 ± 9.3	46.2 ± 9.9	54.1 ± 9.0	46.7 ± 9.6
Smoking (yes/no)	28.9%	31.1%	27.2%	36.7%	28.2%
Diabetes (yes/no)	3.2%	10.4%	1.8%	9.2%	1.5%
Cholesterol (mg/dL)	210.9 ± 40.9	221.0 ± 38.1	207.8 ± 38.2	236.2 ± 48.9	206.6 ± 40.8
HDL Cholesterol (mg/dL)	51.5 ± 14.8	43.4 ± 11.9	46.1 ± 12.1	53.1 ± 15.3	57.8 ± 14.6
BP Treatment (yes/no)	15.4%	27.8%	11.2%	34.5%	12.3%
Current Systolic BP (mm Hg)	123.4 ± 16.6	131.0 ± 15.9	124.1 ± 14.6	131.6 ± 18.1	119.5 ± 16.7
Antecedent Systolic BP (mm Hg)	121.0 ± 14.7	130.1 ± 14.6	123.1 ± 12.6	126.3 ± 17.6	116.1 ± 14.0

Frequencies and means ± standard deviation are shown in the table.

were run with mean arterial pressure [66] instead of systolic BP. To examine if additional antecedent BP measurements can provide additional value, we considered a series of models using exam 5 as baseline and 2,3,or 4 previous exams of antecedent measurements. Finally, we considered models with follow up only for hard CVD events (death by CVD, MI, or stroke.)

2.3 Results

2.3.1 Study Sample Characteristics

A summary of the population sample characteristics is shown in Table 2.1 for the 3344 participants (1604 men, 1740 women) in the study. Men had higher baseline prevalence of diabetes than women (3.9% versus 2.5%), higher current systolic blood pressure (125.8 mm Hg versus 121.1 mm Hg), higher antecedent blood pressure (124.8 mm Hg versus 117.5 mm Hg), and lower HDL cholesterol (45.3 mg/dL versus 57.2 mg/dL). The number of participants on antihypertensive medications at exams 1,2, and 3 were 112, 317, and 515, respectively. The correlation between exam 3 BP and antecedent BP is 0.696, and the variance inflation factors for current and antecedent BP were < 2, indicating no presence of multicollinearity. During 20 years of follow up, there were 643 participants (414 men, 229 women) who experienced a CVD event

Table 2.2: Age and Sex Adjusted Cox Models

		Units	Current BP Model		Antecedent BP Model		Current + Antecedent BP Model	
			HR (95% CI)	p value	HR (95% CI)	p value	HR (95% CI)	p value
Age	1 year		1.06 (1.05-1.07)	<0.001	1.06 (1.05-1.07)	(1.05-1.07)	1.06 (1.05-1.07)	<0.001
Male			2.23 (1.89-2.62)	<0.001	2.08 (1.77-2.45)	<0.001	2.09 (1.77-2.46)	<0.001
Current Systolic BP	10 mm Hg		1.18 (1.12-1.14)	<0.001			1.07 (1.00-1.13)	0.02
Antecedent Systolic BP	10 mm Hg				1.27 (1.20-1.33)	<0.001	1.22 (1.15-1.30)	<0.001
C Statistic			0.735 (0.716,0.753)		0.740 (0.722,0.759)		0.742 (0.724,0.760)	
AIC			9736		9704		9701	
Chi-Square			452		496		499	

(a) Hazard ratio and confidence intervals

Performance	Current + Antecedent vs. Current	Current + Antecedent vs. Antecedent
C Statistic Test	p=0.007	p=0.06
IDI	0.005 (0.001,0.010)	0.001 (0.000,0.003)
Relative IDI	0.050 (0.008,0.092)	0.009 (-0.004,0.024)
NRI continuous	0.149 (0.062,0.238)	0.146 (0.061,0.236)
NRI categories	0.060 (0.0024,0.097)	0.008 (-0.009,0.025)

(b) Model comparison

(19%).

2.3.2 Age and Sex Adjusted Simple Cox Models

Table 2.2 presents the results of the age- and sex- adjusted simple Cox models. Both in the antecedent and the full model, antecedent BP is statistically significant ($p < .001$). Current BP is a statistically significant predictor in both the conventional model and the full model. The C-index of the full model (0.742, CI 95%: 0.724 - 0.760) is significantly higher ($p=0.007$) than that of the conventional model, which implies that considering antecedent BP in addition to current BP significantly improved the reclassification ability. Comparing the full model to the antecedent model, the C-test, NRI, and IDI tests all indicate no significant improvement, suggesting that conventional BP does not improve discrimination by reclassification when antecedent BP is used.

Table 2.3: Multivariate Cox Models

	Units	Current BP Model		Antecedent BP Model		Current + Antecedent BP Model	
		HR (95% CI)	p value	HR (95% CI)	p value	HR (95% CI)	p value
Age	1 year	1.06 (1.05-1.07)	<0.001	1.06 (1.05-1.07)	<0.001	1.06 (1.05-1.07)	<0.001
Male	Yes/No	2.07 (1.74-2.47)	<0.001	1.99 (1.66-2.37)	<0.001	1.99 (1.66-2.37)	<0.001
Smoking	Yes/No	1.64 (1.38-1.94)	<0.001	1.71 (1.44-2.03)	<0.001	1.71 (1.44-2.03)	<0.001
Diabetes	Yes/No	2.48 (1.89-3.25)	<0.001	2.31 (1.75-3.04)	<0.001	2.30 (1.75-3.02)	<0.001
Total Cholesterol	10 mg/dL	1.05 (1.03-1.07)	<0.001	1.05 (1.03-1.07)	<0.001	1.05 (1.03-1.07)	<0.001
HDL Cholesterol	10 mg/dL	0.93 (0.90-0.96)	<0.001	0.93 (0.90-0.96)	<0.001	0.93 (0.90-0.96)	<0.001
Current BP Treatment	Yes/No	1.66 (1.38-2.00)	<0.001	1.42 (1.16-1.74)	<0.001	1.43 (1.17-1.74)	<0.001
Current Sys BP	10 mm Hg	1.09 (1.04-1.15)	<0.001			1.01 (0.95-1.08)	0.73
Ant Sys Bp	10 mm Hg			1.19 (1.12-1.26)	<0.001	1.18 (1.09-1.27)	<0.001
C Statistic		0.771 (0.754,0.788)		0.774 (0.756,0.791)		0.774 (0.757,0.791)	
AIC Statistic		9582		9567		9568	
Chi-square value		693		712		712	

(a) Hazard ratio and confidence intervals

Performance	Current + Antecedent vs. Current	Current + Antecedent vs. Antecedent
C Statistic Test	p=0.04	p=0.29
IDI	0.002 (-0.003,0.007)	0.000 (0.000,0.001)
Relative IDI	0.008 (-0.015,0.033)	0.002 (-0.003,0.007)
NRI continuous	0.153 (0.034,0.277)	0.03 (-0.087,0.149)
NRI categories	0.0289 (0.004,0.054)	-0.001 (-0.010,0.009)

(b) Model comparison

2.3.3 Multivariate Models

Table 2.3 presents the results of the multivariable Cox models. Antecedent BP is a significant predictor in both the antecedent and full models. Current BP is a statistically significant predictor in the conventional model but not in the full model. That is, when considering antecedent BP, antihypertensive treatment, and all other covariates, current BP is not significant. The C-index of the full model (0.774, CI 95%: 0.754 - 0.788) is significantly higher (p=0.04) than that of the conventional model. Both the continuous and categorical NRI tests indicate a significant improvement in the full model over the conventional model, but the IDI test does not indicate a significant improvement. Comparing the full model to the antecedent model, the C-test, NRI, and IDI tests all indicate no significant improvement. The effects of reclassification were assessed with the categorical NRI test using categories found from tertiles

Table 2.4: Antecedent Hypertension Models

	Units	Current BP Model		Current + Antecedent BP Model	
		HR (95% CI)	p value	HR (95% CI)	p value
Age	1 year	1.06 (1.05-1.07)	<0.001	1.06 (1.05-1.07)	<0.001
Male	Yes/No	2.07 (1.74-2.47)	<0.001	2.07 (1.74-2.47)	<0.001
Smoking	Yes/No	1.64 (1.38-1.94)	<0.001	1.66 (1.40-1.96)	<0.001
Diabetes	Yes/No	2.48 (1.89-3.25)	<0.001	2.45 (1.87-3.22)	<0.001
Total Cholesterol	10 mg/dL	1.05 (1.03-1.07)	<0.001	1.05 (1.03-1.07)	<0.001
HDL Cholesterol	10 mg/dL	0.93 (0.90-0.96)	<0.001	0.93 (0.90-0.96)	<0.001
Current BP Treatment	Yes/No	1.66 (1.38-2.00)	<0.001	1.61 (1.32-1.96)	<0.001
Current Sys BP	10 mm Hg	1.09 (1.04-1.15)	<0.001	1.08 (1.03-1.14)	0.004
Antecedent Hypertension	Yes/No			1.12 (0.90-1.40)	0.317
C Statistic		0.771 (0.754,0.788)		0.771 (0.754,0.789)	
AIC Statistic		9582		9583	
Chi-square value		693		699	

(a) Hazard ratio and confidence intervals

Performance	Current + Antecedent vs. Current
C Statistic Test	p=0.51
IDI	0.000 (-0.001,0.001)
Relative IDI	0.000 (-0.001,0.001)
NRI continuous	-0.096 (-0.185,0.000)
NRI categories	0.007 (-0.001,0.018)

(b) Model comparison

of risk to be 0.0457 and 0.1179. The NRI test indicates significant reclassification within these categories. A total of 18 subjects who developed CVD were reclassified upward, and 6 subjects who developed an event were reclassified downwards, for a net estimate of 2.5%. Similar calculations for individuals who did not develop an event revealed 101 subjects reclassified downwards, and 89 subjects reclassified upwards, for a net estimate of 0.4%. The IDI test gave a result of 0.0012 and was not statistical significant. Reclassification information according to the different categories of risk is available in the appendix.

2.3.4 Hypertensive History

Table 2.4 displays the multivariable results using an antecedent hypertension indicator variable. Hypertension, expressed as a yes/no variable in the prediction model, was not statistically significant ($p=0.32$). The hazard ratios for exam 3 systolic BP and antihypertensive treatment were similar to those in the multivariate conventional model.

2.3.5 Secondary Analyses

Diastolic Pressure

Table 2.5 gives the results of running the survival models using diastolic pressure instead of systolic. The results are similar to those of systolic: the full plus antecedent model is a statistically significant improvement over the current model, and there is no improvement in the full plus antecedent model over the antecedent model. The hazard ratio of 10 mm Hg current diastolic pressure is 1.12, while that of antecedent pressure in the antecedent model is 1.33. When both terms are added to the model, current diastolic pressure is insignificant, and antecedent pressure has a hazard ratio of 1.36. We also notice the diminishing effect of BP treatment, as the case with systolic models: in the current model, the hazard ratio of BP treatment is 1.69, while that in the antecedent model is only 1.41.

Mean Arterial Pulse

Table 2.6 gives the results of running the survival models using mean arterial pressure instead of either blood pressure measurement. The results are consistent with the findings from the antecedent blood pressure models. These results are not surprising, since MAP is a convex combination of systolic and diastolic pressures, we would expect the hazard to be consistent with both pressure measurements.

Table 2.5: Antecedent Diastolic Pressure Models

	Units	Current BP Model		Antecedent BP Model		Current + Antecedent BP Model	
		HR (95% CI)	p value	HR (95% CI)	p value	HR (95% CI)	p value
Age	1 year	1.06 (1.05-1.07)	<0.001	1.06 (1.05-1.07)	<0.001	1.06 (1.05-1.07)	<0.001
Male	Yes/No	2.03 (1.70-2.43)	<0.001	1.89 (1.58-2.23)	<0.001	1.90 (1.59-2.27)	<0.001
Smoking	Yes/No	1.65 (1.39-1.95)	<0.001	1.73 (1.46-2.05)	<0.001	1.73 (1.45-2.05)	<0.001
Diabetes	Yes/No	2.57 (1.96-3.36)	<0.001	2.38 (1.81-3.12)	<0.001	2.38 (1.81-3.11)	<0.001
Total Cholesterol	10 mg/dL	1.05 (1.03-1.07)	<0.001	1.05 (1.03-1.07)	<0.001	1.05 (1.03-1.07)	<0.001
HDL Cholesterol	10 mg/dL	0.93 (0.90-0.96)	<0.001	0.93 (0.90-0.96)	<0.001	0.93 (0.90-0.96)	<0.001
Current BP Treatment	Yes/No	1.69 (1.41-2.03)	<0.001	1.41 (1.16-1.73)	<0.001	1.41 (1.16-1.72)	<0.001
Current Dias BP	10 mm Hg	1.12 (1.03-1.22)	0.009			0.97 (0.87-1.08)	0.57
Ant Dias Bp	10 mm Hg			1.33 (1.20-1.48)	<0.001	1.36 (1.20-1.54)	<0.001
C Statistic		0.769 (0.752,0.787)		0.773 (0.755,0.791)		0.773 (0.755,0.791)	
AIC Statistic		9586		9563		9565	
Chi-square value		683		702		703	

(a) Hazard ratio and confidence intervals

Performance	Current + Antecedent vs. Current	Current + Antecedent vs. Antecedent
C Statistic Test	p=0.07	p=0.40
IDI	0.004 (0.001,0.008)	0.000 (0.000,0.001)
Relative IDI	0.033 (0.008,0.059)	0.002 (-0.003,0.003)
NRI continuous	0.125 (0.034,0.214)	-0.053 (-0.143,0.036)
NRI categories	0.054 (0.027,0.082)	-0.003 (-0.013,0.007)

(b) Model comparison

Table 2.6: Mean Arterial Pulse Models

	Units	Current MAP Model		Antecedent MAP Model		Current + Antecedent MAP Model	
		HR (95% CI)	p value	HR (95% CI)	p value	HR (95% CI)	p value
Age	1 year	1.06 (1.05-1.07)	<0.001	1.06 (1.05-1.07)	<0.001	1.06 (1.05-1.07)	<0.001
Male	Yes/No	2.03 (1.70-2.43)	<0.001	1.90 (1.59-2.27)	<0.001	1.90 (1.59-2.27)	<0.001
Smoking	Yes/No	1.65 (1.39-1.95)	<0.001	1.74 (1.46-2.06)	<0.001	1.74 (1.46-2.06)	<0.001
Diabetes	Yes/No	2.51 (1.91-3.29)	<0.001	2.29 (1.74-3.01)	<0.001	2.29 (1.74-3.01)	<0.001
Total Cholesterol	10 mg/dL	1.05 (1.03-1.07)	<0.001	1.05 (1.03-1.07)	<0.001	1.05 (1.03-1.07)	<0.001
HDL Cholesterol	10 mg/dL	0.93 (0.90-0.96)	<0.001	0.93 (0.90-0.96)	<0.001	0.93 (0.90-0.96)	<0.001
Current BP Treatment	Yes/No	1.65 (1.37-1.99)	<0.001	1.36 (1.11-1.67)	<0.001	1.36 (1.10-1.67)	0.003
Current MAP	10 mm Hg	1.14 (1.05-1.23)	0.009			0.99 (0.90-1.09)	0.83
Ant MAP	10 mm Hg			1.31 (1.20-1.43)	<0.001	1.36 (1.20-1.54)	<0.001
C Statistic		0.771 (0.753,0.789)		0.775 (0.757,0.792)		0.775 (0.757,0.792)	
AIC Statistic		9583		9559		9561	
Chi-square value		688		712		712	

(a) Hazard ratio and confidence intervals

Performance	Current + Antecedent vs. Current	Current + Antecedent vs. Antecedent
C Statistic Test	p=0.05	p=0.60
IDI	0.003 (-0.003,0.004)	0.000 (0.000,0.001)
Relative IDI	0.023 (-0.002,0.049)	-0.001 (-0.001,0.001)
NRI continuous	0.161 (0.066,0.249)	-0.068 (-0.165,0.016)
NRI categories	0.050 (0.023,0.076)	0.004 (-0.003,0.011)

(b) Model comparison

When the models were run considering only hard CVD outcomes (death by CVD, MI, and stroke), the results were similar but not statistically significant. This classification lead to a decreased number of events (389), which may explain the loss of statistical power.

In a separate analysis that used Exam 5 as the baseline, we created a series of models with increasing number of antecedent measurements, (in particular, with 2,3, and 4 measurements), and found no statistically significant difference in the discrimination ability (the C-index values were 0.742, 0.744, and 0.745 for the three models respectively, with no statistically significant difference).

2.4 Discussion

These findings show that antecedent systolic blood pressure is a statistically significant predictor of CVD. When antecedent pressure is added to a traditional risk factor model, current BP becomes not statistically significant. The hazard ratio of antecedent BP in both the antecedent and full models is greater than the effect seen for current BP in the traditional risk factor model. An individual's long-term exposure to BP is a stronger predictor of CVD than the current pressure. A reasonable conclusion is that long-term information related to blood pressure continues to be relevant and higher BP levels in the past may exert long term effects on CVD risk.

Consistent with many previous studies and CVD risk scores [55], antihypertensive treatment shows a positive association with risk for CVD, a seemingly contradictory fact. In those studies, treatment may be acting as an indicator of higher blood pressure in the past, which is consistent with our findings. The strength of current BP as a CVD predictor diminishes when antecedent BP is introduced to the model. In the multivariable Cox models, BP treatment has a hazard ratio of 1.66 in the conventional model, and decreases to 1.43 in the full model. As antecedent BP is added to the prediction models, more historical medical information is included for

the individual. In our analyses the indicator variable for antecedent hypertension is not significant in every model. This indicates that knowledge of whether a patient has a history of hypertension is insufficient for the prediction models and the exact pressure measurements are needed to demonstrate significant effects.

In the simple and multivariate models, net reclassification index shows significant improvement in reclassification of individuals without events. This implies that the full model has significantly better specificity than the conventional model. We would not expect an improvement in sensitivity, since individuals with high risk scores in the conventional model will continue to have high risk scores in the full model. However, individuals with intermediate risk scores may be reclassified downwards if they have persistent BP at sub-hypertensive levels. These results must be clinically interpreted, but patients moving between tertiles of risk may be considered for different treatments.

Our study does have limitations. The study population is predominantly white, and may not be generalizable to other racial or ethnic groups. We only consider antecedent BP as the simple average of two previously observed measurements. There are other ways to incorporate historical BP. Considering a weighted average with higher weights on more recent observations might perform better than simple average. An open question is how many years of antecedent information to consider. Our secondary analysis suggests more measurements may improve the model, and further results could quantify the added value of additional measurements. Future work could consider using an exponential weighting scheme on previous observations, incorporating all measurements and simplifying the choice of weightings to a single parameter λ . In our primary models we have only 2 previous BP measurements and are not able to evaluate the potential role of maximum BP attained over a length of time, and other factors such as the age an individual first started treatment, the duration of treatment, and whether treatment lowered the individual's BP. We only

consider antecedent BP as a risk factor, and could consider supplementing the model with antecedent information of other risk factors such as cholesterol and smoking.

This study has demonstrated that antecedent systolic blood pressure is a statistically significant predictor of CVD. The clinical implication of the study is that blood pressure levels in the past are highly associated with greater CVD risk. Clinicians should ask patients about their BP levels in the past and potentially refer to previous medical records, which will be possible with the widening use of electronic health records and health information exchanges. Such patients with elevated antecedent BP may be treated with a more aggressive BP lowering program with weight control, dietary advice, and medications. The latter possibility would most effectively be evaluated with a clinical trial.

CHAPTER 3

ANALYTICS APPROACH TO BLOOD PRESSURE CONTROL

3.1 Introduction

In chapter I, we discussed the health outcomes and cost associated with cardiovascular disease. Elevated blood pressure (BP), referred to as hypertension, is a controllable risk factor. Randomized control trials (RCTs), the gold standard of clinical evidence, have provided abundant evidence that antihypertensive drug treatment can reduce BP and improve health outcomes in patients with hypertension [43, 67]. Many antihypertensive drugs are cheap, effective, and have minimal side effects. Based on the existing RCTs, The Eighth Joint National Committee (JNC8) established the widely adopted guidelines for when to initiate antihypertensive treatment [36], which suggest initiating treatment in patients < 60 years old with SBP ≥ 140 mm Hg or DBP ≥ 90 mm Hg.

While RCTs are powerful and provide strong evidence with respect to the scenarios compared, they also have several inherent limitations. In particular, RCTs are constrained in how many settings they can examine. When the number of potential candidate scenarios/strategies is large, investigating each treatment option becomes infeasible due to time, financial, and sample size limitations. Because of these limitations, while BP progression through time and CVD risk depend on joint systolic and diastolic BP, existing RCTs consider them independently and compare simple strategies such as whether a systolic BP treatment initiation threshold of 130mm Hg is superior to 140mm Hg. Second, due to the same inherent limitations, the existing RCTs of BP control only consider antihypertensive treatment initiation decisions, but not treatment intensity/dosage decisions at various pressure levels. As a result,

current guidelines do not offer suggestions on the intensity of treatment to initiate. Instead, they suggest ad-hoc strategies, such as beginning with one drug and adding more medications until the desired effect is obtained; however, it may be advantageous to begin with a stronger drug regimen in patients with substantially elevated BP to reduce BP and CVD event risk quicker. Finally, RCTs only examine primary outcomes over a limited followup time and do not consider frequency of followup in clinical practice. Evidence that one treatment option is preferred during the length of the trial is not sufficient to guarantee that option is the best over a patient’s lifetime. Antihypertensive treatment decisions should depend not just on present measurements, but how frequently they may be observed in the future, which dictates how many opportunities to initiate treatment exist. Intuitively, clinicians expecting to see a patient frequently may adopt a more conservative treatment strategy than if they see the patient infrequently, because in the former there are more opportunities to initiate treatment if BP progresses adversely.

In this chapter, we propose a data-driven mathematical modeling-based approach to a) study the joint effect of systolic and diastolic BP in optimal treatment initiation decisions and b) characterize the optimal intensity of treatment at various BP levels. We take a population-based approach and model blood pressure as a mixture of geometric Brownian motions, where mixture components correspond to progression of blood pressure in different subpopulations. We analytically characterize the expected value and variance of the hazard ratio which are used in computing the optimal treatment decisions. We carefully calibrate and statistically validate our model using the Framingham dataset and benchmark our findings against the current BP treatment guidelines. Our data-driven model and findings can supplement RCTs in several ways by providing additional evidence that may support the existing guidelines, or may guide the design of future RCTs. Given that it is practically impossible to test all plausible scenarios in RCTs, we believe such a data-driven modeling approach can be

valuable in guiding future RCT development.

Our study also makes several unique contributions to the healthcare analytics and management science literatures. First, while some earlier CVD risk prediction models in the medical literature have considered the J-curve effect and joint effect of systolic and diastolic BP [66], to our knowledge, our work presents the first prescriptive modeling-based study capturing the joint effect of systolic and diastolic BP over time and systematically analyzing the optimal thresholds at which to initiate and intensify anti-hypertensive treatment. Second, unlike commonly used Markov decision process models in disease modeling, our continuous space, continuous time mixture model can be parametrized by arbitrarily timed observations, as commonly observed in BP measurement. Third, our model can capture heterogeneity in population BP progression. We find no simple distribution provides a good fit to real BP data, while our proposed mixture distribution provides excellent fit. Fourth, unlike many of the existing models commonly used in healthcare, our proposed approach provides the hazard ratio and confidence intervals for each available treatment option, which are often important for clinicians in decision making. These confidence intervals allow practitioners and patients to weigh the relative benefit of treatment options with exogeneous factors such as patient preference, cost, comorbidities, and consideration of possible adverse side effects. Last but not the least, our proposed approach provides the hazard ratio and confidence intervals for each available treatment option and can capture various attitudes towards risk, which are important in decision-making in healthcare, but are commonly ignored by most existing studies.

We parameterize and validate our model using the Framingham dataset, one of the largest and most credible longitudinal datasets for studying blood pressure changes over time. We benchmark our findings against the current JNC8 treatment guidelines and draw several policy implications. First, while the JNC8 guidelines consider systolic and diastolic pressure independently, we demonstrate that simultaneously con-

sidering both pressure levels and their interdependent relationship may substantially improve health outcomes. Second, we characterize the optimal systolic and diastolic blood pressure levels for initiating treatment and intensifying dosage, which can be helpful in reducing the variability in clinical practice. Third, our data-driven solutions mostly corroborate current JNC8 guidelines if systolic and diastolic BP are treated independently. Fourth, we find that when the interdependence of BP components is considered, while patients with isolated systolic hypertension should be treated, there might be tradeoffs associated with treating mild isolated diastolic hypertension. Current guidelines suggest treating both cases of isolated hypertension, however, our model indicates that the tradeoffs from the J-Curve effect favor not treating mild isolated diastolic hypertension. These data-driven findings lead to testable hypotheses which merit further empirical analysis and may motivate and guide the design of future trials.

The remainder of this chapter is organized as follows. In §3.2, we review the literature in medical decision making, blood pressure, and stochastic modeling, and discuss our contributions to each. In §3.3, we introduce the model and provide analytical results. §3.4 describes the data and parameter estimation for the numerical study, and §3.5 presents the results of the numerical study and confidence intervals. §3.6 presents sensitivity analysis, and §3.7 contains discussion, conclusions, limitations, and suggestions for future work.

3.2 Literature Review

There are two broad literature areas relevant to our work: medical decision-making studies dealing with long-term management for various chronic diseases and applications of continuous time stochastic processes in other domains.

The medical decision making literature concerning chronic disease management over a long planning horizon typically models health state as a discrete time Markov

chain and solves for optimal policies using a Markov decision process (MDP) framework. [68] consider screening for breast cancer and [69] investigate biopsy referral decisions for prostate cancer, both using a partially observable Markov decision process (POMDP) personalized for individual patients. [70] develops an MDP model for incorporating patient adherence to medication, along with individualized risk factors, to derive personalized optimal hypertension treatment planning strategies. MDP models have also been used to find optimal treatment policies, including finding optimal timings of living donor liver transplantation [71] and related privacy concerns [72], optimizing statin therapy in diabetic patients [73, 74], optimal HIV therapy [75], antibiotic treatment in individuals with sepsis [76], and biopsy decisions in breast cancer patients [77].

In the context of CVD, a few discrete-time Markovian models have been used, mostly in the medical literature, to project long-term impact of current guidelines with given BP treatment threshold levels, or to compare a small set of predefined scenarios [78, 79, 80, 81]. In the management literature, [82] simultaneously optimize systolic blood pressure and cholesterol treatment in diabetic patients, categorizing systolic BP into low, medium, high, or very high states. [83] use a POMDP to personalize anticoagulation therapy to minimize the risk of stroke, considering individual patients' responses and sensitivity to treatment. [84] use an MDP to personalize the optimal sequence of antihypertensive medications considering other risk factors such as age, gender, and smoking. Other research has considered BP as a continuous measure and attempted to describe and predict trajectories of BP without providing a probabilistic model of BP progression [85, 86]. [87] develops a dynamic programming formulation for incorporating patient adherence to medication, along with individualized risk factors, to derive personalized optimal systolic hypertension treatment planning strategies. Our work takes a different perspective, a population-based approach, and differs from this study by considering systolic and diastolic pressure jointly and

the tradeoffs associated with the J-curve effect, as well as considering heterogeneity in BP progression with a mixture model. To our knowledge, this study presents the first continuous longitudinal model of systolic and diastolic BP for assessing the optimal thresholds at which to initiate and intensify anti-hypertensive treatment.

Markovian state models are appropriate when treating the thresholds as given, but are insufficient for investigating optimal treatment thresholds of BP. For example, considering systolic BP from 120 - 170 mm Hg and diastolic BP from 60 - 120 mm Hg at every 1 mm Hg would result in a transition matrix with nearly 10 million entries, estimation and analysis of which would be a major bottleneck. Parameterizing such discrete-time Markovian models is typically infeasible, because as we discussed earlier, BP is typically measured at arbitrarily-spaced time intervals, and existing BP progression datasets reflect these irregular patterns.

Continuous time models have advantages over discrete time models in our application. [88] discuss some of these advantages of continuous time models such as providing physical insights into the system properties, handling non-uniformly sampled data, and incorporating frequent observations. Specifically, when the sampling is non-uniform, as may be case for blood pressure observations, estimation of discrete time model parameters becomes more difficult [89]. Furthermore, studies have demonstrated that continuous time methods may exhibit better predictive performance than discrete time methods when applied to the same data sets [90]. Anticipating the data challenges of Chapter IV, if for example an individual measures their BP twice in a day, three days later, then one week after that, a continuous time model may be better suited to handle these observations than a discrete time model.

Two closely related studies to ours are [91] and [92]. [91] combine machine learning and optimization to predict effective combination of treatment regimens based on historical trial results and help with designing future RCTs. While our work is similar to [91] in the sense that our work also aims to inform the design of RCTs, the approaches

and types of decisions analyzed are very different. In particular, while [91] consider only end points such as survival and toxicity and attempts to identify promising drug combinations, our approach explicitly captures the entire disease trajectory over time, and aims to identify optimal treatment thresholds which depend on progression of disease over time. On the other hand, [92] propose a bandit framework for learning patients' response types to treatment (e.g., responders vs. non-responders) over time, and tailoring treatment to individuals based on their responses to prior treatments. Although [92] apply their model to multiple sclerosis, their framework is applicable to many chronic diseases where treatment is only effective for a subset of patients (responders), and has serious side effects and hence could be harmful to others (non-responders). While our study is similar to [92] in the sense that our work also aims to optimize treatment strategies for a chronic condition, the two studies are different in two key ways: 1) study perspectives and tradeoffs are different: while [92] take an individual patient's perspective and aim to design personalized treatment strategies by learning over time whether a patient is respondent or non-respondent to treatment, we take a population perspective and aim to design population-based guidelines for blood pressure treatment, such that the risk from high or low systolic and diastolic BP is minimized, 2) underlying models and solution approaches are different: while [92] formulate a Markovian model to capture disease progression model over time and utilize multi-armed bandits for identifying optimal control strategies, we show that a Markovian model cannot accurately capture BP change overtime, formulate a Gaussian mixture model for capturing the underlying disease progression, and turn our attention to Ito calculus for solution approaches.

While non-Markovian continuous time, continuous space stochastic processes are common in financial literature [93, 94, 95, 96], they are utilized by only a handful of studies in disease modeling and population health management literature. In that context, two relevant studies to ours are [97] and [98]. [97] model glaucoma progression

as a discrete time, continuous space process, more specifically a discrete time Gaussian state space model, and develop a heuristic approach to find the time of next test to detect glaucoma progression faster than seeing patients on fixed points in time (i.e., only monitoring). Using a similar framework, [98] extend [97] and jointly determine the optimal monitoring regime and treatment such that a weighted sum of disease progression cost, treatment cost, and testing cost is minimized. Our model differs from these works in a few key ways. First, unlike [98] and [97], we model BP as a mixture model, as our empirical analysis based on real data shows that no simple distribution provides a good fit to BP data due to heterogeneity in disease progression. Second, the models by [98] and [97] make monitoring and treatment decisions under the knowledge that glaucoma progression is irreversible, while a blood pressure model must consider the possibility that pressure will revert to a healthy state due to inherent variability or factors other than antihypertensive treatment. Second, in those glaucoma progression models, treatment decisions are based in part on cost and are assumed to cause no harm. In other non-Markovian studies, [99] present a general stochastic model building upon survival analysis to study screening strategies for patients on the kidney transplant waiting list, with the objective of identifying patients who may develop severe conditions while on the wait list, which makes them ineligible for transplant. [100] use a continuous-time semi-Markov model to evaluate the cost effectiveness of disease management programs for heart failure. [101] model progression of AIDS biomarkers, specifically CD4 counts, using Ornstein-Uhlenbeck process, and study a special case of their problem using a Brownian motion model. [102] develop a stochastic model to analyze the health dynamics and management strategies of a population in sub-Saharan Africa, where population health outcomes are captured through a Markov-modulated Brownian motion model. [103] propose a LASSO bandit algorithm and apply it to study the optimal warfarin dosage strategy based on a large number of covariates, including patients' clinical and genetic factors.

3.3 Model and Analysis

An overview of the overall approach is as follows. First, we present a continuous time, continuous space stochastic model to capture BP progression in §3.3.1. Second, we estimate BP reduction from various treatment options in §3.3.2 and characterize the hazard ratio function in §3.3.3. We define the optimization problem, derive closed-form expressions for the mean and variance of the annual hazard ratio, and optimize over treatment options in §3.3.4. Finally, we present our machine learning based approximation of confidence intervals for hazard ratio in §3.3.5.

Notation used in this chapter is summarized on the following page.

Notation within this chapter:

μ_i^N	Average change in log blood pressure per unit time within each mixture component i under natural disease progression
μ^{R_k}, μ^{P_k}	Reduction in log blood pressure from treatment k during the first year and subsequent years, respectively
V_i^N	Covariance matrix of log blood pressure progression per unit time within each mixture component i under natural disease progression
V^{R_k}, V^{P_k}	Change in covariance of log blood pressure progression from treatment k during the first year and subsequent years, respectively
L_i	The Cholesky decomposition of a given covariance matrix V_i
w_i	Mixture weight of i th component Gaussian distribution
X_t	Log of population-level observed systolic and diastolic blood pressure at time t
$HR(X_0, \mu_i, V_i, T)$	Hazard ratio a patient with initial log BP X_0 experiences over the following T time if log BP evolves with mean μ_i and covariance V_i
$y(X_0, T, k)$	Hazard ratio a patient with initial log BP X_0 experiences over the following T time when placed on anti-hypertensive treatment k
$y^*(X_0, T)$	Minimum over available treatment options of expected hazard ratio for a patient with initial log BP X_0 over the following T time
A, b, c	Parameters of the quadratic fit model of hazard ratio
B_t	Standard Brownian Motion

3.3.1 A Model for Blood Pressure Progression

Our aim is to identify the optimal population-level BP treatment strategies and compare our findings against the existing BP treatment guidelines, and for this purpose we need to capture the progression of BP at the population level over time. Taking a data-driven approach, we have considered various distributions to capture BP progression at the population level. Our empirical analysis based on the Framingham data, one of the largest BP progression datasets in the US, has shown that BP progression in population is poorly fit by a simple distribution, but is well-captured by a mixture distribution. Therefore, using the observed population-level data, we model BP progression as a mixture distribution, where each patient is allowed to belong to one or more of the mixture components, representing different subpopulations in the overall population. More specifically, let $X_t = \log\left(\begin{matrix} \text{systolic BP}(t) \\ \text{diastolic BP}(t) \end{matrix}\right)$ represent the log BP at time t ; then the observed rate of change in BP in population-level data, denoted by dX_t , is modeled as a Gaussian mixture distribution as follows:

$$dX_t = \sum_{i=1}^n w_i (\mu_i^N dt + L_i^N dB_t), \quad (3.1)$$

where w_i are the mixture weights, μ_i^N are the mean change per unit time within each mixture component under natural history progression, B_t is a standard 2-dimensional Brownian motion, L_i^N is the lower triangular Cholesky decomposition of the variance V_i^N , namely, $V_i^N = L_i^N (L_i^N)'$; and $V_i^N = \begin{bmatrix} \sigma_{i,1}^2 & \sigma_{i,1}\sigma_{i,2}\rho \\ \sigma_{i,1}\sigma_{i,2}\rho & \sigma_{i,2}^2 \end{bmatrix}$, $L_i^N = \begin{bmatrix} \sigma_{i,1} & 0 \\ \sigma_{i,2}\rho & \sigma_{i,2}\sqrt{1-\rho^2} \end{bmatrix}$. We note that similar functional forms have been used in finance [104] and climate research [105], and in addition to the statistical evidence we present later (see §3.4), we remark that this model also makes physical sense: BP progression is known to be heterogeneous across different subpopulations [106], and mixture com-

ponents correspond to BP progression in different subpopulations. Finally, before moving to the analyses, we reiterate that, similar to the existing BP management guidelines, we take a policy-level perspective, rather than a clinical level perspective of managing individual patients. However, while modeling the observed BP progression at the population level, this model also allows for capturing heterogeneity of BP progression across subpopulations by allowing different means and variances of BP changes in the overall population.

In the following proposition, we present the unique solution to Equation 4.1, which allows us to capture the trajectory of the population-level BP change at any time in the future, and is used in the calculation of hazard ratios.

Proposition 1. *The unique solution to (3.1) is given by*

$$X_t = X_0 + \sum_{i=1}^n w_i (\hat{\mu}_i t + L_i^N B_t) \quad (3.2)$$

where $\hat{\mu}_i = \mu_i^N - \frac{1}{2}D(V_i^N)$ and $D(A)$ is the $n \times 1$ vector of diagonal elements of A .

Proof. Ito's lemma [107] in multiple dimensions states that for any twice differentiable function $f(X, t) : R^m \rightarrow R$ where X follows the stochastic equation (3.1)

$$df = \left(\frac{\partial f}{\partial t} + \frac{1}{2} \sum_{j=1}^m \frac{\partial^2}{\partial B_{t,j}^2} \right) dt + \sum_{j=1}^m \left(\frac{\partial f}{\partial B_{t,j}} \right) dB_t,$$

where $B_{t,j}$ is the j th component of the Brownian Motion B_t . Take $f(X_j, t) = X_{t,j} = X_{0,j} \exp\{(\mu_{i,j}^N - \frac{1}{2}\sigma_i^2)t + L_{i,j}^N B_t\}$, where $X_{t,j}$ is the j th entry of the $m \times 1$ vector X_t , $\mu_{i,j}^N$ is the j th entry of the vector μ_i^N , and $L_{i,j}^N$ is the j th row of the matrix L_i^N . Then

$$\frac{\partial f}{\partial t} = (\mu_{i,j}^N - \frac{1}{2}\sigma_i^2) X_{0,j} \exp\{(\mu_{i,j}^N - \frac{1}{2}\sigma_i^2)t + L_{i,j}^N B_t\} = (\mu_{i,j}^N - \frac{1}{2}\sigma_i^2) X_{t,j},$$

$$\sum_{j=1}^m \left(\frac{\partial f}{\partial B_{t,j}} \right) = L_{i,j}^N X_t,$$

$$\frac{1}{2} \sum_{j=1}^m \frac{\partial^2}{\partial B_{t,j}^2} = \frac{1}{2} \sum_{j=1}^m (L_{i,j}^N)^2 X_{t,i} = \frac{1}{2} \sigma_i^2 X_{t,i}.$$

Thus by Ito's lemma we have

$$dX_{t,j} = ((\mu_{i,j}^N - \frac{1}{2} \sigma_i^2) X_{t,j} + \frac{1}{2} \sigma_i^2 X_{t,j}) dt + L_{i,j}^N X_t dB_t.$$

Ito's lemma guarantees uniqueness of this solution. \square

The next proposition demonstrates that the change in BP per unit time follows a Gaussian mixture model (GMM), i.e. a weighted sum of n component Gaussian densities given by:

$$p(x|\lambda) = \sum_{i=1}^n w_i g(x|\mu_i^N, V_i^N),$$

where x is a d -dimensional continuous vector, $w_i \geq 0, i = 1, \dots, n$ are the mixture weights where $\sum_{i=1}^n w_i = 1$, and $g(x|\mu_i^N, V_i^N), i = 1, \dots, n$ are d -variate Gaussian densities: $g(x|\mu_i^N, V_i^N) = \frac{1}{(2\pi)^{d/2} |V_i^N|^{1/2}} \exp\{-\frac{1}{2}(x - \mu_i^N)'(V_i^N)^{-1}(x - \mu_i^N)\}$.

Proposition 2. *The distribution of the increments of (3.2) is a Gaussian mixture Z .*

Proof. Let F_t and f_t be the distribution and probability density functions of (3.1), respectively, and let $f_{i,t}$ be the density of a mixture component. Then:

$$F_t(x) = P(X_t - X_0 \leq x) = \sum_{i=1}^n w_i P(\hat{\mu}_i t + L_i^N B_t \leq x).$$

Differentiating with respect to x to find the density:

$$\begin{aligned} f_t(x) &= \sum_{i=1}^n w_i \frac{1}{2\pi |L_i^N|^{1/2}} \exp\{-\frac{1}{2}(x - \hat{\mu}_i t)'(L_i^N)^{-1}(x - \hat{\mu}_i t)\} \\ &= \sum_{i=1}^n w_i f_{i,t}(x). \end{aligned}$$

Therefore the density is the sum of Gaussian densities, and is therefore a Gaussian mixture. This result can be seen as a multidimensional generalization of [104]. \square

GMMs can form a smooth approximation to arbitrarily shaped densities [108] making them appropriate for modeling change in BP. GMMs are frequently used in finance due to their capability of representing a large class of sample distributions [109, 104, 110]. The complete model is parameterized by the mean vectors, covariance matrices, and mixture weights, collectively represented by the notation $\lambda = \{w_i, \mu_i^N, V_i^N\}, i = 1, \dots, n$ and the parameters are estimated by an Expectation Maximization algorithm [111].

We next show how to calculate the population parameter estimates from the component distributions. Let Y be the mixture random variable, and W_i be the component random variables. The mean μ_Y and covariance Σ_Y of the mixture distribution Y can be calculated as

$$\mu_Y = E\left[\sum_{i=1}^n w_i W_i\right] = \sum_{i=1}^n w_i E[W_i] = \sum_{i=1}^n w_i \mu_i \quad (3.3)$$

$$\Sigma_Y = E[(Y - E[Y])(Y - E[Y])'] = E[YY'] - \mu_Y \mu_Y'$$

$$= \sum_{i=1}^n w_i E[W_i W_i'] - \mu_Y \mu_Y' = \sum_{i=1}^n w_i (\Sigma_i + \mu_i \mu_i') - \mu_Y \mu_Y' \quad (3.4)$$

The mixture mean is a weighted sum of the means of the component distributions, and the mixture covariance is a weighted sum of the component covariances plus an extra term to represent the shift to the new mean. Note that by Jensen's inequality the term $\sum_{i=1}^n w_i \mu_i \mu_i' - \mu_Y \mu_Y'$ is non-negative. Thus, the mixture covariance is greater than the weighted sum of the component covariances.

3.3.2 Anti-hypertensive Treatment

In line with clinical practice, we consider a discrete number of antihypertensive treatment options, each representing a possible dosage, including standard or half standard dose of a one, two, or three drug combination. We allow the treatment effect in BP reduction to follow any distribution with mean μ^{R_k} and covariance V^{R_k} , and also possibly depend on initial log BP X_0 , but suppress this dependence on X_0 for the simplicity of the notation. As widely accepted and supported by clinical evidence [112], in our base case analysis, we assume that the almost full potential effect of blood pressure reduction from treatment is achieved within a year and after the first year, remaining on treatment confers some relatively small adjustment to the progression under natural history with mean μ^{P_k} and covariance V^{P_k} . Later in our sensitivity analysis, we consider various time lengths for initial treatment effect, and show that our results are robust as long as benefit from treatment is achieved within the time frame considered. Then, the expected BP change during the first year and the following years are captured by $\dot{\mu}_i^k = \mu_i^N - \mu^{R_k}$ and $\tilde{\mu}_i^k = \mu_i^N - \mu^{P_k}$ respectively, and the overall rate of BP change in patients under treatment is given by:

$$dX_t = \begin{cases} \sum_{i=1}^n w_i (\dot{\mu}_i^k dt + \dot{L}_i^k dB_t), & \text{for } T \leq 1 \\ \sum_{i=1}^n w_i (\tilde{\mu}_i^k dt + \tilde{L}_i^k dB_t), & \text{for } T > 1 \end{cases} \quad (3.5)$$

where $\dot{L}_i^k \times (\dot{L}_i^k)' = \dot{V}_i^k$, $\dot{V}_i^k = V_i^N + V^{R_k}$, $\tilde{L}_i^k \times (\tilde{L}_i^k)' = \tilde{V}_i^k$, and $\tilde{V}_i^k = V_i^N + V^{P_k}$.

3.3.3 Characterization of the Hazard Ratios

The hazard ratio is a commonly used risk measure in the CVD literature, corresponding to the increased chance of an adverse event from uncontrolled BP (e.g., mortality or ESRD) compared to a patient with some reference BP, such as 135 mm Hg Systolic BP and 85 mm Hg diastolic BP [113, 35]. The outcomes of drug studies in clinical trials are frequently summarized by the use of hazard ratios because they make use

of all available information, including patients who fail to complete the trial [113].

Prior studies in the clinical literature have shown empirically that a quadratic model forms a quality approximation to the relationship between SBP/DBP and hazard ratio (see Figure 1.1) [114]. Thus, we define the annual average hazard ratio that patients initially at log BP X_0 with annual drift μ_i and covariance V_i experience over the following T years in reference to benchmark systolic and diastolic BP values (135 mm Hg Systolic BP and 85 mm Hg diastolic BP, as:

$$HR(X_0, \mu_i, V_i, T) := \frac{1}{T} \int_0^T X_t' A X_t + b' X_t + c dt, \quad (3.6)$$

where X_t is the stochastic process $dX_t = \mu_i dt + L_i dB_t$ corresponding to a single mixture of (4.1), and $A \in R^{2 \times 2}$, $b \in R^2$ and $c \in R$ are the best fit quadratic surface from above.

3.3.4 Minimum Risk-Adjusted Hazard Ratio

We are interested in selecting treatment action k that minimizes the hazard ratio patients at log BP X_0 experience over the following T time units, which is defined as:

$$y(X_0, T, k) = \begin{cases} \sum_{i=1}^n w_i (HR(X_0, \mu_i^k, \dot{V}_i^k, T)) & \text{for } T \leq 1 \\ \sum_{i=1}^n w_i \frac{1}{T} HR(X_0, \mu_i^k, \dot{V}_i^k, 1) \\ \quad + \frac{T-1}{T} \int_{-\infty}^{\infty} f_{i,k,X_0}(x) HR(X_0 + x, \tilde{\mu}_i^k, \tilde{V}_i^k, T-1) dx, & \text{for } T > 1 \end{cases} \quad (3.7)$$

where $f_{i,k,X_0}(x)$ is the density function conditional on mixture component i of a patient on treatment k initially at log BP X_0 experiencing a change in BP of x in one year. Equation (3.7) states that during the first year of treatment, patients experience BP reduction according to the predicted reduction for the treatment and their initial

BP [112], and after one year, continued use of the treatment offers some marginal benefit over natural history progression captured in $\mu_i^{P_k}$ and $V_i^{P_k}$. As noted earlier, in our sensitivity analysis, we consider various time lengths for initial treatment effect, and show that our results are robust, as long as benefit from treatment is achieved at some point within the planning horizon T . As such, in the calculation for $T > 1$, we condition on the patient's BP after one year and calculate the hazard ratio of the remaining $T - 1$ years given this BP at year one. Then, the objective is to select the treatment option that achieves the minimum expected hazard ratio over T years, which is given by:

$$y^*(X_0, T) = \min_k E[y(X_0, T, k)]. \quad (3.8)$$

Alternatively, in order to capture different attitudes towards risk, we can also consider a mean-variance optimization approach:

$$y^*(X_0, T) = \min_k (E[y(X_0, T, k)] + \lambda Var[y(X_0, T, k)]). \quad (3.9)$$

where $\lambda \geq 0$ measures the degree of risk aversion: when $\lambda = 0$, (3.9) captures a risk-neutral objective function; otherwise, the larger λ is, the more risk averse the decision maker is. Mean-variance optimization models such as this are common in financial studies [115, 116, 117]. We remark that the medical decision-making literature has primarily taken a risk-neutral approach (see for example [82] and [75]), and our flexible formulation and approach extends this literature by explicitly considering variation in addition to expectation. In order to solve the model in (3.9), we need to know the values of $E[y(X_0, T, k)]$ and $Var[y(X_0, T, k)]$, which we analytically characterize.

We first present two lemmas that characterize the mean and variance of average hazard over T time with fixed drift and covariance, which will aid in proving the main theorems.

Lemma 1.

$$E[HR(X_0, \mu_i, V_i, T)] = \frac{T^2}{3} \hat{\mu}_i' A \hat{\mu}_i + \frac{T}{2} (\text{Tr}(AV_i) + 2\hat{\mu}_i' AX_0 + b' \hat{\mu}_i) + (X_0' AX_0 + b' X_0 + c),$$

where $\hat{\mu}_i = \mu_i - \frac{1}{2}D(V_i)$, $D(A)$ is the $n \times 1$ vector of diagonal elements of A , and $\text{Tr}(A)$ is the trace of the matrix A .

Proof: We first consider the case with a standard Brownian motion process. Suppose $C_1 \in R^{m \times m}$, $c_2 \in R^m$, $c_3 \in R^m$, and B_t is m dimensional standard (uncorrelated) Brownian motion. Let

$$U = \int_0^T B_t' C_1 B_t + c_2' t B_t + c_3' B_t dt.$$

We will first show $E[U] = \frac{T^2}{2} \text{Tr}(C_1)$. Since $B(t)$ is a continuous function of t , U is a Riemann integral with a random integrand. Therefore we calculate the expectation and variance by Riemann sum approximations and take the limit.

For $n > 0$ let $\Delta_n = \frac{T}{n}$ and $t_k = k\Delta_n$ for $k = 0, \dots, n$. Using right Riemann sums, the area under the curve from t_{k-1} to t_k is approximated by

$$\Delta_n (B_{t_k}' C_1 B_{t_k} + t_k c_2' B_{t_k} + c_3' B_{t_k}).$$

We rewrite

$$B_{t_k} = \sum_{i=1}^k B_{t_i} - B_{t_{i-1}},$$

so the Riemann sum approximation of the integral is

$$U_n = \Delta_n \sum_{k=1}^n \left(\begin{array}{l} (\sum_{i=1}^k B_{t_i} - B_{t_{i-1}})' C_1 (\sum_{i=1}^k B_{t_i} - B_{t_{i-1}}) \\ + t_k c_2' (\sum_{i=1}^k B_{t_i} - B_{t_{i-1}}) \\ + c_3' (\sum_{i=1}^k B_{t_i} - B_{t_{i-1}}) \end{array} \right).$$

By the independent increments property of Brownian motion, $B_{t_i} - B_{t_{i-1}}$ is inde-

pendent of $B_{t_j} - B_{t_{j-1}}$ for all $i \neq j$, and the components of $B_{t_i} - B_{t_{i-1}}$ are elementwise independent. Because increments are normally distributed, $E[(B_{t_i} - B_{t_{i-1}})_j] = 0$, $E[(B_{t_i} - B_{t_{i-1}})_j(B_{t_i} - B_{t_{i-1}})_l] = 0$ and $E[(B_{t_i} - B_{t_{i-1}})_j^2] = t_i - t_{i-1}$ for all i, j , and l . Therefore

$$\begin{aligned}
E[U_n] &= \Delta_n \sum_{k=1}^n \sum_{i=1}^k E[(B_{t_i} - B_{t_{i-1}})' C_1 (B_{t_i} - B_{t_{i-1}})] \\
&= \Delta_n \sum_{k=1}^n \sum_{i=1}^k E\left[\sum_{j=1}^m ([C_1]_{j,j} (B_{t_i} - B_{t_{i-1}})_j^2 + \sum_{l=j+1}^m ([C_1]_{j,l} + [C_1]_{l,j}) (B_{t_i} - B_{t_{i-1}})_j (B_{t_i} - B_{t_{i-1}})_l)\right] \\
&= \Delta_n \sum_{k=1}^n \sum_{i=1}^k E\left[\sum_{j=1}^m [C_1]_{j,j} (B_{t_i} - B_{t_{i-1}})_j^2\right] \\
&= \Delta_n \sum_{k=1}^n \sum_{i=1}^k \text{Tr}(C_1) \Delta_n \\
&= \text{Tr}(C_1) \Delta_n^2 \sum_{k=1}^n k \\
&= \text{Tr}(C_1) \Delta_n^2 \frac{n(n+1)}{2} \\
&= \frac{T^2}{2} \text{Tr}(C_1) \left(1 + \frac{1}{n}\right).
\end{aligned}$$

Therefore

$$E[U] = \lim_{n \rightarrow \infty} E[U_n] = \frac{T^2}{2} \text{Tr}(C_1).$$

Now consider the general case:

$$HR(X_0, \mu_i, V_i, T) = \frac{1}{T} \int_0^T X_t' A X_t + b' X_t + c \, dt$$

Using Proposition 1 to give the solution for a single mixture component of X_t

$$= \frac{1}{T} \int_0^T (X_0 + \hat{\mu}_i t + L_i B_t)' A (X_0 + \hat{\mu}_i t + L_i B_t) + b' (X_0 + \hat{\mu}_i t + L_i B_t) + c \, dt$$

$$\begin{aligned}
&= \frac{1}{T} \int_0^T B_t' (L_i' A L_i) B_t + (2(\hat{\mu}_i)' A L_i) t B_t + (2X_0' A L_i + b' L_i) B_t \\
&\quad + t^2 (\hat{\mu}_i)' A \hat{\mu}_i + t(2(\hat{\mu}_i)' A X_0 + b' \hat{\mu}_i) + X_0' A X_0 + b' X_0 + c \, dt.
\end{aligned}$$

Using the specific case above with $C_1 = L_i' A L_i$, $c_2 = 2\hat{\mu}_i' A L_i$, and $c_3 = 2\hat{\mu}_i' A X_0 + b' \hat{\mu}_i$,

$$\begin{aligned}
E[HR(X_0, \mu_i, V_i, T)] &= \frac{T}{2} \text{Tr}(L_i' A L_i) + \frac{1}{T} \int_0^T t^2 \hat{\mu}_i' A \hat{\mu}_i + t(2\hat{\mu}_i' A X_0 + b' \hat{\mu}_i) + X_0' A X_0 + b' X_0 + c \, dt \\
&= \frac{T}{2} \text{Tr}(L_i' A L_i) + \frac{T^2}{3} \hat{\mu}_i' A \hat{\mu}_i + \frac{T}{2} (2\hat{\mu}_i' A X_0 + b' \hat{\mu}_i) + (X_0' A X_0 + b' X_0 + c).
\end{aligned}$$

Noting that by properties of trace, $\text{Tr}(L_i' A L_i) = \text{Tr}(A L_i L_i') = \text{Tr}(A V_i)$, the desired result follows.

Lemma 2.

$$\begin{aligned}
\text{Var}[HR(X_0, \mu_i, V_i, T)] &= \frac{T}{3} (2X_0' A L_i + b' L_i)' (2X_0' A L_i + b' L_i) + \frac{8T^3}{15} (\hat{\mu}_i' A L_i)' (\hat{\mu}_i' A L_i) \\
&\quad + \frac{T^2}{6} (2\text{Tr}(A^2 V_i^2) + 5(\hat{\mu}_i' A L_i)' (2X_0' A L_i + b' L_i)).
\end{aligned}$$

Proof:

Let U and U_n be defined as in Lemma 1. We will first show $\text{Var}(U) = \frac{c_3' c_3 T^3}{3} + \frac{2c_2' c_2 T^5}{15} + \frac{5c_2' c_3 T^4}{12} + \frac{\text{Tr}(C_1' C_1) T^4}{3}$. By the independent increments property of Brownian motion, $B_{t_i} - B_{t_{i-1}}$ is independent of $B_{t_j} - B_{t_{j-1}}$ for all $i \neq j$, and the components of $B_{t_i} - B_{t_{i-1}}$ are elementwise independent. Because increments are normally distributed, $\text{Var}[(B_{t_i} - B_{t_{i-1}})_j] = t_i - t_{i-1}$, $\text{Var}[(B_{t_i} - B_{t_{i-1}})_j (B_{t_i} - B_{t_{i-1}})_l] = (t_i - t_{i-1})^2$ and $\text{Var}[(B_{t_i} - B_{t_{i-1}})_j^2] = 2(t_i - t_{i-1})^2$ for all i, j , and l . We furthermore observe that $\text{Cov}[(B_{t_i} - B_{t_{i-1}})_j, (B_{t_i} - B_{t_{i-1}})_j^2] = \text{Cov}[(B_{t_i} - B_{t_{i-1}})_j, (B_{t_i} - B_{t_{i-1}})_j (B_{t_i} - B_{t_{i-1}})_l] =$

$Cov[(B_{t_i} - B_{t_{i-1}})_j^2, (B_{t_i} - B_{t_{i-1}})_j(B_{t_i} - B_{t_{i-1}})_l] = 0$. Therefore

$$Var[U_n] = Var[\Delta_n \sum_{k=1}^n \left(\begin{array}{l} ((n-k+1)c'_3 + \Delta_n \sum_{i=k}^n i \cdot c'_2)(B_{t_i} - B_{t_{i-1}}) \\ + (n-k+1)(B_{t_i} - B_{t_{i-1}})' C_1(B_{t_i} - B_{t_{i-1}}) \\ + \sum_{j=k+1}^n 2(n-j+1)(B_{t_i} - B_{t_{i-1}})' C_1(B_{t_j} - B_{t_{j-1}}) \end{array} \right) \quad (3.10)$$

Now

$$\begin{aligned} & Var[(n-k+1)c'_3 + \Delta_n \sum_{i=k}^n i \cdot c'_2](B_{t_i} - B_{t_{i-1}})] \\ &= \sum_{j=1}^m ((n-k+1)[c_3]_j + \Delta_n \sum_{i=k}^n i \cdot [c_2]_j)^2 Var[(B_{t_i} - B_{t_{i-1}})_j] \\ &+ 2 \sum_{l=j+1}^m ((n-k+1)[c_3]_j + \Delta_n \sum_{i=k}^n i \cdot [c_2]_j)((n-k+1)[c_3]_l \\ &\quad + \Delta_n \sum_{i=k}^n i \cdot [c_2]_l) Cov[(B_{t_i} - B_{t_{i-1}})_j, (B_{t_i} - B_{t_{i-1}})_l] \\ &= \Delta_n \sum_{j=1}^m ((n-k+1)[c_3]_j + \Delta_n \sum_{i=k}^n i \cdot [c_2]_j)^2 \\ &= \Delta_n \sum_{j=1}^m (n-k+1)^2 [c_3]_j^2 + \Delta_n^2 \left(\sum_{i=k}^n i \right)^2 [c_2]_j^2 + 2\Delta_n (n-k+1) \sum_{i=k}^n i \cdot [c_2]_j [c_3]_j, \quad (3.11) \end{aligned}$$

and

$$\begin{aligned} & Var[(n-k+1)(B_{t_i} - B_{t_{i-1}})' C_1(B_{t_i} - B_{t_{i-1}})] \\ &= Var[(n-k+1) \sum_{j=1}^m ([C_1]_{j,j}(B_{t_i} - B_{t_{i-1}})_j)^2 + \sum_{l=j+1}^m ([C_1]_{j,l} + [C_1]_{l,j})(B_{t_i} - B_{t_{i-1}})_j (B_{t_i} - B_{t_{i-1}})_l] \\ &= (n-k+1)^2 (2\Delta_n^2 \sum_{j=1}^m [C_1]_{j,j}^2 + \Delta_n^2 \sum_{j=1}^m \sum_{l=j+1}^m ([C_1]_{j,l} + [C_1]_{l,j})^2), \quad (3.12) \end{aligned}$$

and

$$Var[2(n-j+1)(B_{t_i} - B_{t_{i-1}})' C_1(B_{t_j} - B_{t_{j-1}})]$$

$$\begin{aligned}
&= 4(n-j+1)^2 \sum_{h=1}^m \sum_{l=1}^m [C_1]_{j,l}^2 \text{Var}[(B_{t_i} - B_{t_{i-1}})_h (B_{t_j} - B_{t_{j-1}})_l] \\
&= 4(n-j+1)^2 \Delta_n^2 \sum_{h=1}^m \sum_{l=1}^m [C_1]_{j,l}^2. \tag{3.13}
\end{aligned}$$

Substituting (3.11), (3.12), and (3.13) into (3.10),

$$\text{Var}[U_n] = \Delta_n^2 \sum_{k=1}^n \left(\begin{aligned} &\Delta_n \sum_{j=1}^m (n-k+1)^2 [c_3]_j^2 + \Delta_n^2 (\sum_{i=k}^n i)^2 [c_2]_j^2 \\ &+ 2\Delta_n (n-k+1) \sum_{i=k}^n i \cdot [c_2]_j [c_3]_j \\ &+ (n-k+1)^2 (2\Delta_n^2 \sum_{j=1}^m [C_1]_{j,j}^2 + \Delta_n^2 \sum_{j=1}^m \sum_{l=j+1}^m ([C_1]_{j,l} + [C_1]_{l,j})^2) \\ &+ 4(n-j+1)^2 \Delta_n^2 \sum_{h=1}^m \sum_{l=1}^m [C_1]_{j,l}^2 \end{aligned} \right)$$

$$\begin{aligned}
&= \Delta_n^3 \frac{1}{6} (2n^3 + 3n^2 + n) \sum_{j=1}^m [c_3]_j^2 \\
&+ \Delta_n^5 \frac{1}{30} (4n^5 + 10n^4 + 10n^3 + 5n^2 + n) \sum_{j=1}^m [c_2]_j^2 \\
&+ \Delta_n^4 \frac{1}{6} (5n^4 + 10n^3 + 7n^2 + 2n) \sum_{j=1}^m [c_2]_j [c_3]_j \\
&+ \Delta_n^4 \frac{1}{6} (2n^3 + 3n^2 + n) \left(\sum_{j=1}^m [C_1]_{j,j}^2 + \sum_{j=1}^m \sum_{l=j+1}^m ([C_1]_{j,l} + [C_1]_{l,j})^2 \right) \\
&+ \Delta_n^4 \frac{1}{3} (n^4 - n^2) \sum_{j=1}^m \sum_{l=1}^m [C_1]_{j,l}^2
\end{aligned}$$

Therefore

$$\begin{aligned}
\text{Var}[U] &= \lim_{n \rightarrow \infty} \text{Var}[U_n] = \frac{(\sum_{j=1}^m [c_3]_j^2) T^3}{3} + \frac{2(\sum_{j=1}^m [c_2]_j^2) T^5}{15} + \frac{5(\sum_{j=1}^m [c_2]_j [c_3]_j) T^4}{6} \\
&+ \frac{(\sum_{j=1}^m \sum_{l=1}^m [C_1]_{j,l}^2) T^4}{3} \\
&= \frac{c'_3 c_3 T^3}{3} + \frac{2c'_2 c_2 T^5}{15} + \frac{5c'_2 c_3 T^4}{6} + \frac{\text{Tr}(C'_1 C_1) T^4}{3}
\end{aligned}$$

To calculate variance of $HR(X_0, \mu_i, V_i, T)$:

$$HR(X_0, \mu_i, V_i, T) = \frac{1}{T} \int_0^T X_t' A X_t + b' X_t + c \, dt$$

Using Proposition 1,

$$\begin{aligned} &= \frac{1}{T} \int_0^T (X_0 + \hat{\mu}_i t + L_i B_t)' A (X_0 + \hat{\mu}_i t + L_i B_t) + b' (X_0 + \hat{\mu}_i t + L_i B_t) + c \, dt \\ &= \frac{1}{T} \int_0^T B_t' (L_i' A L_i) B_t + (2\hat{\mu}_i' A L_i) t B_t + (2X_0' A L_i + b' L_i) B_t \\ &\quad + t^2 \hat{\mu}_i' A \hat{\mu}_i + t(2\hat{\mu}_i' A X_0 + b' \hat{\mu}_i) + X_0' A X_0 + b' X_0 + c \, dt \end{aligned}$$

Therefore

$$\begin{aligned} Var[HR(X_0, \mu_i, V_i, T)] &= Var\left(\frac{1}{T} \int_0^T B_t' (L_i' A L_i) B_t + (2\hat{\mu}_i' A L_i) t B_t + (2X_0' A L_i + b' L_i) B_t \right. \\ &\quad \left. + t^2 \hat{\mu}_i' A \hat{\mu}_i + t(2\hat{\mu}_i' A X_0 + b' \hat{\mu}_i) + X_0' A X_0 + b' X_0 + c \, dt\right) \\ &= \frac{1}{T^2} Var\left(\int_0^T B_t' (L_i' A L_i) B_t + (2\hat{\mu}_i' A L_i) t B_t + (2X_0' A L_i + b' L_i) B_t \, dt\right) \end{aligned}$$

Using the result with Y above, taking $C_1 = L_i' A L_i$, $c_2 = (2\hat{\mu}_i' A L_i)$, and $c_3 = (2X_0' A L_i + b' L_i)$, the result follows.

We are now ready to analytically calculate the values of $E[y(X_0, T, k)]$ and $Var[y(X_0, T, k)]$:

Theorem 3. *The expected risk-adjusted hazard ratio that patients with initial log BP X_0 experience under treatment k (including no treatment) over $T \geq 1$ years is characterized by:*

$$E[y(X_0, T, k)] = X_0' A X_0 + b' X_0 + c$$

$$\begin{aligned}
& + \sum_{i=1}^n w_i \left(\frac{2T-1}{2T} \left(\text{Tr}(A\dot{V}_i^k) + 2(\hat{\mu}_i^k)' AX_0 + b' \hat{\mu}_i^k \right) \right. \\
& \quad + \frac{3T-2}{3T} (\hat{\mu}_i^k)' A \hat{\mu}_i^k \\
& \quad + \frac{T-1}{T} \left(\frac{T-1}{2} (\text{Tr}(A\tilde{V}_i^k) + 2(\bar{\mu}_i^k)' AX_0 + b' \bar{\mu}_i^k) \right. \\
& \quad \quad \left. \left. + \frac{(T-1)^2 (\bar{\mu}_i^k)' A \bar{\mu}_i^k}{3} + (T-1) (\bar{\mu}_i^k)' A \hat{\mu}_i^k \right) \right),
\end{aligned}$$

where $\hat{\mu}_i^k = \dot{\mu}_i^k - \frac{1}{2}D(\dot{V}_i^k)$, $\bar{\mu}_i^k = \tilde{\mu}_i^k - \frac{1}{2}D(\tilde{V}_i^k)$, and $D(A)$ is the $n \times 1$ vector of diagonal elements of A .

Proof. We first consider a single mixture component. From Lemma 1:

$$E\left[\frac{1}{T}HR(X_0, \dot{\mu}_i^k, \dot{V}_i^k, 1)\right]$$

$$= \frac{1}{T} \left(\frac{1}{2} \text{Tr}(A\dot{V}_i^k) + \frac{1}{3} (\hat{\mu}_i^k)' A \hat{\mu}_i^k + \frac{1}{2} (2(\hat{\mu}_i^k)' AX_0 + b' \hat{\mu}_i^k) + (X_0' AX_0 + b' X_0 + c) \right), \quad (3.14)$$

and:

$$\begin{aligned}
& E\left[\frac{T-1}{T} \int_{-\infty}^{\infty} f_{i,k,X_0}(x) HR(X_0 + x, \tilde{\mu}_i^k, \tilde{V}_i^k, T-1) dx\right] \\
& = \frac{T-1}{T} \int_{-\infty}^{\infty} f_{i,k,X_0}(x) E[HR(X_0 + x, \tilde{\mu}_i^k, \tilde{V}_i^k, T-1) dx].
\end{aligned}$$

By Lemma 1:

$$\begin{aligned}
& = \frac{T-1}{T} \int_{-\infty}^{\infty} f_{i,k,X_0}(x) \left(\frac{T-1}{2} \text{Tr}(A\tilde{V}_i^k) + \frac{(T-1)^2}{3} (\bar{\mu}_i^k)' A \bar{\mu}_i^k + \frac{T-1}{2} b' \bar{\mu}_i^k \right. \\
& \quad \left. + \frac{T-1}{2} 2(\bar{\mu}_i^k)' A(X_0 + x) + (X_0 + x)' A(X_0 + x) + b'(X_0 + x) + c \right) dx \\
& = \frac{T-1}{T} \left(\frac{T-1}{2} \text{Tr}(A\tilde{V}_i^k) + \frac{(T-1)^2}{3} (\bar{\mu}_i^k)' A \bar{\mu}_i^k + \frac{T-1}{2} b' \bar{\mu}_i^k + (T-1) (\bar{\mu}_i^k)' AX_0 + X_0' AX_0 + b' X_0 + c \right. \\
& \quad \left. + \int_{-\infty}^{\infty} f_{i,k,X_0}(x) ((T-1) (\bar{\mu}_i^k)' Ax + x' Ax + 2x' AX_0 + b' x) dx \right)
\end{aligned}$$

$$\begin{aligned}
&= \frac{T-1}{T} \left(\frac{T-1}{2} \text{Tr}(A\tilde{V}_i^k) + \frac{(T-1)^2}{3} (\bar{\mu}_i^k)' A \bar{\mu}_i^k + \frac{T-1}{2} b' \bar{\mu}_i^k + (T-1) (\bar{\mu}_i^k)' A X_0 + X_0' A X_0 + b' X_0 + c \right. \\
&\quad \left. + (T-1) (\bar{\mu}_i^k)' A \hat{\mu}_i^k + \text{Tr}(A(\hat{\mu}_i^k (\hat{\mu}_i^k)' + V_i^k)) + 2(\hat{\mu}_i^k)' A X_0 + b' \hat{\mu}_i^k \right) \quad (3.15)
\end{aligned}$$

Therefore combining (3.14) and (3.15) we have

$$\begin{aligned}
&E\left[\frac{1}{T} \text{HR}(X_0, \dot{\mu}_i^k, \dot{V}_i^k, 1) + \frac{T-1}{T} \int_{-\infty}^{\infty} f_{i,k,X_0}(x) \text{HR}(X_0 + x, \tilde{\mu}_i^k, \tilde{V}_i^k, T-1) dx\right] \\
&= X_0' A X_0 + b' X_0 + c \\
&\quad + \frac{2T-1}{2T} \left(\text{Tr}(A\dot{V}_i^k) + 2(\hat{\mu}_i^k)' A X_0 + b' \hat{\mu}_i^k \right) \\
&\quad + \frac{3T-2}{3T} (\hat{\mu}_i^k)' A \hat{\mu}_i^k \\
&\quad + \frac{T-1}{T} \left(\frac{T-1}{2} (\text{Tr}(A\tilde{V}_i^k) + 2(\bar{\mu}_i^k)' A X_0 + b \bar{\mu}_i^k) \right. \\
&\quad \quad \left. + \frac{(T-1)^2}{3} (\bar{\mu}_i^k)' A \bar{\mu}_i^k + (\bar{\mu}_i^k)' A \hat{\mu}_i^k (T-1) \right).
\end{aligned}$$

Summing the weighted mixture components produces the desired result. \square

Theorem 4. *The variance of the risk-adjusted hazard ratio that patients with initial log BP X_0 experience under treatment k (including no treatment) over $T \geq 1$ years is characterized by:*

$$\begin{aligned}
&\text{Var}[y(X_0, T, k)] = \\
&\sum_{i=1}^n w_i \left(\frac{1}{T^2} \left(\frac{1}{3} (2X_0' A \dot{L}_i^k + b' \dot{L}_i^k)' (2X_0' A \dot{L}_i^k + b' \dot{L}_i^k) \right. \right. \\
&\quad \left. \left. + \frac{8}{15} ((\hat{\mu}_i^k)' A \dot{L}_i^k)' ((\hat{\mu}_i^k)' A \dot{L}_i^k) \right) \right)
\end{aligned}$$

$$\begin{aligned}
& + \frac{5}{6}((\hat{\mu}_i^k)' A \dot{L}_i^k)' (2X_0' A \dot{L}_i^k + b' \dot{L}_i^k) + \frac{1}{3} \text{Tr}(A^2(\dot{V}_i^k)^2) \\
& + \left(\frac{T-1}{T}\right)^2 \left(\frac{(T-1)}{3} (2(X_0 + \hat{\mu}_i^k)' A \tilde{L}_i^k + b' \tilde{L}_i^k)' (2(X_0 + \hat{\mu}_i^k)' A \tilde{L}_i^k + b' \tilde{L}_i^k) \right. \\
& \quad + \frac{4(T-1)}{3} \text{Tr}(A^2(\dot{V}_i^k)^2) \\
& \quad + \frac{(T-1)^2}{6} (2\text{Tr}(A^2(\tilde{V}_i^k)^2) + 5((\tilde{\mu}_i^k)' A \tilde{L}_i^k)' (2(X_0 + \hat{\mu}_i^k)' A \tilde{L}_i^k + b' \tilde{L}_i^k)) \\
& \quad \left. + \frac{8(T-1)^3}{15} ((\tilde{\mu}_i^k)' A \tilde{L}_i^k)' ((\tilde{\mu}_i^k)' A \tilde{L}_i^k) \right).
\end{aligned}$$

Proof.

$$\begin{aligned}
\text{Var}[y(X_0, T, k)] &= \sum_{i=1}^n w_i \left(\frac{1}{T^2} \text{Var}[HR(X_0, \dot{\mu}_i^k, \dot{V}_i^k, 1)] \right. \\
& \quad \left. + \left(\frac{T-1}{T}\right)^2 \int_{-\infty}^{\infty} f_{i,k,X_0}(x) \text{Var}[HR(X_0 + x, \tilde{\mu}_i^k, \tilde{V}_i^k, T-1)] dx \right)
\end{aligned}$$

The result follows from Lemma 2 applied to both variance terms and noting

$$\begin{aligned}
& \int_{-\infty}^{\infty} f_{i,k,X_0}(x) \frac{5}{6} (T-1)^2 (\tilde{\mu}_i^k)' A \tilde{L}_i^k)' (2(X_0 + x)' A \tilde{L}_i^k + b' \tilde{L}_i^k) dx \\
& = \frac{5}{6} (T-1)^2 (\tilde{\mu}_i^k)' A \tilde{L}_i^k)' (2(X_0 + \hat{\mu}_i^k)' A \tilde{L}_i^k + b' \tilde{L}_i^k)
\end{aligned}$$

and

$$\begin{aligned}
& \int_{-\infty}^{\infty} f_{i,k,X_0}(x) \frac{1}{3} (T-1) (2(X_0 + x)' A \tilde{L}_i^k + b' \tilde{L}_i^k)' (2(X_0 + x)' A \tilde{L}_i^k + b' \tilde{L}_i^k) dx \\
& = \frac{1}{3} (T-1) \left((2(X_0 + \hat{\mu}_i^k)' A \tilde{L}_i^k + b' \tilde{L}_i^k)' (2(X_0 + \hat{\mu}_i^k)' A \tilde{L}_i^k + b' \tilde{L}_i^k) \right. \\
& \quad \left. + 4 \text{Tr}(A^2(\dot{V}_i^k)^2) \right)
\end{aligned}$$

□

The computational complexity of these calculations is low, requiring only arithmetic and matrix multiplication. This implies that the model-based optimal dosage decisions can be computed nearly instantaneously in a spreadsheet or other non-specialized tool, which is very appealing from a practical perspective.

3.3.5 Approximate Confidence Intervals for Hazard Ratio

In this section, we present an approach for constructing confidence intervals on the T-year hazard ratio experienced by patients under various treatment options. The traditional approach to constructing such intervals is to assume the quantity of interest follows some known simple distribution and construct the intervals as a fixed number of standard deviations above and below the sample mean. However, as we describe in detail in the following paragraph, analytical and empirical evidence demonstrate this approach is insufficient for our problem. As such, the remainder of this section develops an accurate approximation to these confidence intervals.

In obtaining the expected hazard ratio in Theorem 2, we observed that the Brownian increments $(B_{t_i} - B_{t_{i-1}})_j$ are normally distributed, and therefore $(B_{t_i} - B_{t_{i-1}})_j^2$ has a scaled chi-squared distribution. The distribution of a weighted sum of chi-squared random variables has no analytical form [118], and since the hazard ratio is a generalization of this, it does not have a simple closed form distribution. Furthermore, in our simulation model, the distribution of the hazard ratio was poorly fit by the distributions considered (normal, lognormal, exponential, beta, and gamma). This leads to poor fit of confidence intervals constructed by assuming a distributional form.

To address these challenges, we approximate the confidence interval bounds by radial basis functions (RBFs) [119]. RBFs are a method of multivariate approximation / interpolation for arbitrary functions that have been successfully applied in various applications [120]. Given data points $x_1, x_2, \dots, x_n \in R^d, d > 1$ and corresponding

observations f_1, f_2, \dots, f_n , the goal is finding a continuous function $s(x)$ which approximates/interpolates the data well. RBFs construct $s(x)$ as a linear combination of basis functions, $s(x) = \sum_{i=1}^n \alpha_i \theta_i(x)$. The weights α_j are found by solving a system of linear equations, equivalent to linear regression of the observations on the data points.

For our basis functions we use the well known Wendland function [121] with dimension $d = 2$ and smoothness $k = 2$. This function fits our data well and takes the form

$$\theta_j(x) = (1 - r)^6 \frac{(3 + 18r + 35r^2)}{1680}$$

where $r = \|x_j - x\|$ is the Euclidean norm. The procedure is to first impose a mesh on a range of BP values, each point of which corresponds to a basis function. We chose Systolic from 110 to 170 mm Hg, and Diastolic from 50 to 120 mm Hg, dividing that range evenly into 10 along each dimension (yielding 100 total basis functions). At each point and for each treatment option, the hazard ratio is simulated for a large number of replications, and the sample confidence interval bounds are recorded. The weights α_j in the linear combination above for lower or upper bound and a specific treatment are found by solving

$$\begin{pmatrix} \alpha_1 \\ \alpha_2 \\ \vdots \\ \alpha_n \end{pmatrix} = \begin{pmatrix} \theta_1(x_1) & \theta_2(x_1) & \dots & \theta_n(x_1) \\ \theta_1(x_2) & \theta_2(x_2) & \dots & \theta_n(x_2) \\ \vdots & \vdots & \ddots & \vdots \\ \theta_1(x_n) & \theta_2(x_n) & \dots & \theta_n(x_n) \end{pmatrix}^{-1} \begin{pmatrix} f_1 \\ f_2 \\ \vdots \\ f_n \end{pmatrix}$$

where f_i is the simulated bound. Then for any point in the range of BP values, we can construct an approximate confidence bound by calculating the basis functions and taking the weighted sum.

The advantages of this approach are the high accuracy in approximation and the

low computational effort to calculate the confidence interval bounds once the weights have been solved. This calculation requires the weighted sum of 100 basis function evaluations, a negligible computation time. These weights can be programmed in a decision support tool and users can receive near instantaneous access to the confidence bounds.

A disadvantage of this method is that it is less intuitive than normal approximations or other schemes that establish confidence interval bounds as a fixed number of standard deviations above or below the mean. However, given the heavy-tailed nature and the lack of fit to traditional distributions, we argue an intuitive approach is insufficient and this more complicated method is necessary. Another disadvantage is moderate apriori computational time to solve for the weights. For each mesh point, a large sample must be simulated over the full time horizon, a non-trivial task. If parameters of the model change, such as the hazard function or the population BP dynamics, this simulation must be performed again to recalibrate new weights.

3.4 Data and Parameter Estimations

In this section, we describe our input datasets as well as the model parameterization approaches and parameter values.

3.4.1 Blood Pressure Change: Gaussian Mixture Models

All parameters for the stochastic blood pressure models were fit from the Framingham Heart Study, described in §1.1.2. The Framingham Original Cohort was chosen instead of the Framingham Offspring Cohort because compared to the latter, the former has more observations, smaller inter-observation times, and less confounding due to treatment effects. This data set included 43,801 BP observations from 5,079 patients. BP readings at each exam were the average of two measurements to reduce variability and measurement error. For each patient, BP readings at each exam and

Table 3.1: Gaussian Mixture Model for Systolic and Diastolic BP

n	AIC	BIC
1	-284949	-284905
2	-286988	-286893
3	-287043	-286896
4	-287149*	-286949*
5	-287139	-286887

Table 3.2: Fitted Parameters for Systolic and Diastolic BP Gaussian 4-mixture model

Component	w_i	$(\mu_i^N)_1$	$(\mu_i^N)_2$	$(V_i^N)_{11}$	$(V_i^N)_{12}$	$(V_i^N)_{22}$
1	0.4119	0.0046	-0.0005	0.0003	0.0002	0.0003
2	0.4079	0.0042	-0.0003	0.0005	0.0003	0.0005
3	0.1123	0.0021	-0.0044	0.0034	0.0022	0.0029
4	0.0679	0.0040	0.0012	0.0017	0.0009	0.0028

inter-observation times were recorded. No observations were recorded after a patient experienced a CVD event or from patients above 70 years of age.

Based on the Framingham dataset, we find a Gaussian 4-mixture fits the systolic and diastolic BP changes over time. The choice of $n=4$ mixture components has the best AIC and BIC (Table 3.1 reports the fits of the Gaussian mixture model for varying number of mixture components n). The estimated parameters of the best fit mixture components are listed in Table 3.2. The mean and covariance of the change in log BP per unit time are estimated using equations (3.3) and (3.4) as

$$\mu_Y = \begin{bmatrix} 0.003 \\ -0.0018 \end{bmatrix}, \Sigma_Y = \begin{bmatrix} 0.0031 & 0.002 \\ 0.002 & 0.0031 \end{bmatrix}.$$

As expected from clinical knowledge, the systolic component is increasing over time, and diastolic is slightly decreasing over time.

3.4.2 Antihypertensive Treatment

The effects of drug treatment on BP progression were estimated from a meta-analysis of 147 randomized trials [43]. They construct equations for the expected reduction

in systolic and diastolic pressure resulting from different treatment options. They find:

"From the average blood pressure of 154 mm Hg systolic and 97 mm Hg diastolic, one drug at standard dose lowered blood pressure by 9.1 mm Hg systolic and 5.5 mm Hg diastolic on average. At lower or higher pretreatment blood pressures the blood pressure reduction decreased (or increased) by 0.10 mm Hg systolic and 0.11 mm Hg diastolic per mm Hg decrease (or increase) in pretreatment blood pressure. ... The estimated blood pressure reduction for two or three drugs at standard dose was calculated by applying these equations to each drug in turn, allowing for the effect of the first in lowering pretreatment blood pressure for the second, and the second for the third. ... Using drugs at half standard dose, taking dose and pretreatment blood pressure into account, it was estimated in the meta-analysis of 354 trials that one, two, and three drugs at half standard dose reduced a pretreatment systolic pressure of 150 mm Hg by 6.7 mm Hg, 13.3 mm Hg, and 19.9 mm Hg, respectively, and reduced a pretreatment diastolic pressure of 90 mm Hg by 3.7 mm Hg, 7.3 mm Hg, and 10.7 mm Hg, respectively (allowing for the effect of one drug in lowering pretreatment blood pressure for the next). These blood pressure reductions decreased (or increased) by an estimated 0.078 mm Hg systolic and 0.088 mm Hg diastolic, per mm Hg decrease (or increase) in pretreatment blood pressure per drug."

The authors therefore provide a recursive way of calculating blood pressure treatment. To save on calculations, we derive a simple linear regression model for the BP reduction at any pretreatment pressure which exactly fits their described effects by

Table 3.3: Expected BP reductions for initiating treatment in a patient at pretreatment SBP X , DBP Y

	Systolic Reduction	Diastolic Reduction
No Rx	0	0
1 drug, half dose	.078X - 5	0.088Y - 4.22
1 drug, std dose	0.1X - 6.3	0.11Y - 5.17
2 drugs, half dose	0.156X - 10.1	0.176Y - 8.54
2 drugs, std dose	0.19X - 11.97	0.208Y - 9.77
3 drugs, half dose	0.234X - 15.2	0.264Y - 13.06
3 drugs, std dose	0.271X - 17.07	0.295Y - 13.87

without the need for recursive calculations. For example, for a patient at pretreatment systolic X taking two drugs standard dose, we solve:

$$\begin{aligned}
 Red(X) &= 9.1 + 0.1 * (X - 154) + Red(NewPressure) \\
 &= 9.1 + 0.1 * (X - 154) + (9.1 + 0.1 * (X - (9.1 + 0.1(X - 154)) - 154)) \\
 &= 0.19X - 11.97
 \end{aligned}$$

Table 3.3 gives the regression equations for the expected BP reductions for initiating treatment in a patient with pretreatment systolic pressure X , diastolic pressure Y .

It is also necessary to generate equations for the effects of treatment reduction, that is, switching to a less aggressive treatment. A patient with excessively low BP on aggressive treatment may wish to switch to a less aggressive treatment, thereby raising their BP. Since the BP reductions from initiating treatment are linear in pretreatment pressure, the expected gain from reducing treatment has a unique solution. We can calculate the effects of removing all treatment as follows: assume a patient's posttreatment BP is X , and we wish to solve for their pretreatment BP Z . Then we can calculate $X = Z - Red(Z)$. For example, a patient at posttreatment SBP X

Table 3.4: Expected BP gain for removing all treatment in a patient at posttreatment SBP X , DBP Y

	Systolic Gain	Diastolic Gain
No Rx	0	0
1 drug, half dose	$0.085X - 5.42$	$0.096Y - 4.63$
1 drug, std dose	$0.111X - 7$	$0.124Y - 5.81$
2 drugs, half dose	$0.185X - 11.97$	$0.214Y - 10.36$
2 drugs, std dose	$0.235X - 14.78$	$0.263Y - 12.34$
3 drugs, half dose	$0.305X - 19.84$	$0.359Y - 17.74$
3 drugs, std dose	$0.372X - 23.42$	$0.418Y - 19.67$

taking one half dose drug, we solve:

$$X = Z - (0.078Z - 5) = 0.922Z + 5$$

$$\rightarrow Z = \frac{X - 5}{0.922}$$

Therefore the expected gain is $Z - X = 0.085X - 5.42$. Table 3.4 gives the regression equations for the expected BP gain for removing all treatment in a patient with posttreatment systolic pressure X , diastolic pressure Y .

To calculate the effects of switching from a more aggressive treatment k_0 to a less aggressive treatment k_1 , we first remove all influence of k_0 by calculating the pretreatment pressure using the equations in table 3.4, compute the posttreatment pressure using the equations from table 3.3 and the calculated pretreatment pressure, then compute the gain as the difference between the current pressure (on k_0) and this predicted pressure (on k_1). To calculate the effects of a more aggressive treatment, by linearity and the way the equations were constructed, it is sufficient to consider current pressure and the addition of the difference in treatments. For example, for a patient on 2 drugs standard dose, the BP reduction from switching to 3 drugs standard dose can be calculated using current pressure and the equation for 1 drug standard dose from table 3.3. Sample expected systolic BP reductions for a patient currently on no treatment can be found in table 3.5, and diastolic in table 3.6.

Table 3.5: Expected systolic BP reduction from antihypertensive treatment

Pretreatment Systolic BP	One drug Half Dose	One drug Standard Dose	Two drugs Half Dose	Two drugs Standard Dose	Three drugs Half Dose	Three drugs Standard Dose
180	9.0	11.7	18.0	22.2	26.9	31.7
170	8.3	10.7	16.4	20.3	24.6	29.0
160	7.5	9.7	14.5	18.4	22.2	26.3
150	6.7	8.7	13.3	16.5	19.9	23.6
140	5.9	7.7	11.7	14.6	17.6	20.9
130	5.1	6.7	10.2	12.7	15.2	18.2
120	4.4	5.7	8.6	10.8	12.9	15.5

Table 3.6: Expected diastolic BP reduction from antihypertensive treatment

Pretreatment Diastolic BP	One drug Half Dose	One drug Standard Dose	Two drugs Half Dose	Two drugs Standard Dose	Three drugs Half Dose	Three drugs Standard Dose
110	5.5	6.9	10.8	13.1	16.0	18.6
105	5	6.4	9.9	12.1	14.7	17.1
100	4.6	5.8	9.1	11.0	13.3	15.6
95	4.1	5.3	8.2	10.0	12.0	14.2
90	3.7	4.7	7.3	8.9	10.7	12.7
85	3.3	4.2	6.4	7.9	9.4	11.2
80	2.8	3.6	5.5	6.9	8.1	9.7
75	2.4	3.1	4.7	5.8	6.7	8.3

3.4.3 Hazard Ratio

Mortality and end-stage renal disease (ESRD), i.e. kidney failure, are two primary outcomes resulting from uncontrolled hypertension [36]. We obtained hazard ratio estimates for all cause mortality / ESRD from [35]. The study population included 398,419 treated hypertensive patients from the Kaiser Permanente Southern California health system. The average patient age was 64 years old, the population was 55% female, had mixed racial demographics, and had a variety of comorbidities. The reported hazard ratios were adjusted for age, sex, race, body-mass index (BMI), chronic kidney disease, diabetes, and comorbidities. Given this diversity in the study population, the authors consider this study to be representative of a general hypertensive population. The reported hazard ratios are listed in table 3.7, independently for systolic and diastolic pressure. Following the conventions of that study, 135 mm Hg systolic BP and 85 mm Hg diastolic BP were used as the reference pressures for constructing the hazard ratios.

Table 3.7: Hazard Ratio estimates from Sim et.al.

Systolic BP	HR	Diastolic BP	HR
< 110	4.10	< 50	3.14
110-119	1.81	50-59	0.96
120 - 129	1.12	60 - 69	0.72
130 - 139	1.00	70 - 79	0.70
140 - 149	1.44	80 - 89	1.00
150 - 159	2.34	90 - 99	1.92
160 - 169	3.33	≥ 100	3.83
≥ 170	4.91		

We fit a quadratic model to log systolic BP and diastolic BP separately using polynomial regression by randomly sampling from the reported hazard ratios. Specifically, for each pressure category we uniformly generate a pressure within the category and generate a hazard ratio as a normal random variable using the reported mean and confidence intervals, and repeat for 1000 observations. The associated R^2 values were 0.911 and 0.82 respectively, indicating good fit of the models. We constructed the fitted hazard ratio surface by averaging the hazard of systolic and diastolic pressure. The resulting surface is presented in Figure 3.1, and the corresponding equation was $X_t' \begin{bmatrix} 24.35 & 0 \\ 0 & 7.23 \end{bmatrix} X_t + \begin{bmatrix} -238.05 & -60.89 \end{bmatrix} X_t + 710.7$. We remark that averaging of hazards is common in clinical practice [112], and in a supplemental study of §3.6 that jointly characterizes the hazards, we present statistical evidence showing that the interaction effect is not significantly different from 0. The surface exhibits the J-curve effect in both systolic and diastolic BP: for a fixed systolic BP, the minimum hazard ratio is attained at some intermediate value of diastolic BP, and vice-versa.

3.4.4 External Validation

To assess the validity of our BP progression model on unseen data, we conducted an external validation on the Framingham Offspring Cohort. This study began in 1971, recruiting 5,124 relatives of the participants of the Framingham Original Cohort,

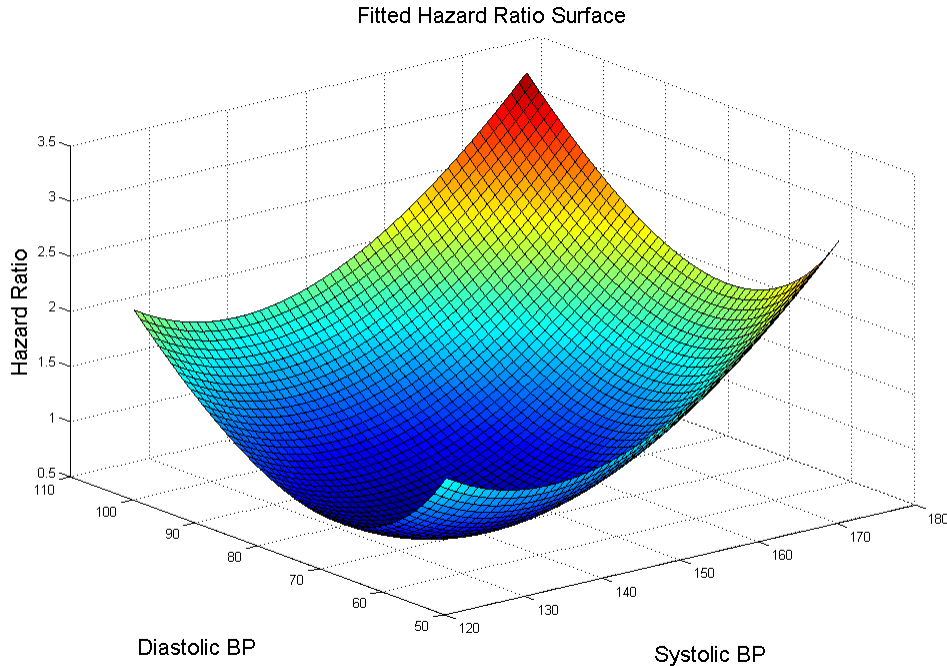


Figure 3.1: Fitted Hazard Ratio Surface

forming an independent population. 9,126 observations of blood pressure in non-CVD patients not on antihypertensive treatment were recorded, and the observed pressures in the population 4 years later were compared to the predictions from our fitted model. For comparison, both observed and predicted pressures were binned according to the categories reported in [35]. Figure 3.2 compares the observed and predicted frequencies of the population systolic and diastolic pressures, and shows that predicted values are close to the observed ones for both systolic and diastolic blood pressures. Table 3.8 presents the joint pressure predictions and observations, which also confirms the fit of our model.

In a supplementary analysis, we repeated the same procedure as above, but examining an 8 year validation window. Figure 3.3 shows this validation. We observe that while the diastolic pressure prediction is accurate, our model underestimates the true percentage of systolic pressure at the lowest category, less than 110 mm Hg. Nonetheless, these differences are mild and we consider the model sufficiently

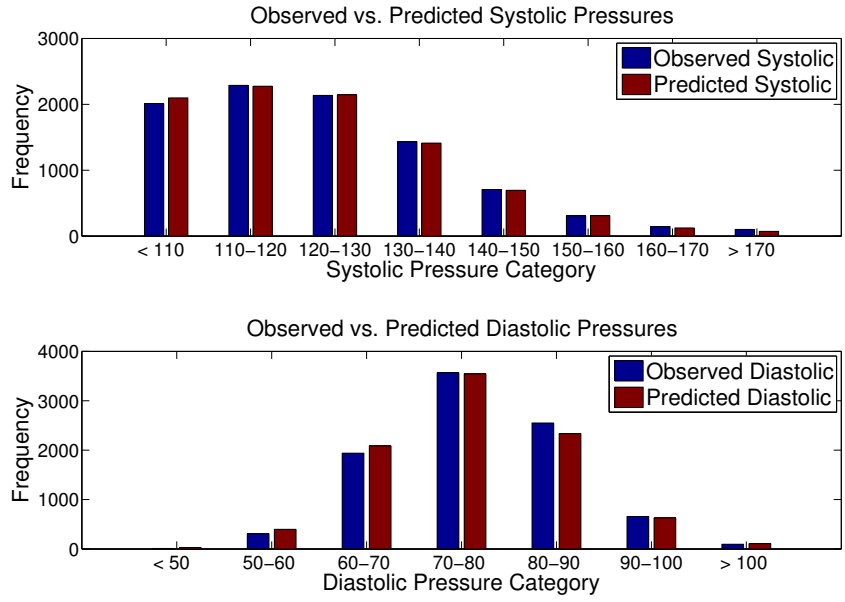


Figure 3.2: 4 Year Validation of BP progression model predictions in external Framingham Offspring data

validated.

3.5 Numerical Results

In this section, we first discuss results about treatment initiation thresholds in §3.5.1 and treatment dosage intensification thresholds in §3.5.2. Then, we extend our results to study treatment intensification and reduction decisions for patients currently on treatment in §3.5.3. Next, we explore the implications of our treatment policy in a simulation model in §3.5.4. Finally, we develop approximate confidence intervals in §3.5.5. In our base case results, we take we take a risk-neutral perspective, as population-based guidelines typically aim to minimize expected adverse events and ignore variance ([122] and [123]). Later in §3.6, we also assess the sensitivity of our base case results against different risk attitudes, as well as several other key model parameters.

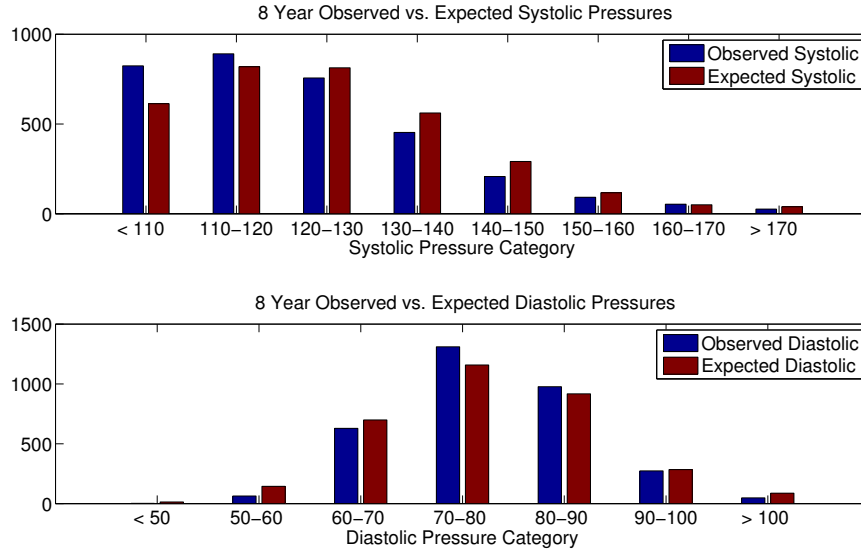


Figure 3.3: 8 Year Validation of BP progression model predictions in external Framingham Offspring data

3.5.1 Treatment Initiation Thresholds

The thresholds for initiating one drug standard dose antihypertensive treatment in patients currently on no treatment to minimize expected 10 year hazard ratio are given in figure 3.4. 10 years was chosen because it is the standard prediction horizon for cardiovascular disease risk calculators [124]. The dotted line shows the JNC 8 thresholds of systolic 140 and diastolic 90. We observe the optimal treatment decision depends on both systolic and diastolic BP, and is nonlinear in both arguments. The thresholds derived from our model are similar to the JNC8 thresholds, but differ in two key ways. First, our findings imply that patients with systolic and diastolic pressure medium-high should initiate treatment, even if not crossing the JNC thresholds. For example, the results indicate that a patient with BP 135/85 should initiate treatment. Second, while these results agree with JNC8 guidelines that patients with isolated systolic hypertension should initiate treatment, they suggest that mild isolated diastolic hypertension should not be treated. For example, consider a patient with BP 120/95. The current JNC8 guidelines, due to aforementioned inherent limitations of RCTs,

Table 3.8: Comparison of joint Systolic / Diastolic BP in external Framingham Offspring data. Upper right of each cell are observed counts, lower left are predicted counts.

Systolic Diastolic	<110	110-120	120-130	130-140	140-150	150-160	160-170	>170
<50	8 25	0 2	0 0	2 1	0 0	0 0	0 0	0 0
50-60	247 320	43 52	9 16	6 6	2 2	1 0.4	1 0	1 0
60-70	1045 1073	543 624	239 275	71 79	30 25.5	8 6	2 1	1 0
70-80	654 616	1294 1231	935 1002	449 473	146 151	57 47	17 15	13 6
80-90	57 59	395 344	860 757	717 667	324 321	113 124	52 42	31 21.6
90-100	0 3	12 18	92 88	183 173	185 168	102 106	51 47	32 26
>100	0 0	0 1	0 5	6 13	19 27	27 27	21 18	23 17

treat systolic and diastolic BP independently by ignoring the interaction and joint J-curve effect between the two and recommend treatment initiation for this patient as their diastolic BP is greater than 90. On the other hand, our findings, which capture this nonlinear effect, indicate that the benefits of reducing diastolic pressure in this case are outweighed by the increase in risk from reducing systolic pressure due to the J-curve effect. Given that it is not feasible to design RCTs to test all possible scenarios, we believe such data-driven findings can help guide the design of future antihypertensive treatment RCTs, and merit further empirical testing via trials.

To assess where the benefit from this policy primarily comes from, we examined the distribution of blood pressure in the population and considered the 10 year hazards coresponding to the JNC8 policy or our policy. Specifically, we considered a one-time decision of whether to initiate treatment or not initiate treatment and compared the resulting hazard ratios. The average 10-year hazard was 1.437 under the JNC8 policy, and 1.411 under our policy. We consider the improvement in our policy broken

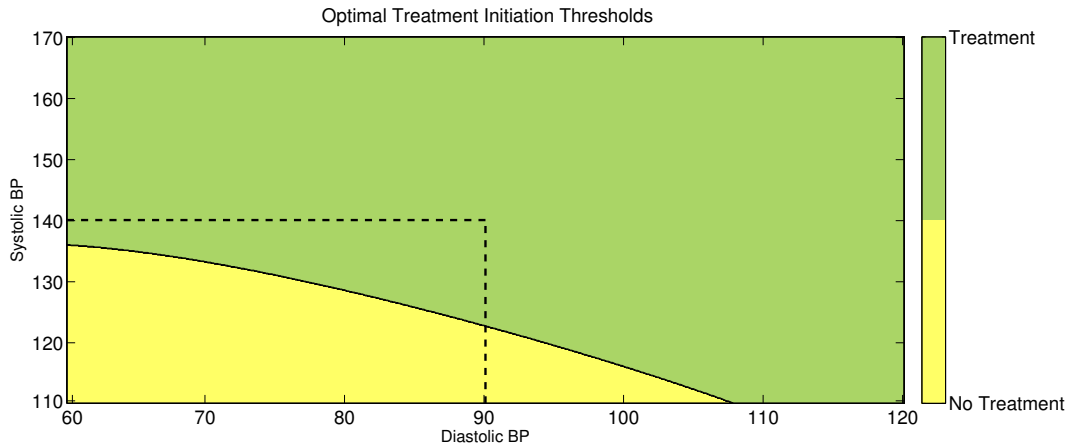


Figure 3.4: Optimal thresholds for initiation of treatment
 Note. The dotted line shows the thresholds given by JNC8

down into two sources, the first arising from the additional treatment recommended in medium-high systolic and diastolic patients below the JNC8 guidelines, and the second coming from the cessation of treatment in patients with isolated diastolic hypertension. We find 99.6% of the reduction in hazard comes from the former, with only 0.4% of the reduction coming from the latter. This result follows from first, the fact that medium-high systolic and diastolic pressure was common in the Framingham data set, while isolated diastolic pressure was fairly uncommon; and second, a greater reduction in hazard was observed for patients in the first region compared to reduction in the isolated diastolic hypertension region. This indicates the improvement of our treatment initiation policy primarily follows from the increased treatment in patients with medium-high systolic and diastolic pressures.

3.5.2 Treatment Intensification Thresholds

In addition to treatment initiation thresholds, our proposed approach can also help calculate the thresholds for the optimal drug dosages. Figure 3.5 shows the optimal dosages for a patient currently on no antihypertensive medication. We make several important observations from this figure. First, as would be expected, treatment dosages in this range of BP values are nondecreasing in systolic and diastolic pres-

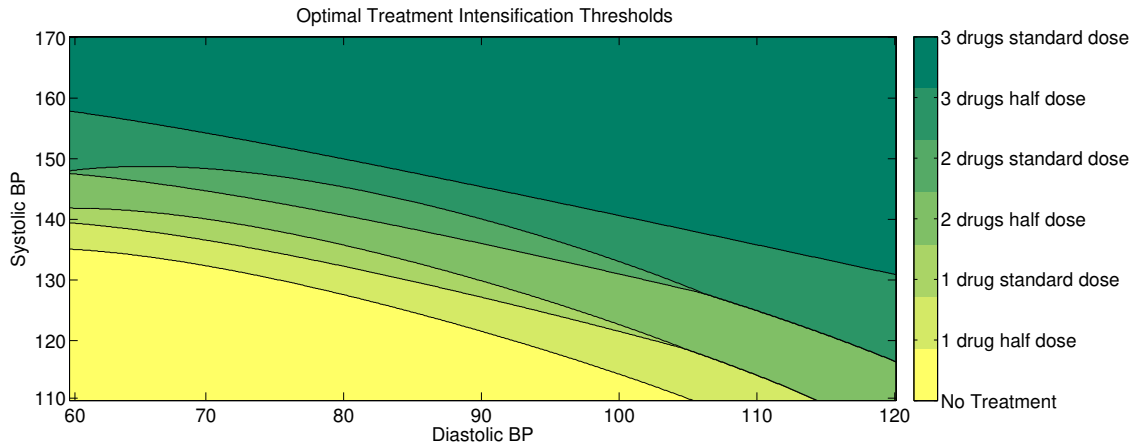


Figure 3.5: Optimal dosage intensification thresholds

sure. For a given systolic pressure, dosage increases as diastolic pressure increases, and vice-versa. Second, optimal dosage usually tends to increase relatively quickly. For example, for a patient with diastolic BP of 80, the weakest treatment (one drug half dose) is initiated at systolic BP 130 and increases in dosage approximately every 5 mm Hg systolic. These dosage thresholds are the first such published results to our knowledge, and can assist clinicians in determining optimal dosages to expediently return patients to desirable BP ranges and reduce variation in clinical practice. In particular, [125] reports high variability in clinical practice of hypertension management owing, in part, to physician difficulty in integrating results from clinical findings and doubts about improvement in outcomes from following guidelines. Our findings may help in alleviating these concerns and lower variability in practice by providing a framework to integrate findings about BP progression, antihypertensive treatment effects, and risk of mortality as a function of BP.

3.5.3 Results for Patients Currently on Treatment

Our base case results presented above focus on patients not on treatment; however, our modeling framework is flexible and can be also used in assisting with the optimal dosage intensification or reduction decisions for patients on existing treatment, as

illustrated below.

As noted in [112], intensifying (or reducing) treatment confers additional BP reduction (or gain) equal to the marginal difference in BP reduction from the two treatments, adjusted for pretreatment pressure. These BP changes from treatment can then be used in calculating the expectation and variance of hazard in Theorems 3 and 4. As an example, Figure 3.6 shows optimal treatment decisions for patients currently on 1 drug, standard dose. The structure of the thresholds is very similar to that of patients not currently on antihypertensive treatment, shifted to account for the expected change in BP from removing or intensifying dosage. For example, the risk of a patient with systolic BP 130 and diastolic BP 70 not currently on antihypertensive treatment would be minimized by not initiating treatment. However, a patient with the same pressures currently on 1 drug standard dose would minimize risk by staying on 1 drug standard dose treatment, since reducing or removing this drug would lead to an expected rise in pressure back to pretreatment levels.

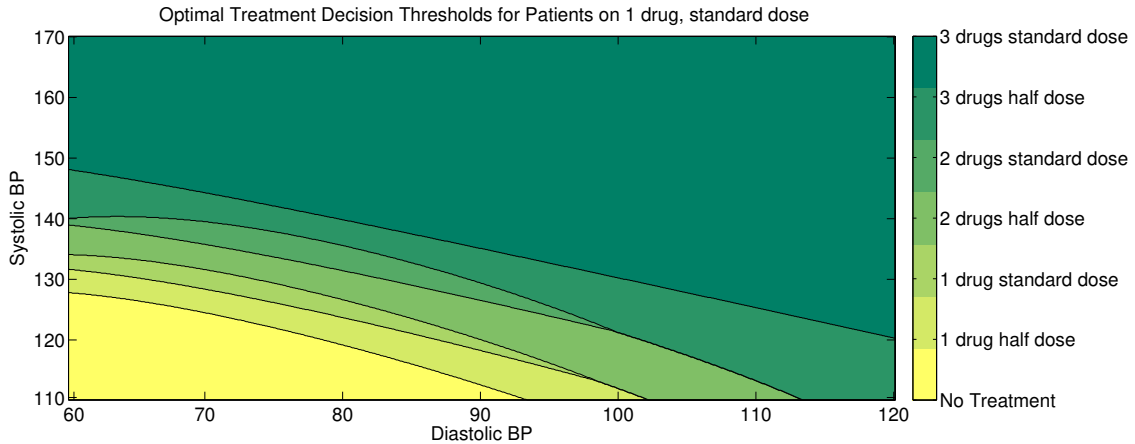


Figure 3.6: Optimal dosage intensification thresholds for patients on 1 drug standard dose

3.5.4 Simulation Model

To evaluate the performance of our policy against the baseline clinical guidelines from JNC8, we created a simulation model of blood pressure progression. A patient's

initial BP was randomly generated from a GMM of initial pressures, and a progression mixture component is chosen based on the mixture weights. Their blood pressure was simulated over 10 years using (3.2) to a discretization of 0.01 years. At 1 year intervals starting at time 0 and proceeding through time 9, the patient's BP was observed and a treatment decision was made according to JNC8 guidelines or our policy. One year decision intervals were chosen because blood pressure is typically observed at annual physician checkups. The JNC8 policy initiates one drug standard dose in untreated patients with systolic BP above 140 or diastolic BP above 90, or intensifies treatment by one standard dose if patients are currently on treatment and above these thresholds, up to a maximum of three drugs standard dose. Our policy picks the treatment at each step that solves (3.8). Initiating or intensifying treatment modified the simulated BP path according to the treatment equations in Tables 3.5 and 3.6. At the end of 10 years, the hazard ratio of the treatment-modified path was calculated by integrating (3.6).

With 10^6 replications, the average hazard ratios following no treatment, the JNC8 policy, and our suggested policy were 2.197, 1.639 and 1.541, respectively. To put these results into perspective, [38] estimate that use of antihypertensives prevented 86,000 premature deaths from cardiovascular disease in 2001. If these 86,000 deaths are attributable to the reduction of hazard from 2.197 to 1.639 (an absolute reduction of 0.558), the additional reduction of 0.098 from our policy could proportionally prevent an estimated 15,100 premature deaths from cardiovascular disease annually. However, we interpret these results cautiously. Clinical implementation of JNC8 guidelines may be more sophisticated than the written policy, for example, by allowing reduction in treatment or implementing different dosages. Therefore actual gains from our proposed policy may be more modest.

3.5.5 Approximate Confidence Intervals for Hazard Ratio

See Figure 3.7 for a histogram of the simulated distribution of the 10-year hazard ratio 20,000 patients initially at BP 150/100 on two drug standard dose treatment. This heavy tailed distribution is poorly fit by all standard distributions considered (exponential, beta, lognormal, gamma). Figure 3.8 shows the associated QQ plot for fitting a normal distribution, demonstrating serious deviations from normality. It may be reasonable to believe that even if the distribution is poorly fit by a normal distribution, the resulting confidence intervals may still be accurate. The most easily recognizable confidence interval is of the form $\mu_{HR} \pm z_{\alpha/2}\sigma_{HR}$, which assumes the distribution of hazard ratio is normal. This assumption is frequently made in practice, so we attempt to construct such an interval, despite a proof that hazard ratio is not normally distributed. On the training data of 100 points, we compute the mean and variance given by the theorems above, and simulate the hazard ratio many times to calculate the exact upper and lower α confidence intervals. We then optimize z to minimize the average error in the hazard ratio approximation. Our numerical results for 95% confidence intervals find the optimal value of z is 1.174. However, on the test data, this choice of z gives an average error of 12.2%. For example, for a patient with BP 150/90 taking no treatment, the mean hazard ratio is 2.136 and standard deviation is 1.12. The exact lower confidence bound is 0.930, and the predicted bound using the above formulation is 0.821, a 11.7% error.

The confidence interval approximation by RBFs is accurate. On a training set of 100 points forming a grid of systolic and diastolic pressures, the approximation of lower and upper bounds have a relative error $< 0.01\%$ for all treatment options. On a test set of 20 points sampled uniformly at random from the BP range, Table 3.9 shows the resulting approximation errors. The average relative error in approximating the lower bound was 0.84% across all samples, and 3.64% for the upper bound. Figure 3.9 shows the upper and lower 95% confidence bounds over a range of systolic

Table 3.9: Relative error in approximation of 95% confidence interval bounds across randomly sampled test data

	No Rx	One drug half dose	One drug standard dose	Two drugs half dose	Two drugs standard dose	Three drugs half dose	Three drugs standard dose	Average
Lower Bound	0.96%	0.89%	0.80%	0.72%	0.78%	0.84%	0.88%	0.84%
Upper Bound	2.88%	3.37%	3.47%	3.75%	3.93%	3.96%	4.14%	3.64%

pressures for a patient with diastolic BP 90 undergoing treatment of two drugs, standard dose. From these results, we conclude these approximate confidence intervals are computationally efficient and may provide additional evidence to assist users in decision making.

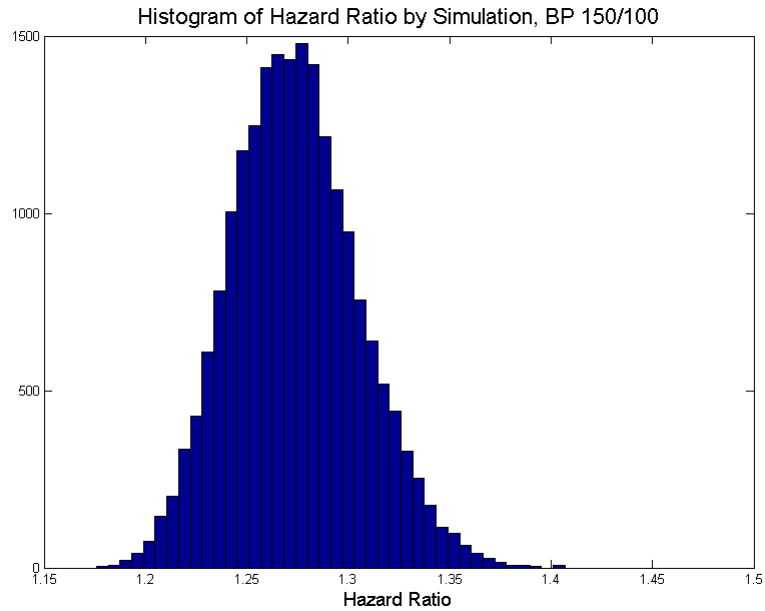


Figure 3.7: Histogram of simulated hazard ratios, initial BP 150/100

3.6 Sensitivity Analysis

In this section, we assess the sensitivity of our findings against key model parameters, including the hazard ratio, BP progression rate, risk behavior, BP measurements, treatment effect, time to achieve treatment effect, and planning horizon.

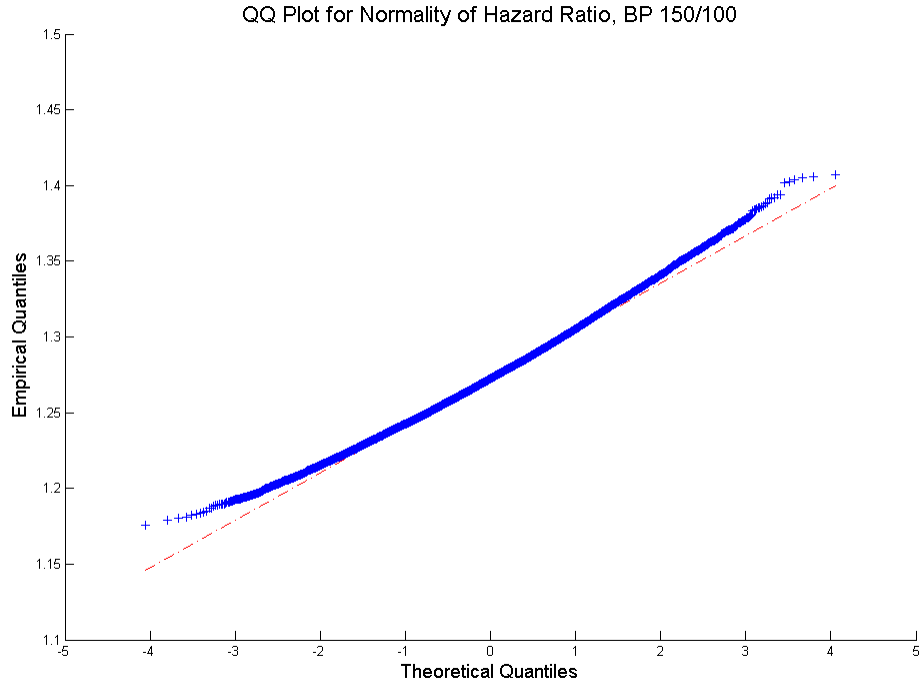


Figure 3.8: QQ plot of simulated hazard ratios, initial BP 150/100

3.6.1 Sensitivity to Hazard Ratio

To assess the sensitivity of our policy against perturbations in the hazard ratio, we conducted a sensitivity analysis by perturbing the reported hazard ratios by up to $\pm 25\%$. More specifically, in each replication, each hazard ratio for different BP values was multiplied by a uniformly distributed random variable to generate hazard ratios between plus or minus 25% of the reported value. The best fit quadratic model of these perturbed hazards was used as the true hazard, and treatment decisions were made according to our policy described in §3.5.2. With 1000 replications, the relative loss in achieved hazard averaged across population BP levels was 0.17%, indicating our model performs well even under moderately misspecified hazards.

While robust against moderately misspecified hazards, the performance of our policy may suffer if the shape of the hazard surface is drastically different. Studies reporting a stronger J-curve effect suggest less aggressive treatment, as the potential

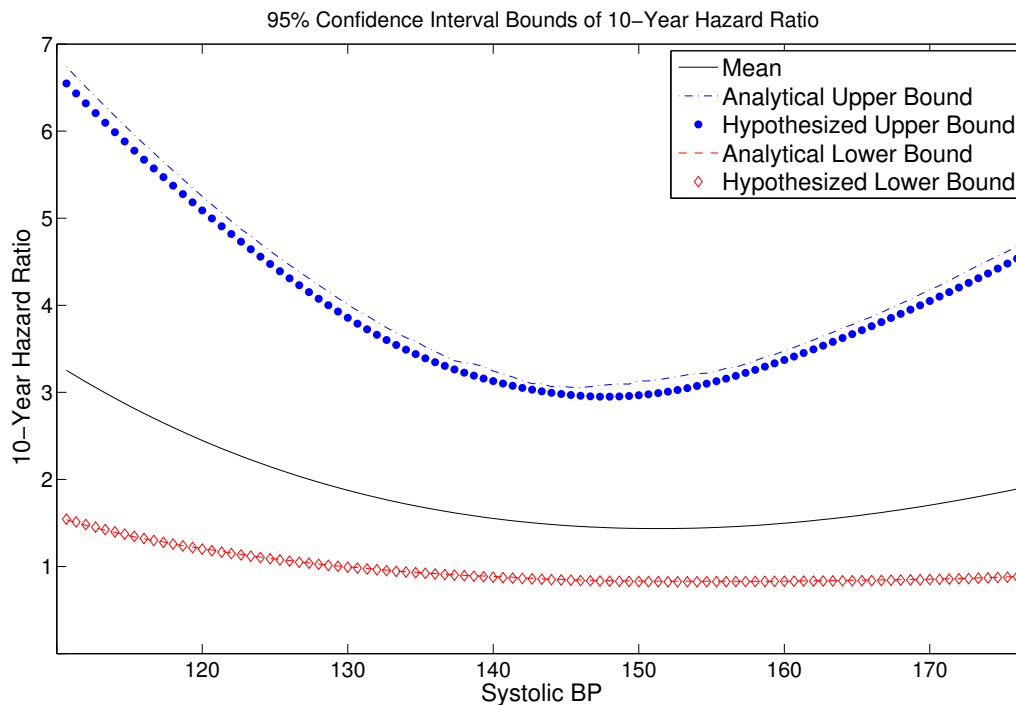


Figure 3.9: Simulated and exact confidence interval bounds for a patient with diastolic BP 90 taking two drugs, standard dose

harms from over-treatment are greater [24]. To examine the model solution under a different parameterization of the hazard ratio surface, we obtain hazard ratio estimates for all cause mortality/ ESRD from [126]. That study followed 651,749 US Veterans with chronic kidney disease (CKD) for a median follow-up of 5.8 years. In comparison to the main result study population, this population is older (average age 73.8 years), almost exclusively male (97.3% male), and each patient suffers from a specific comorbidity. Therefore this study is not appropriate for drawing population level conclusions, but instead to demonstrate the capacity of our model for easy adoption to new data and its power in application to subpopulations. It is further of interest because they provide hazard ratio estimates based jointly on systolic and diastolic BP. Table 3.10 lists the hazard ratios associated with categories of systolic and diastolic BP, and Figure 3.10 for the fitted surface. The fitted hazard ratio function exhibits the J-curve effect more intensely than that in our primary analysis. In fact,

from the data and subsequent parametrization, we observe higher risk for patients at the lowest categories of pressure than at the highest categories.

The optimal intensification thresholds under this parametrization are given in Figure 3.11. These results differ considerably from the main results. The policy is more conservative than in our primary results. This is expected due to the stronger J-curve effect. Patients suffering from CKD can suffer physiological damage from excessively low blood pressure owing to arterial stiffness [127], so it is consistent that hypertension treatment should only be applied in patients with excessively high pressures. Using our policy to make treatment decisions in this subpopulation resulted in a relative error of 3.23%, unacceptably high. This emphasizes the importance of ensuring the correct shape of the hazard ration surface in the population being studied.

Table 3.10: Hazard ratios for all cause mortality associated with Systolic and Diastolic BP in patients with CKD. Source: [30]

	SBP <80	80 ≤ SBP <90	90 ≤ SBP <100	100 ≤ SBP <110	110 ≤ SBP <120	120 ≤ SBP <130	130 ≤ SBP <140	140 ≤ SBP <150	150 ≤ SBP <160	160 ≤ SBP <170	170 ≤ SBP <180	180 ≤ SBP <190	190 ≤ SBP <200	200 ≤ SBP <210	210 ≥ SBP
DBP <40	2.56	2.42	2.55	2.15	1.73	1.69	1.91	-	-	-	-	-	-	-	-
40 ≤ DBP <50	2.99	2.69	2.31	1.77	1.58	1.39	1.37	1.30	1.50	1.83	-	-	-	-	-
50 ≤ DBP <60	3.25	2.88	2.24	1.77	1.51	1.27	1.14	1.17	1.27	1.32	1.63	1.20	-	-	-
60 ≤ DBP <70	-	3.11	2.32	1.82	1.48	1.23	1.09	1.09	1.12	1.13	1.28	1.36	1.00	-	-
70 ≤ DBP <80	-	-	2.05	1.70	1.34	1.14	1.01	1.01	1.04	1.07	1.12	1.19	1.11	1.17	1.26
80 ≤ DBP <90	-	-	-	1.82	1.27	1.08	0.98	1.00	1.01	1.07	1.13	1.22	1.43	1.25	1.35
90 ≤ DBP <100	-	-	-	-	1.57	1.26	1.08	1.10	1.15	1.18	1.25	1.23	1.16	1.38	1.04
100 ≤ DBP <110	-	-	-	-	-	-	1.53	1.16	1.31	1.33	1.37	1.30	1.62	1.40	1.42
110 ≤ DBP <120	-	-	-	-	-	-	-	-	1.11	1.28	1.81	1.35	1.89	1.85	1.71
DBP ≥ 120	-	-	-	-	-	-	-	-	-	-	1.62	-	-	2.44	2.06

3.6.2 Sensitivity to BP Progression

To quantify the sensitivity of the optimal policy against the estimate of mean BP progression, we considered increasing the mean of each mixture component by 25% and assessed the performance of our policy compared to the true optimal treatment policies. The resulting treatment policy is visually depicted in Figure 3.12, and treatment decisions made according to our policy induced average relative loss in achieved

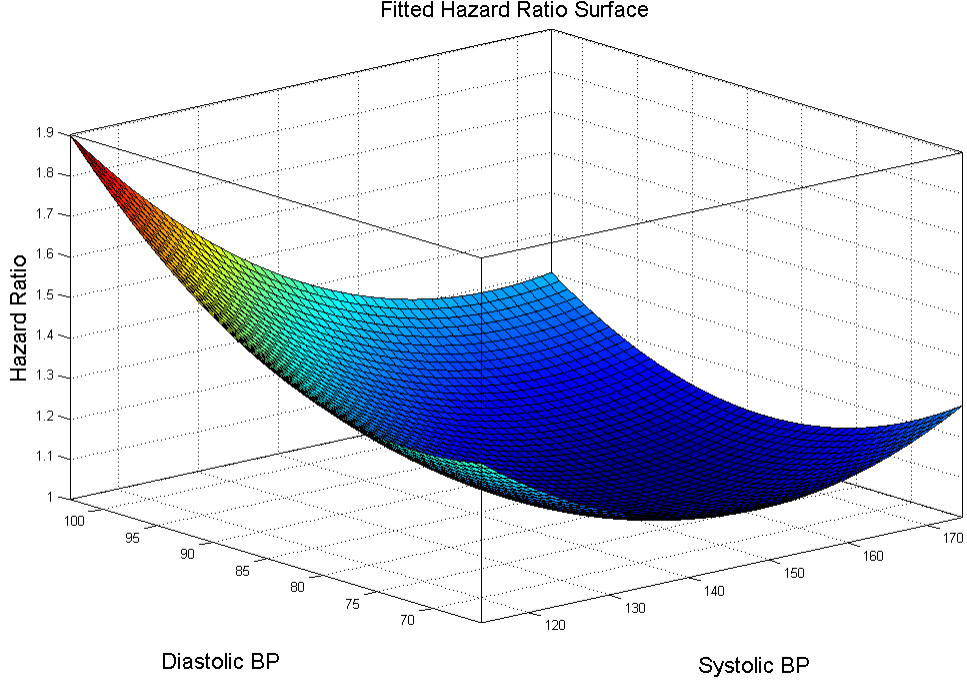


Figure 3.10: Fitted hazard ratio surface. Data source: [30]

hazard of 0.027%, indicating that our model is robust against moderately misspecified estimates of mean BP progression.

In the following proposition, we show that the optimal treatment strategy does not depend on the mixture covariance V_i^N . The intuition behind this result is that treatment affects the BP level but not the variability in progression, hence optimal treatment decisions are not impacted by the covariance of BP progression.

Proposition 3. *Under a risk-neutral perspective ($\lambda = 0$), as the inter-observational blood pressure variance V_i^N changes, there is no change in the difference between the expected hazard ratios of treatment k_1 and treatment k_2 .*

Proof. Using Theorem 3, the difference in expected T-year hazard ratio between two treatments k_1 and k_2 for a patient at log BP X_0 is

$$D_{k_1, k_2}(X_0, T) = \sum_{i=1}^n w_i \left(\frac{2T-1}{2T} (\text{Tr}(AV_i^{k_1}) + 2(\hat{\mu}_i^{k_1})' AX_0 + b' \hat{\mu}_i^{k_1}) \right)$$

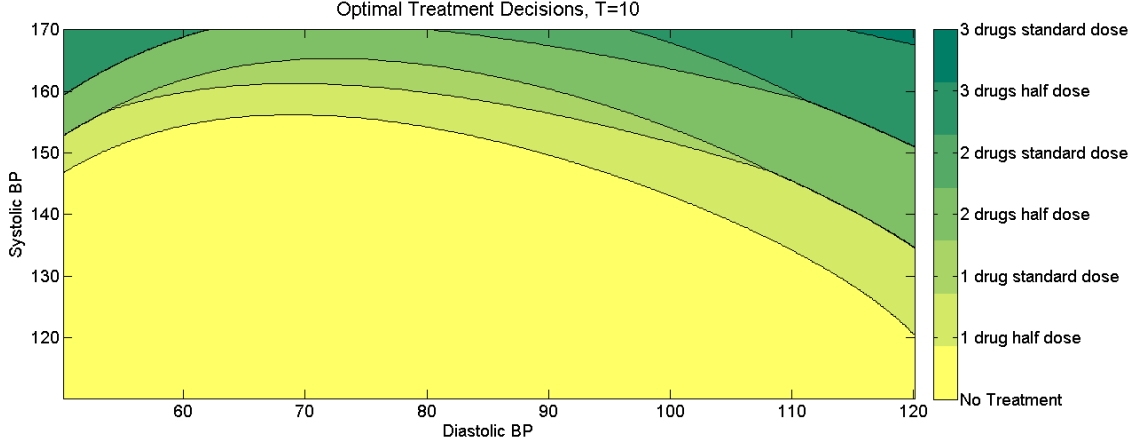


Figure 3.11: Optimal treatment decisions. Data source: [30]

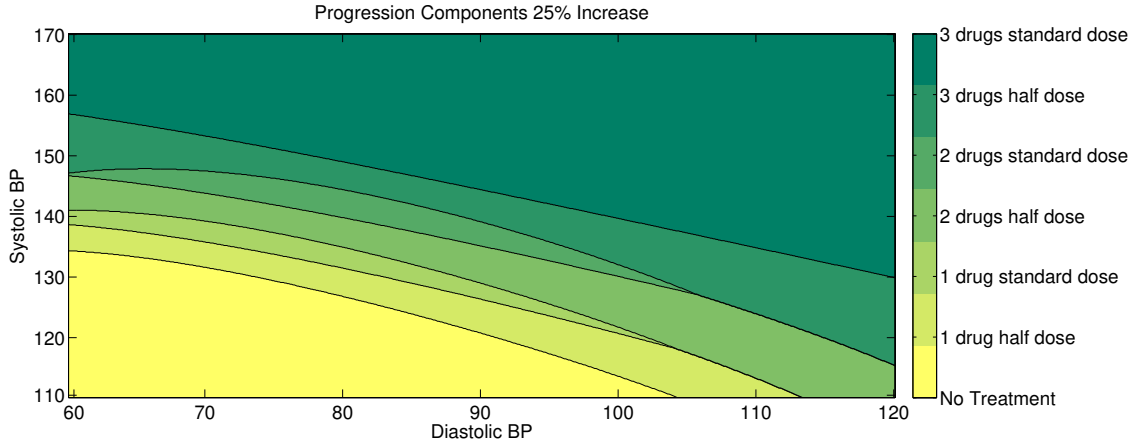


Figure 3.12: Optimal intensification thresholds with BP progression 25% higher than estimated

$$\begin{aligned}
& -Tr(A\hat{V}_i^{k_2}) - 2(\hat{\mu}_i^{k_2})'AX_0 - b'\hat{\mu}_i^{k_2} \\
& + \frac{3T-2}{3T}((\hat{\mu}_i^{k_1})'A\hat{\mu}_i^{k_1} - (\hat{\mu}_i^{k_2})'A\hat{\mu}_i^{k_2}) \\
& + \frac{(T-1)^2}{2T}(Tr(A\tilde{V}_i^{k_1}) - Tr(A\tilde{V}_i^{k_2})) \\
& + \frac{T-1}{T}(2(\bar{\mu}_i^{k_1})'AX_0 + b'\bar{\mu}_i^{k_1} - 2(\bar{\mu}_i^{k_2})'AX_0 - b'\bar{\mu}_i^{k_2}) \\
& + \frac{(T-1)^3}{3T}((\bar{\mu}_i^{k_1})'A\bar{\mu}_i^{k_1} - (\bar{\mu}_i^{k_2})'A\bar{\mu}_i^{k_2}) \\
& + \frac{(T-1)^2}{T}((\bar{\mu}_i^{k_1})'A\hat{\mu}_i^{k_1} - (\bar{\mu}_i^{k_2})'A\hat{\mu}_i^{k_2})
\end{aligned}$$

To examine the sensitivity of the optimal solution to the mixture covariance V_i^N ,

we examine the rate of change by taking the partial derivative:

$$\frac{\partial D_{k_1, k_2}(X_0, T)}{\partial V_i^N} = 0.$$

That is, the expected hazard ratio does not depend on V_i^N . □

The implication of this result is that the scale and shape of variance in blood pressure change does not affect the optimal solution in a given population under a risk-neutral perspective. We remark that this result would not hold under a risk averse perspective ($\lambda > 0$), as the variance of risk is affected by treatment decision. We further remark that this is a simple yet powerful result, because population based guidelines typically take an expectation minimization/maximization approach and ignore variance (See for example population-based cancer screening guidelines by recommended CISNET simulation models (cisnet.gov), which influenced clinical guidelines). The intuition behind this result is that treatment affects the BP level but not the variability in progression, hence optimal treatment decisions are not impacted by the covariance of BP progression.

3.6.3 Sensitivity to the Risk Behavior

In our main analysis we adopted a risk-neutral perspective, where $\lambda = 0$. Here we consider how the treatment decisions depend on the choice of the risk consideration λ . Figure 3.13 demonstrates the optimal decisions when the objective to be minimized is an equal weighting of mean and variance of hazard ($\lambda = 1$). We observe that overall the results are similar to our main risk neutral results, with slightly more aggressive treatment in patients with isolated systolic pressure and less aggressive treatment in patients with isolated diastolic pressure. For example, under a risk neutral decision, a patient with Systolic BP 110 and Diastolic BP 105 would be advised to begin one drug half dose, while under the $\lambda = 1$ perspective the same patient would be advised not

to initiate treatment. Intuitively, the decisions are not very different because from Figure 3.1, we observe that regions with smaller hazard also tend to have smaller variability in hazard. While this holds for BP management, in other applications these decisions may change depending on the desired level of risk.

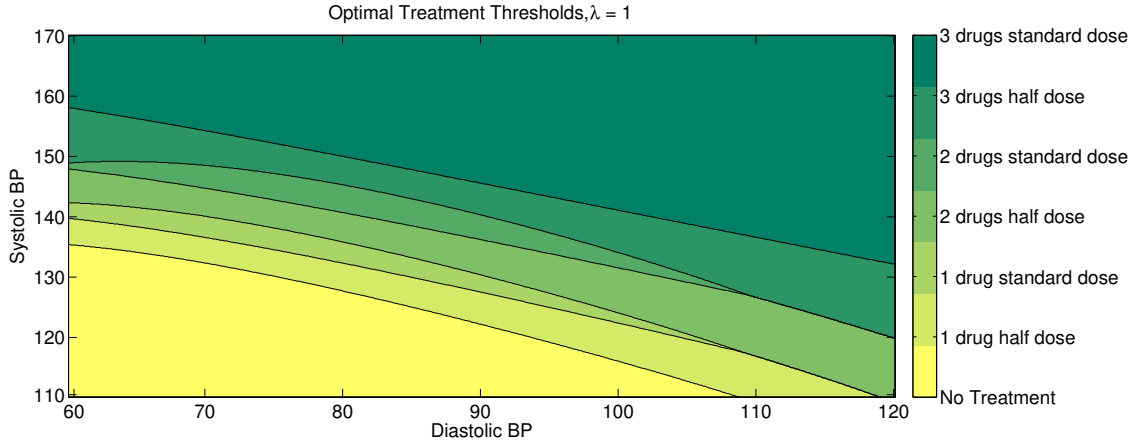


Figure 3.13: Optimal intensification thresholds with $\lambda = 1$

3.6.4 Sensitivity to Blood Pressure Measurements

We consider how our policy performs if the measurement of current BP is incorrect. White-coat hypertension is a phenomenon where BP observed in clinical settings can be up to 5 mm Hg higher than true pressure in both systolic and diastolic components [128]. Our analysis shows that our results are sensitive to BP readings and that using our policy to make treatment decisions in these patients would lead to overly aggressive treatment decisions because of the overestimation of current pressure. Furthermore, the treatment effects in this case would also be miscalculated because the reduction from treatment depend on initial pressure. The treatment decisions made according to our policy induced average relative losses in achieved hazard of 1.75%, emphasizing the importance of the guideline’s recommendation of confirming true BP before initiating treatment [36].

3.6.5 Sensitivity to Treatment Effect

To assess our policy against sensitivity to benefit from treatment, we considered increasing and decreasing the cumulative BP reduction from each treatment option by 25%. The resulting optimal policies are given in Figures 3.14 and 3.15, and the resulting losses in relative hazard are 0.86% and 0.51% respectively, indicating our model is mildly to moderately sensitive to the treatment effect.

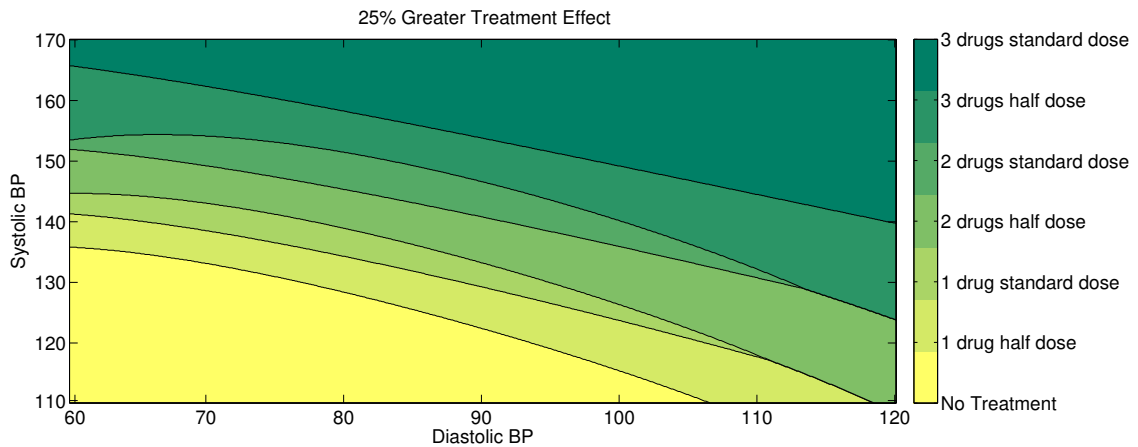


Figure 3.14: Optimal treatment decisions, treatment effect + 25%

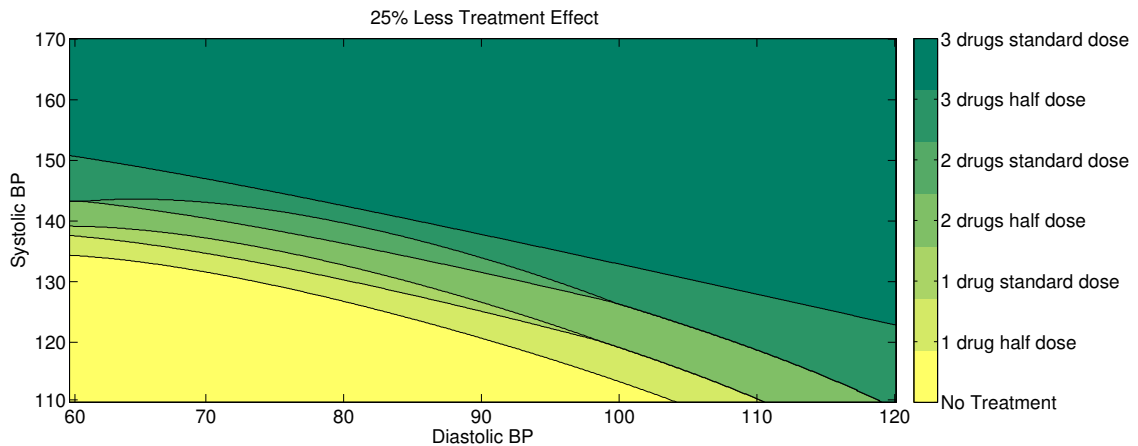


Figure 3.15: Optimal treatment decisions, treatment effect - 25%

3.6.6 Sensitivity to Length of Time to Achieve Treatment Benefit

In our main analysis we assume the almost full benefit of treatment is achieved within one year. Here we consider how the treatment decisions perform if the BP reduction

is instead achieved within different time intervals, anywhere within 3 months to 5 years. While we consider a wide range, here we only present the two extreme cases, corresponding to within 3 months and 5 years treatment benefit effect in Figures 3.16 and 3.17, respectively. Comparing these results with our base case results shows them to be quite similar. The corresponding losses in relative hazard are 0.004% and 0.13%, indicating that the time to achieve benefit of treatment is not critical to the policy, as long as the full benefit of treatment is achieved within the planning horizon T considered.

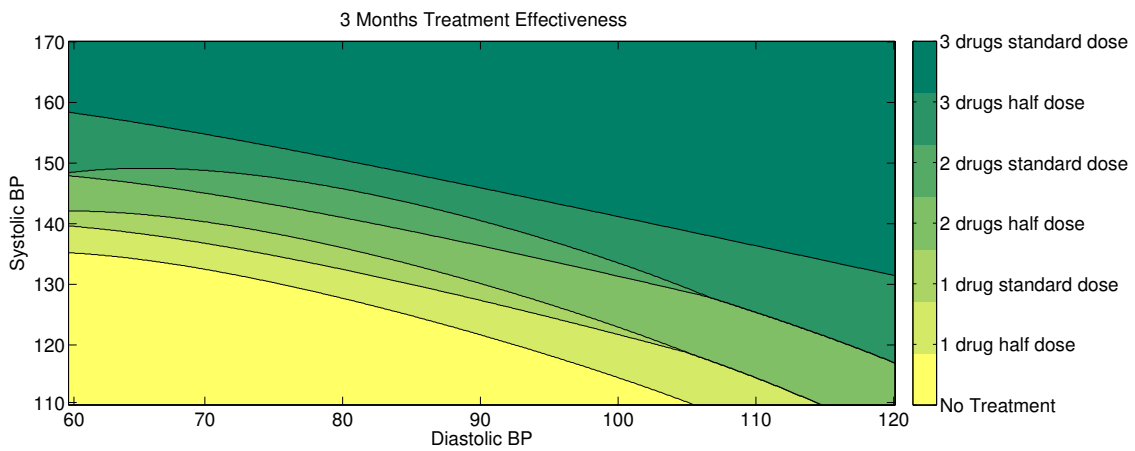


Figure 3.16: Optimal treatment decisions, treatment occurring in 3 months

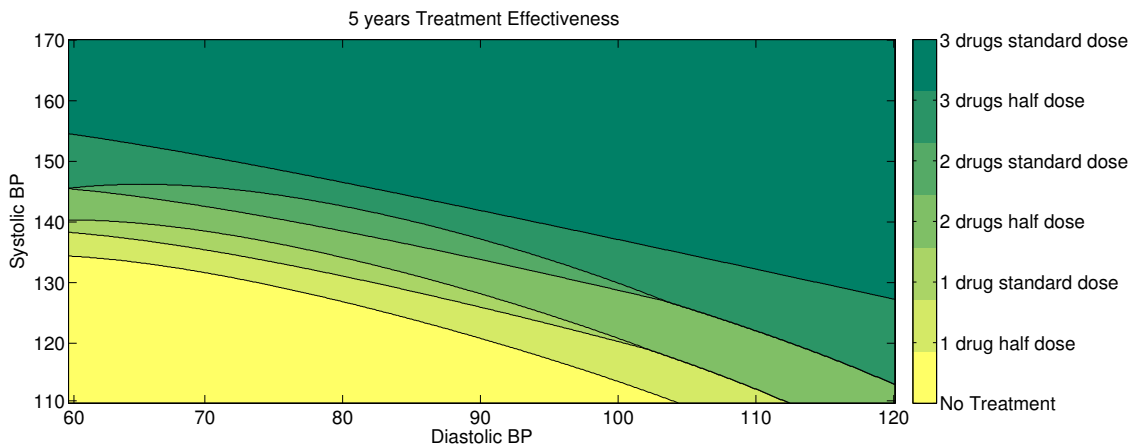


Figure 3.17: Optimal treatment decisions, treatment occurring in 5 years

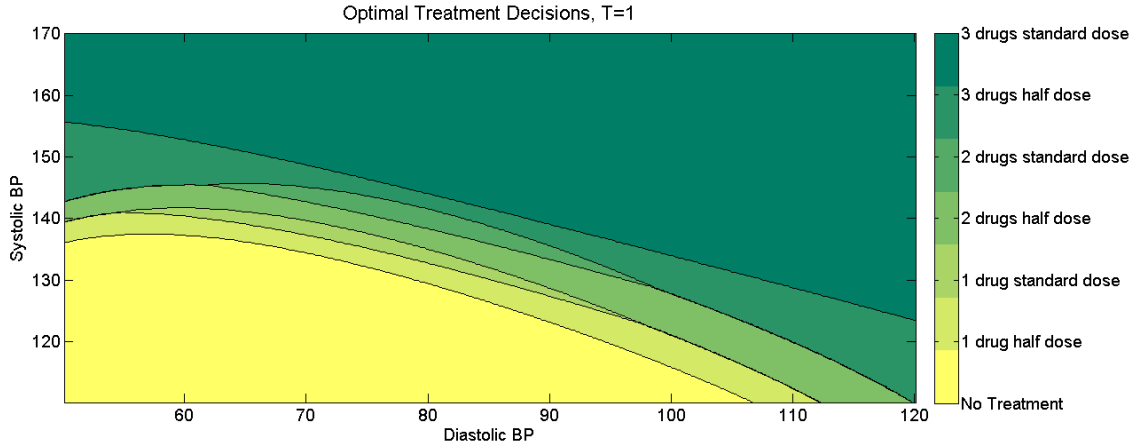


Figure 3.18: Optimal treatment decisions, $T=1$.

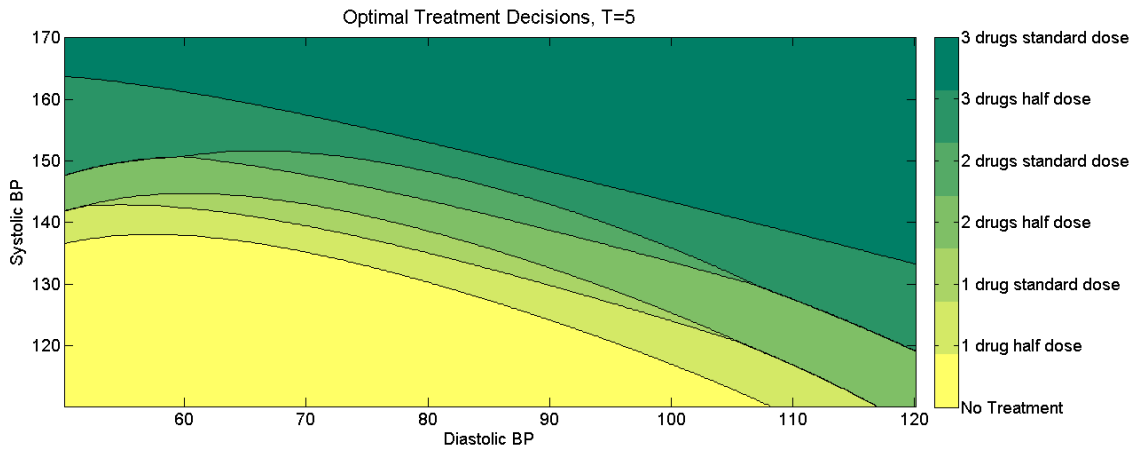


Figure 3.19: Optimal treatment decisions. $T=5$.

3.6.7 Sensitivity to Planning Horizon T

We find little change in treatment decision as the planning horizon T changes. For example, Figures 3.18 and 3.19 compare the optimal treatment policy under planning horizons $T = 1$ and $T = 5$ respectively, where we observe some small differences in the thresholds for initiating various treatment options, but overall the policy is similar as under the base case with $T = 10$. Treatment decisions made according to our policy induced average relative losses in achieved hazard of 0.26% and 0.04%, respectively. Therefore, we conclude that our results are not very sensitive to the planning horizon T .

3.7 Discussion and Conclusion

Among the principles recommended by the American Heart Association, the American College of Cardiology, and the Centers for Disease Control for creating an effective hypertension management algorithm are the following four [129]. First, to base the algorithm on best available science. Second, format the algorithm to be simple to update as better information becomes available. Third, the algorithm should have a feasible, simple implementation strategy. Finally, it should be developed in a format able to be incorporated into electronic health records for use as a clinical decision support tool.

Our model meets all of these recommendations. First, it has been built on the best available science, incorporating the best known results about BP change over time, risk of cardiovascular disease for a given BP, and the effects of antihypertensive treatment. Second, our model is simple to update as better information emerges. The expected average T -year hazard ratio is a simple arithmetic function of the parameterizations. If new data become available, the fitted parameters only need to be recalculated and optimal thresholds can be solved using Theorem 3. The model is easily updateable for new estimates of BP progression, CVD hazard ratio, or antihypertensive treatment benefit. This ease of calculation is a major advantage over MDP models that would require implementing the process and resolving if new information became available, a process requiring specialized expertise and significant computational effort. As mentioned previously, this algorithm is simple to implement. Despite the visual complexity of the expression of the expected hazard ratio in Theorem 3, it is a simple arithmetic expression. Calculation of the expected hazard ratio and 95% confidence interval using the radial basis function approach for each treatment option is near instantaneous on any modern computer. Finally, this algorithm can easily be incorporated into electronic health records as a decision support tool. Because of the

simplicity of calculation, any programming language or spreadsheet can calculate the hazard ratios for each treatment option. We stress that the calculation of confidence intervals makes this a decision support tool, and not a decision maker. Clinicians can weigh the relative benefit of each treatment against exogenous information such as patient preference, cost of treatment, comorbidities, and risk of side effects.

Our findings can help guide the design of future antihypertensive treatment RCTs. Given that it is not feasible to test all possible scenarios in RCT settings, our data-driven methods may prove helpful in identifying the promising scenarios, which could then be tested empirically through actual trials. In particular, our findings of a) initiation and intensification thresholds depending jointly on systolic and diastolic pressure, b) intensification thresholds standardizing clinical practice, and c) tradeoffs associated with treating mild isolated diastolic hypertension merit testing by RCTs, the gold standard of evidence. Specifically, our results indicate that a trial comparing outcomes in treated and untreated patients at moderate-high systolic and diastolic pressure but below JNC8 guidelines, such as 135/85, may yield benefit. Similarly, our treatment intensification thresholds suggest that patients at 145/90 should initiate 2 drugs standard dose, so this policy could be compared to initiating 1 drug standard dose as prescribed by JNC8. Such trials may provide evidence to verify our findings and improve health outcomes.

3.7.1 Limitations

Our work has various limitations due to data availability and necessary assumptions for computational tractability. Our parameterization of blood pressure change is based on the Framingham study, an older data source. This was necessary because it is the only clinical trial with longitudinal BP observations. In particular, we demonstrated that the change in BP per unit time is well modeled by a Gaussian mixture, but the majority of our inter-observation times were 2 year intervals. Therefore we

are unable to establish the model (3.1) is valid for all inter-observation times. The expectation maximization algorithm used to fit the GMM returns only a local solution. In particular, running the algorithm with different initial solutions or random seed results in different component mixtures. However, the mean and variance of the mixture distribution remains nearly the same, which are the only important features for our calculations. In addition, the model that we propose is general and can be easily recalibrated using other comprehensive datasets or subpopulations as they become available in the future.

Our assumption of perfect knowledge of blood pressure requires clinicians to take repeated measurements before implementing our solutions. This is simple to satisfy, as blood pressure would be measured several times in clinic or with an at home device to gather an accurate estimate before an antihypertensive regiment was initiated. All Framingham measurements were averages of several observation, so our progression model is built on perfect measurements of BP. This limitation does make the threshold inappropriate for use as a screening tool.

We have assumed hazard ratio is well fit by a second degree quadratic surface for computational tractability, and demonstrated sufficient statistical fit. Higher degree surfaces would render the necessary stochastic calculus calculations unwieldy. Our calculation of the average expected T -year hazard ratio assumes no future actions may be taken. Specifically, it assumes treatment must be initiated today or not at all. While this is a limitation, cardiovascular disease risk calculators adopt this same assumption, predicting 10-year risk based only on present measurements. In addition, we demonstrate in the simulation model that our policy outperforms existing clinical guidelines, even when future actions are possible.

In this study we optimized treatment decisions based solely on hazard ratio. Cost of treatment was not considered because it is extremely low. One year of generic BP treatment is estimated at \$212 and one cardiovascular event costs over \$ 10000

in hospitalization, rehabilitation, and long-term care [39], so even small reductions in risk are cost effective. The major trade-off considered is increased hazard ratio from over aggressive BP reduction due to the J-curve effect. Other side effects of BP treatment such as dizziness or fainting [131] and diuretic induced low potassium levels [132] should be considered qualitatively by practitioners when comparing the relative benefits of different treatment options and their associated confidence intervals.

3.7.2 Future Work and Conclusion

Future work should expand this model to include personalizable results. Currently, this model uses population level estimates of drift and variance of BP change. Algorithms that track an individual's BP and forecast future progression can be imbedded within our main result as an improvement over population level estimates. Such an algorithm could monitor trends within an individual and predict, for example, when a patient with presently controlled BP may be rapidly increasing and therefore wish to initiate treatment. Such algorithms could accommodate unequally spaced observations and could incorporate information from office, home, and ambulatory measurements. Future work could also consider applying this model to other continuous state health measurements with available control strategies, such as cholesterol, blood glucose level in diabetics, or body mass index.

We have presented a model that aids in the decision of initiating anti-hypertensive treatment. For a given current BP, the model exactly calculates the mean and variance of the average hazard ratio a patient will experience over the following T years under various treatment options. The model optimizes treatment by picking the treatment that results in the lowest risk adjusted hazard ratio. In addition, it calculates approximate confidence intervals so decision makers can weigh the relative benefits of treatment with exogenous information. The advantages of this model are the flexibility of handling BP as a continuous time, continuous state process, the simplicity

of calculation, and the ease of updating the model with new data. We hope this work may inspire future work in mathematical models of continuous health measurements.

CHAPTER 4

PERSONALIZED BLOOD PRESSURE MANAGEMENT

4.1 Introduction

Personalized medicine has become a prominent topic in recent history for its potential value to public health [133, 134, 135]. The term “personalized medicine” broadly refers to providing care according to the individual patient’s susceptibility to a disease, rate of disease progression, and response to specific treatment options [136]. Population level guidelines are built on aggregated results from randomized control trials. Yet, it is recognized that individuals respond differently to treatment due to biological, behavior, and life history characteristics [133]. With advances in big data, computational power, and algorithms, researchers and practitioners have recognized the value in personalized approaches in the management of chronic diseases.

In Chapter I, we discussed how wearables and other devices associated with the Internet of Things, collectively known as mobile health (mHealth), have the potential to revolutionize the management of chronic disease. Fitness trackers and smart watches measure and record vital measurements (VMs) such as pulse, heart rate variability, blood oxygenation, and blood sugar. In January 2018, Omron Healthcare debuted a wearable BP monitor that will enter the marketplace fall 2018 [50]. New mHealth devices offer access to unprecedented amounts of individual, patient-level data that are recorded at short intervals. Many of these technologies integrate with smartphones to provide data tracking and visualization. However, the analytics potential of these data remains largely unexplored [52].

As discussed in Chapter I, CVD is the leading cause of death both in the United States and worldwide [137] and has many controllable risk factors; therefore it is one

of the largest areas in which mHealth can improve health care [138]. Traditionally, BP was measured at annual clinical examinations and treatment was initiated in patients above a threshold value [36]. With the rise of mHealth, new opportunities exist for screening and monitoring BP in non-clinical settings [46]. In addition to the existing devices mentioned above, it is anticipated that by 2020 more wearables may be capable of blood pressure monitoring [51]. For these reasons, BP is an excellent candidate to study in an analytics framework. In this chapter we design analytics based tools and approaches for BP monitoring. While designed primarily for BP monitoring, we believe our proposed approaches could be generalizable to a variety of VMs.

A concern from the health community about mHealth is their highly noisy measurements due to mis-calibration or improper user training. For example, [139] found 30% of home blood pressure monitors exceeded 5 mm Hg error on average and were declared inaccurate according to FDA regulations. The problem is exacerbated by wearables - examining a popular unregulated consumer smartphone app for measuring BP, [140] found the mean absolute difference between true and reported BP was 12.4 mm Hg, which they refer to as ‘highly inaccurate’. While this is problematic for single uses of such technology, as long as the noise is unbiased (or we know the distribution of the noise), this problem is alleviated by the large number of observations typically collected by mHealth. Observations at the daily level, as provided by wearables and other technologies, can still provide accurate information about the VM when aggregated. Highly noisy daily measurements can lead to effective monitoring policies when statistical tests are designed to balance Type I/Type II errors.

In this chapter we propose statistical and mathematical methods that use measurements from wearables and other technologies to make screening decisions for chronic diseases. We propose changepoint detection-based algorithms that signal when the likelihood the VM of interest has exceeded some threshold value is high. Such a

signal may suggest the user follow up with a clinician for diagnosis and treatment options (for example, in the case of blood pressure or cholesterol) or take immediate action (for example, an elevated heart rate or low blood glucose level). We first design a Bayesian belief-based changepoint method that uses knowledge of the disease progression. Then, we develop a Naive changepoint procedure that is simpler and is applicable to a wide variety of VMs. Finally, we demonstrate the effectiveness of our algorithms on simulated blood pressure data and show the improvement in our algorithm over benchmark policies.

4.2 Literature Review

There are three broad literature areas relevant to our work: wearables, internet of things, and other emerging technologies for VMs; personalized screening in chronic diseases; and statistical process control and changepoint detection.

The medical community is cautiously optimistic about the potential of wearables to improve health in chronic disease populations [141, 142]. Studies demonstrating successes have included physical activity monitoring in patients with multiple sclerosis [143], rehabilitation in individuals with chronic conditions [144], obesity tracking [145], and heart failure self-care [146]. In a review of existing mobile apps, the American Heart Association (AHA) found “the evidence ... clearly demonstrates the great potential that mobile technologies can have” in cardiovascular disease prevention [147], yet they also found a lack of scientific rigor in evaluating the algorithms and technologies. In a recommendation on telehealth, the AHA said “the future of healthcare delivery will likely involve increased reliance on mobile computing (e.g., smartphones) that can support a variety of operating systems and healthcare applications (e.g., FDA-approved blood pressure monitors)” [148]. Reviews have remarked that “mobile health technologies offer promise with regard to the management and prevention of cardiovascular disease via risk factor modification” [149] and suggested

future research explore analytical methods for data analysis [150].

Personalized medicine has the potential to improve public health in the screening, monitoring, and treating of chronic disease [133, 134, 135]. Within cardiology, [151] uses a personalized chronotherapy approach to informing patients when throughout the day to take their antihypertensive treatment to achieve maximum BP reduction. [152] predict when a patient will attain or leave hypertension control based on current BP and comorbid conditions. [153] propose making treatment decisions for individuals on the basis of the difference in 10-year risk score taking or not taking antihypertensive treatment. [154] uses a Markov modeling approach and an imbedded risk score to make treatment decisions subject to budget constraints in a population setting. [155] uses clustering methods to categorize patients' BP progression into fixed trajectories. Personalized medicine has also found great success in oncology and cancer treatment [156]. Personalized approaches to cancer span the full care spectrum from risk stratification to prevention, screening, and therapy [157]. [158] develop a partially observable Markov decision model to find personalized optimal policies for mammography screenings. Targeted therapy based on genetic analysis has yielded improvement over population level treatment strategies [159]. In other domains, [160] use a stochastic model to create a personalized prediction of Glaucoma progression and decide the time until next screening. The contribution of this work is to design algorithms for monitoring BP from noisy observations and detecting when it has risen above a threshold.

Bayesian methods are useful for integrating information from multiple sources of noisy observations [161]. They have been used in many domains of science and engineering, such as decision theory [162], ecology [163], and finance [164, 165]. Within the medical decision making domain, they have explored cost effectiveness [166], integrated the findings from clinical studies [167, 168], and aided in decision support tools for cancer care [169, 170]. Specifically in cardiology, older studies have proposed

Bayesian approaches to classifying hypertension [171, 172, 173]. Those studies considered a fixed threshold for diagnosing hypertension and calculated positive predictive value of multiple observations using Bayes theorem. To our knowledge, no prior study has used Bayesian methods to construct belief of current pressure based on a longitudinal model of BP change and full history of observations. Our contribution is to provide such a model, basing our belief of current pressure on a statistically validated disease progression model and observational noise model.

Sequential analysis is concerned with testing two hypotheses in an on-line fashion with sequential observations. Changepoint detection is specifically concerned with detecting a change in the state of a process subject to a tolerable limit on the risk of false alarms [174]. Changepoint detection has been used in applications in computer network anomaly detection [175], climate data [176], and computer vision [177]. In the healthcare domain, changepoint detection has been used in infectious disease surveillance [178], diagnosing speech disorders [179], and monitoring surgery outcomes [180]. Changepoint detection has primarily been studied from an i.i.d. perspective, that is, sequential observations are independent and identically distributed. For our application, BP observations will be highly correlated, as pressure is serially correlated over time. This work expands the changepoint detection literature by developing methods for considering correlated observations.

4.3 Method

Without loss of generality, we are interested in detecting when the true VM exceeds some threshold K . All methods in this study can be easily adapted when the detection of interest is the VM decreasing below the threshold or leaving some interval. In this section we first present a Bayesian belief-based changepoint detection procedure in §4.3.1 that utilizes specific knowledge of the disease progression and observation error, and develop computationally efficient methods. A contribution of our Bayesian

Table 4.1: Notation in this Study

K	vital measurement threshold
x_t	true vital measurement at time t
y_t	noisy vital measurement at time t
σ^2	Variance of observation noise
p_t	probability true vital measurement at time t exceeds threshold K
S_t	test statistic at time t
b	test statistic decision threshold
Bayesian Changepoint §4.3.1	
w_i	mixture weights
μ_i	mixture means
L_i	mixture standard deviations
n	number of mixture components
f_{X_0}	the pdf of initial true BP
$f_{X_t,i}$	the pdf of true BP X_t at time t from mixture component i
$f_{Y_t,i}$	the pdf of observation Y_t at time t from mixture component i
$f_{\Delta,i}$	the pdf of change in BP per unit time from mixture component i
Naive Changepoint §4.3.2	
λ	allowance term for test statistic
Performance Evaluation §4.3.3	
Γ	time the algorithm declares a change has occurred
η_0	false alarm window
τ	first time the vital measurement exceeds the threshold K
ℓ	detection power window

change point procedure is to incorporate mixture models, which can capture a wide range of distributions. While our analyses find this method performs well, it requires perfect knowledge of the disease dynamics, which may not be reasonable in practice, and in addition we are forced to rely on simulation for calibrating the decision criteria. Motivated by these concerns, we present a naive change point detection algorithm in §4.3.2. This procedure is generalizable to many VMs and requires mild assumptions on the observation error but no explicit knowledge of the disease progression. The notation we use in this chapter is summarized in table 4.1.

4.3.1 Bayesian Belief Changepoint Detection

In this section we describe a Bayesian belief-based changepoint algorithm. Specifically, we model systolic BP as a continuous time, continuous space Gaussian mixture process and develop a Bayesian filtering procedure to model our belief of current true pressure from noisy measurements.

We model log systolic BP, denoted by $X_t = \log(\text{systolic BP}(t))$, as a mixture of Brownian motions as in Chapter 3:

$$dX_t = \sum_{i=1}^n w_i(\mu_i dt + L_i dB_t), \quad (4.1)$$

where w_i are the mixture weights, μ_i and L_i are the mean and standard deviation of change per unit time within each mixture component respectively, and B_t is a standard Brownian motion. Noisy observations of BP are gathered with some normally distributed random noise:

$$y_t = x_t + \epsilon_t, \quad (4.2)$$

where $\epsilon_t \sim N(0, \sigma^2)$.

We consider the following setup. Under the null hypothesis, the patient is healthy and the true BP is consistently below a threshold K . Alternatively, when the patient's blood pressure is elevated, there will be an unknown moment κ after which their BP will be constantly above K . We need to test between these two situations based on noisy observations. Formally, consider the following hypothesis test.

$$\begin{aligned} H_0 : X_i < K & \quad \forall i = 1, \dots, t, \\ H_1 : X_i < K, X_j > K & \quad \forall i = 1, \dots, \kappa, j = \kappa + 1, \dots, t \text{ for some } \kappa. \end{aligned}$$

Since we use this procedure in an online fashion, the belief of true pressure at time

t is dependent only on observations up until that time, and therefore

$$\mathbb{P}(X_1, \dots, X_t | Y_1, \dots, Y_t) = \mathbb{P}(X_1 | Y_1) \mathbb{P}(X_2 | Y_1, Y_2) \dots \mathbb{P}(X_t | Y_1, \dots, Y_t).$$

Our goal is to detect the changepoint κ of the true BP $\{X_t\}$ as soon as possible from a sequence of noisy observations $\{Y_t\}$. We next derive the likelihood ratio based detection procedure. For an assumed changepoint time $\kappa = k$, the log-likelihood of the hypothesis test can be written as

$$\begin{aligned} & \log \frac{\mathbb{P}(X_1 < K, \dots, X_k < K, X_{k+1} > K, X_t > K | Y_1, \dots, Y_t)}{\mathbb{P}(X_1 < K, \dots, X_t < K | Y_1, \dots, Y_t)} \\ &= \log \frac{\prod_{i=1}^k \mathbb{P}(X_i < K | Y_1, \dots, Y_i) \prod_{i=k+1}^t \mathbb{P}(X_i > K | Y_1, \dots, Y_i)}{\prod_{i=1}^t \mathbb{P}(X_i < K | Y_1, \dots, Y_i)} \\ &= \sum_{i=k+1}^t \log \frac{\mathbb{P}(X_i > K | Y_1, \dots, Y_i)}{1 - \mathbb{P}(X_i > K | Y_1, \dots, Y_i)}, \end{aligned} \tag{4.3}$$

due to cancellation of the first k terms. Define the Bayesian log-odds ratio at time t as

$$O_t = \log \frac{\mathbb{P}(X_t > K | Y_1, \dots, Y_t)}{1 - \mathbb{P}(X_t > K | Y_1, \dots, Y_t)}.$$

Hence, the likelihood ratio based changepoint detection procedure can be derived by maximizing with respect to the unknown k . This leads to the following detection procedure that stops the first time it hits a pre-specified threshold b :

$$T_{\text{Bayesian}} = \inf\{t \geq 1 : \max_{1 \leq k \leq t} \sum_{i=k+1}^t O_i \geq b\}.$$

Notice that the computation of the procedure amounts to computing the posterior probability O_t at each time. Alternatively, we can recursively implement this proce-

ture, which has a similar structure to the CUSUM:

$$T_{\text{Bayesian}} = \inf\{t \geq 1 : S_t \geq b, \quad S_t = \max\{S_{t-1} + O_t, 0\}, S_0 = 0\}.$$

Note that the log-odds ratio under the null hypothesis tends to be negative, and under the alternative hypothesis tends to be positive. Hence, when a patient's true BP is under K the test statistic will tend to stay small, and when the true BP is over K it will tend to increase linearly.

Bayesian filtering

In the following, we describe how to compute the Bayesian belief and $\mathbb{P}(X_t > K | Y_1, \dots, Y_t)$ in an efficient manner. Define

f_{X_0} - the pdf of initial true BP.

$f_{X_t,i}$ - The pdf of true BP X_t at time t from mixture component i .

$f_{Y_t,i}$ - The pdf of observation Y_t at time t from mixture component i .

$f_{\Delta,i}$ - The pdf of change in BP per unit time from mixture component i .

f_ϵ - The pdf of the observation error ϵ .

We can compute the Bayesian posterior belief of true pressure x_t given observations y_1, \dots, y_t under the i th mixture component as:

$$\begin{aligned} & f_{X_t,i}(x_t | y_1, \dots, y_t) \\ & \propto \int_{-\infty}^{\infty} \dots \int_{-\infty}^{\infty} f_{X_0}(x_0) \left(\prod_{j=1}^t f_{\Delta,i}(x_j - x_{j-1}) \right) \left(\prod_{j=1}^t f_{Y_j,i}(y_j | x_j) \right) dx_0 dx_1 \dots dx_{t-1} \\ & = f_{Y_t,i}(y_t | x_t) \int_{-\infty}^{\infty} \dots \int_{-\infty}^{\infty} f_{X_0}(x_0) \left(\prod_{j=1}^{t-1} f_{\Delta,i}(x_j - x_{j-1}) f_{Y_j,i}(y_j | x_j) \right) \\ & \qquad \qquad \qquad f_{\Delta,i}(x_t - x_{t-1}) dx_0 dx_1 \dots dx_{t-1} \\ & \propto f_\epsilon(y_t - x_t) \int_{-\infty}^{\infty} f_{X_{t-1},i}(x_{t-1} | y_1, \dots, y_{t-1}) f_{\Delta,i}(x_t - x_{t-1}) dx_{t-1}. \end{aligned} \tag{4.4}$$

We maintain this belief separately for each mixture component i . This calcula-

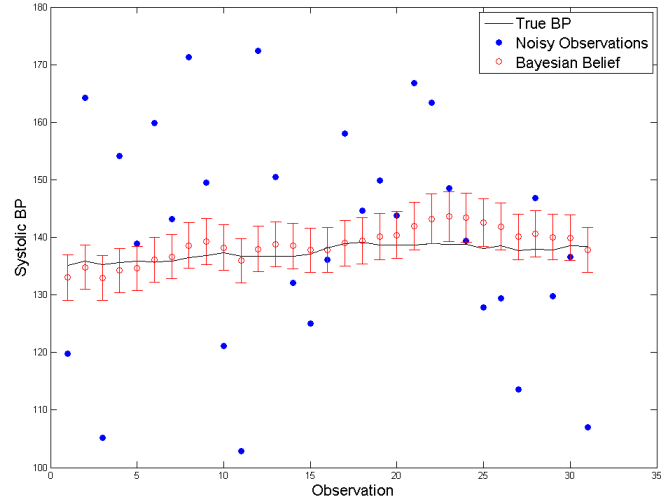
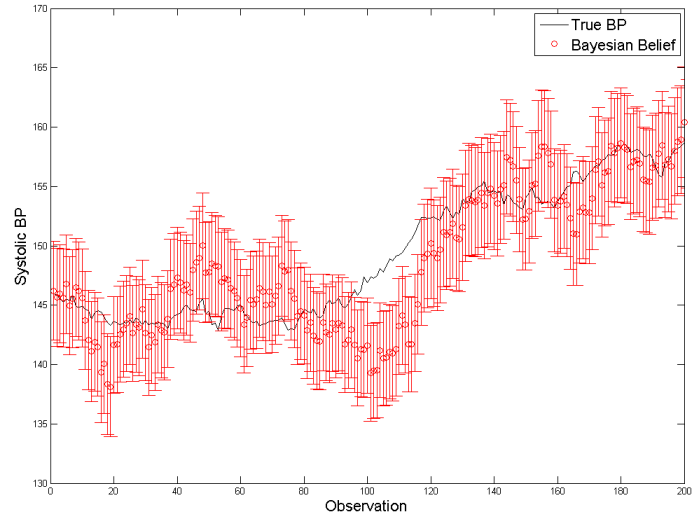


Figure 4.1: Result of Bayesian filtering (Left) complete path; (Right) Zoom-in.

tion requires low computational effort, utilizing the prior distribution and a single integration. (4.4) says the posterior belief of this period's true pressure is found by integrating the prior belief and transition probability, multiplied by the likelihood of noisy observations from this period. See Figure 4.1 for an example of this filter operating on noisy BP observations. This figure demonstrates that even with highly noisy observations we can create accurate belief of true BP.

The tail probability of threshold exceedance for each mixture component is easily calculated by integrating the tail of the Bayesian posterior belief:

$$\hat{p}_{t,i} = \int_K^\infty f_{X_t,i}(x_t|y_1, \dots, y_t) dx_t. \quad (4.5)$$

The aggregate tail probability is constructed from the mixture weights:

$$\hat{p}_t = \sum_{i=1}^n w_i \hat{p}_{t,i}. \quad (4.6)$$

Finally, the test statistic S_t is constructed as:

$$S_t = \max[0, S_{t-1} + \log(\frac{\hat{p}_t}{1 - \hat{p}_t})]. \quad (4.7)$$

For an overview of the steps of the Bayesian changepoint algorithm, see figure 4.2 and the following algorithm:

Algorithm 1 Bayesian algorithm for BP changepoint detection

Inputs: Threshold b

Initialization: Initial belief f_{X_0}

- 1: Gather noisy observation y_t .
 - 2: Compute Bayesian posterior belief within each component according to (4.4).
 - 3: Compute tail probability $\hat{p}_{t,i}$ within each component with (4.5).
 - 4: Compute aggregate tail probability \hat{p}_t with (4.6).
 - 5: Compute test statistic S_t with (4.7).
 - 6: Signal a change has occurred if $S_t \geq b$, otherwise return to step 1.
-

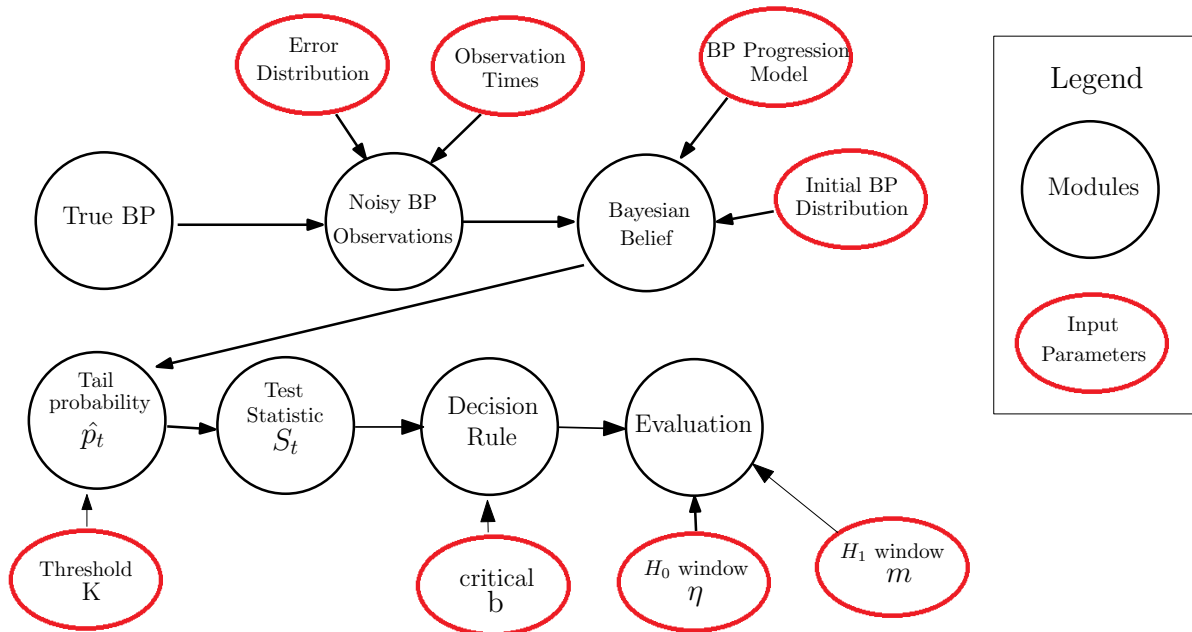


Figure 4.2: Bayesian Changepoint Detection Procedure

4.3.2 Naive CUSUM Changepoint

In this section, we develop a procedure that does not require assumptions on the VM progression, making it relevant to a wide variety of applications. Specifically, we assume the observations are i.i.d., which ignores the temporal correlation between the observations. As we explain below, while this i.i.d. assumption does not hold in practice, it provides bounds on the performance when the true VM is temporally correlated. We further demonstrate that we achieve good performance using it on simulated BP observations. Our only assumption in this section is that the observation noise is normally distributed with mean 0 and variance σ^2 . This assumption can be easily relaxed to allow the noise to follow any distribution with known parameters.

Our goal is as follows: we are interested in detecting when the true VM is above K , and not detecting a change when the true VM is below $K - \delta$. Thus, the minimal

change of interest is δ . We formally define our hypotheses:

$$\begin{aligned} \mathbf{H}_0 : X_i &= K - \delta & \forall i = 1, \dots, t, \\ \mathbf{H}_1 : X_i &= K - \delta, X_j = K & \forall i = 1, \dots, \kappa, j = \kappa + 1, \dots, t \text{ for some } \kappa. \end{aligned}$$

From this setup, we can derive a naive algorithm, based on the following intuition. When there is no change (true VM is $K - \delta$), the probability of the observed VM exceeding the threshold K will be small. On the other hand, when there is a change (true VM is K), the probability that the observed BP exceeding K will be significantly larger. Hence, we can monitor the likelihood using a cumulative sum (CUSUM) procedure. As we will show later on, this simple algorithm has reasonably good performance, and its theoretical performances can be well calibrated. The algorithm is as follows:

Algorithm 2 Naive algorithm for BP changepoint detection

Inputs: Threshold b

Initialization: Set

$$\lambda = \frac{0.5 + \Phi\left(\frac{-\delta/\sigma}{\sqrt{2}}\right)}{2}$$

- 1: Gather noisy observation y_t .
- 2: Compute

$$p_t = \Phi\left(\frac{y_t - K}{\sigma}\right), \tag{4.8}$$

where $\Phi()$ is the CDF of the standard normal distribution.

- 3: Compute

$$S_t = \max[0, S_{t-1} + p_t - \lambda]. \tag{4.9}$$

- 4: Signal a change has occurred if $S_t \geq b$, otherwise return to step 1.
-

The intuition of this algorithm is based around the distribution of p_t . As we formally prove in Theorem 5 below, the expected value of p_t is 0.5 under the alternate hypothesis (true VM is K), and is $\Phi\left(\frac{-\delta/\sigma}{\sqrt{2}}\right)$ under the null hypothesis (true VM is $K - \delta$). By choosing the allowance term λ as the midpoint between these expectations, the expectation of $p_t - \lambda$ is positive under the alternate hypothesis and hence S_t tends

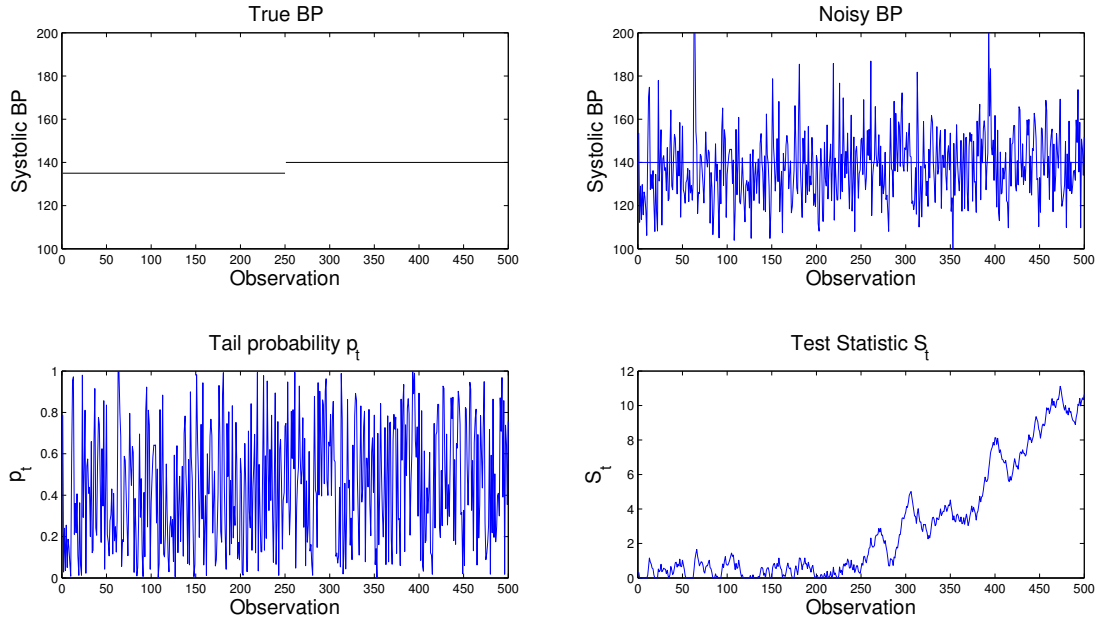


Figure 4.3: Example sample path. Upper left: true blood pressure. Upper right: Noisy observations of blood pressure. Lower left: tail probabilities calculated from (4.8). Lower right: Test statistic calculated from (4.9).

to linearly increase, while the expectation is negative under the null hypothesis and S_t tends to stay close to 0.

For an example of these statistics with $K = 140\text{mm Hg}$ and $\delta = 5\text{mm Hg}$, see figure 4.3. From observation 1 to 250, the true BP is 135 mm Hg, and the test statistic S_t stays close to 0. From observations 251 to 500, the true BP is 140 mm Hg, and the test statistic linearly increases.

The fundamental tradeoff in the design of any statistical process control problems is between false alarms, that is, the algorithm declaring the VM above the threshold when the true value is below the threshold, and detection power, correctly declaring the VM above the threshold when it truly is. The typical performance evaluation with i.i.d. samples are average run length (ARL) and detection delay (DD), the mean number of observations until a change has been declared under the null or alternate hypotheses, respectively. That is, ARL is the mean number of observations until the algorithm declares a patient's VM is above the threshold when the true

VM is below the threshold, and DD is the mean number of observations until the algorithm declares a patient's VM is above the threshold when the true VM is above the threshold.

Theorem 5. *Following the Naive algorithm, the average run length is approximately*

$$ARL = \frac{e^{\delta^*c} - \delta^*c - 1}{(\delta^*)^2/2}(1 + o(1)),$$

and the detection delay is approximately

$$DD = \frac{e^{-\delta^*c} + \delta^*c - 1}{(\delta^*)^2/2}(1 + o(1)),$$

where

$$\delta^* = \frac{0.5 - \Phi\left(\frac{-\delta/\sigma}{2}\right)}{s},$$

$$c = \frac{b}{s} + 1.166,$$

$$s = \sqrt{\frac{1/12 + \Phi\left(\frac{-\delta/\sigma}{\sqrt{2}}\right) - \Phi\left(\frac{-\delta/\sigma}{\sqrt{2}}\right)^2 - 2T\left(\frac{-\delta/\sigma}{\sqrt{2}}, \frac{1}{\sqrt{3}}\right)}{2}},$$

and $T(\cdot, \cdot)$ is Owen's T function [181].

Proof. We first examine the moments of p_t under the null and alternate hypotheses.

To do so, we first note that if $X \sim N(\mu, \sigma^2)$ and c and d are constants,

$$\begin{aligned} E\left[\Phi\left(\frac{X+c}{d}\right)\right] &= \int \frac{1}{\sigma} \phi\left(\frac{x-u}{\sigma}\right) \Phi\left(\frac{x+c}{d}\right) dx \\ &= \int \phi(x) \Phi\left(\frac{\sigma x + \mu + c}{d}\right) dx \\ &= \Phi\left(\frac{\mu + c}{\sqrt{\sigma^2 + d^2}}\right), \end{aligned}$$

where ϕ and Φ are the pdf and cdf of the normal distribution respectively, and

$$\begin{aligned} E[\Phi(\frac{X+c}{d})^2] &= \int \frac{1}{\sigma} \phi(\frac{x-u}{\sigma}) \Phi(\frac{x+c}{d})^2 dx \\ &= \int \phi(x) \Phi(\frac{\sigma x + \mu + c}{d})^2 dx \\ &= \Phi(\frac{\mu+c}{\sqrt{\sigma^2+d^2}}) - 2T(\frac{\mu+c}{\sqrt{\sigma^2+d^2}}, \frac{d}{\sqrt{2\sigma^2+d^2}}). \end{aligned}$$

Therefore, under the alternate hypothesis that the VM is equal to K ,

$$E_1[p_t] = \Phi(\frac{0}{\sqrt{2}}) = 0.5,$$

and

$$Var_1[p_t] = \Phi(\frac{0}{\sqrt{2}}) - 2T(\frac{0}{\sqrt{2}}, \frac{1}{\sqrt{3}}) - \Phi(\frac{0}{\sqrt{2}})^2 = \frac{1}{12}.$$

Under the null hypothesis that the VM is equal to $K - \delta$,

$$E_0[p_t] = \Phi(\frac{-\delta/\sigma}{\sqrt{2}}),$$

and

$$Var_0[p_t] = \Phi(\frac{-\delta/\sigma}{\sqrt{2}}) - 2T(\frac{-\delta/\sigma}{\sqrt{2}}, \frac{1}{\sqrt{3}}) - \Phi(\frac{-\delta/\sigma}{\sqrt{2}})^2.$$

The remainder of the algorithm is a traditional CUSUM approach, see for example [182]. Since traditional CUSUM methods assume a constant variance, we define s^2 as the average of the variance under the null and alternate hypotheses, similar to as λ is defined as the average expected value. Even though the p_t are not normally distributed under either hypothesis, the CUSUM approach does not require the normality assumption. \square

Our computational analyses show that these approximations are quite accurate.

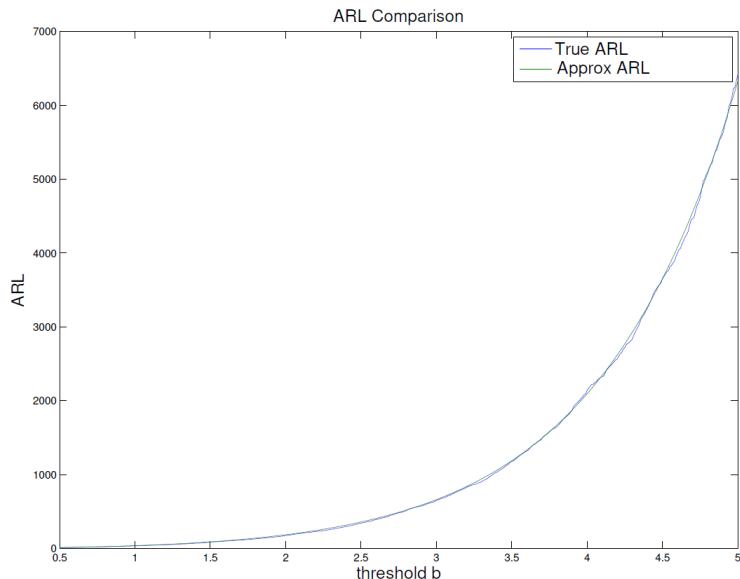


Figure 4.4: Naive Changepoint Procedure ARL

See figures 4.4 and 4.5 for comparison of the true and approximate ARL and DD for the BP problem, respectively.

When the VM dynamically progresses in a more complex form than the step function of the hypotheses presented above, the run length statistics of Theorem 5 provide a bound on the algorithm performance. When the true VM is at least δ below the threshold K , the average run length is at least that presented in Theorem 5, and when the true VM is greater than or equal to K , the detection delay is at most that from the theorem. This implies the run lengths in the theorem are worst case analyses, and the decision threshold b can be chosen using these as a conservative measure. For an example of these statistics on simulated BP with $K = 140\text{mm Hg}$ and $\delta = 5\text{mm Hg}$, see figure 4.6. As expected, at the start when true BP is below the threshold of 140, the test statistic S_t stays very close to 0, despite nonzero tail probabilities p_t owing to measurement noise. When true BP approaches the threshold around observation 150, the test statistic S_t begins to rise but stays low, reflecting the weak evidence BP is above 140. When true BP experiences a sustained shift above

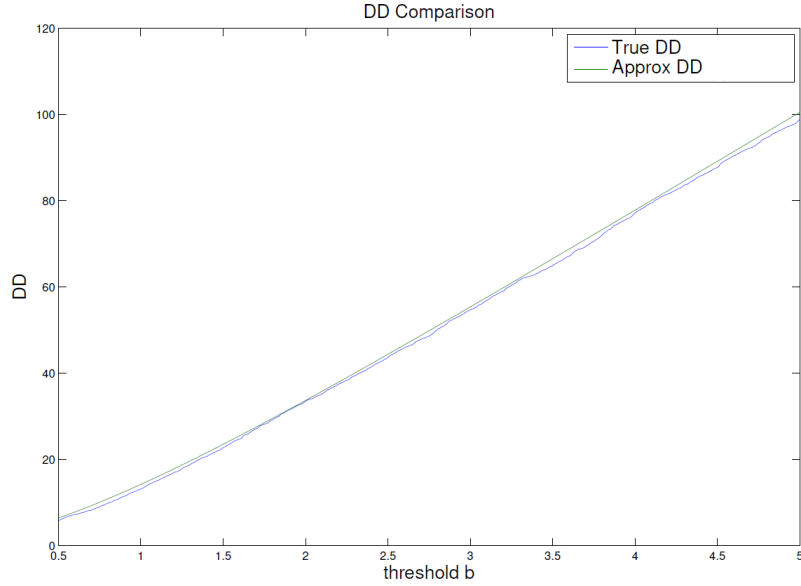


Figure 4.5: Naive Changepoint Procedure DD

the threshold around observation 250 , the test statistic increases linearly.

4.3.3 Performance Evaluation

In this section we describe the criteria for evaluating decision rules under either changepoint algorithm proposed above. When observations are i.i.d. under either hypothesis, the ARL and DD are sensible evaluation criteria, as the process signals with probability 1 and the ARL is finite. In the non-i.i.d. case that we face here, this is not necessarily true - for example, consider a VM with a negative drift over time. Then, with positive probability the process never signals, and thus the ARL is infinite. To overcome this limitation, we consider false alarm and detection rates as described in the following paragraphs.

To examine false alarm rates, we are interested in studying $P_{H_0}(\Gamma < \eta_0)$, where Γ is the time the changepoint process signals and η_0 is a fixed length of time, for example 1 year. This quantity represents the probability that we give a false signal within this length of time when the process is in control, that is, true VM is under

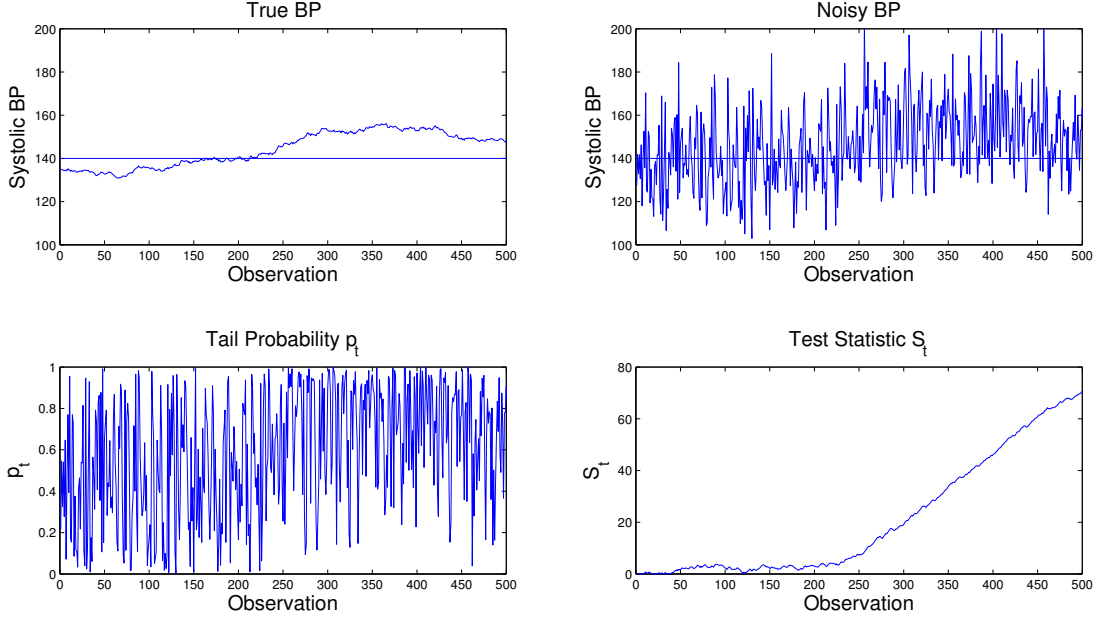


Figure 4.6: Example sample path. Upper left: simulated true blood pressure. Upper right: Noisy observations of blood pressure. Lower left: tail probabilities calculated from (4.8). Lower right: Test statistic calculated from (4.9).

K.

To examine detection power, we are interested in $P_{H_1}(\Gamma < \tau + \ell | \Gamma > \tau)$, where τ is the true changepoint time. This expression is the probability that the change is detected within ℓ additional observations given that it has not been detected by the true changepoint.

Note there is a natural connection between ARL and alarm rates in the i.i.d. case - [183] show an approximation to the probability of false alarm $P_{H_0}(\Gamma < \eta_0)$ is related to the ARL by:

$$P_{H_0}(\Gamma < \eta_0) \approx 1 - e^{-\eta_0/ARL}. \quad (4.10)$$

4.4 Numerical Results

In this section we conduct a numerical study on simulated BP data to demonstrate the efficiency of our algorithms. We simulate systolic BP of 10,000 patients for 10 years using (4.1). Patients have initial BP 135 mm Hg and we are interested in

detecting an exceedance of threshold 140 mm Hg. Observations are gathered once a day. The false alarm window η_0 was set to 10 years. Parameter estimates for the progression model were identical to chapter III. The observation noise was estimated from [140], who conducted a validation of the Instant Blood Pressure Smartphone App, a smartphone based application which measures blood pressure. They found the application highly inaccurate, reporting a mean absolute difference between the BP measured from this app and standard calibrated automated sphygmomanometer reading of 12.4 for systolic BP. The results of this section may therefore be conservative, and we may expect better performance of our methods as the accuracy of the wearable measurements improves with further development.

The ROC curve for various choices of threshold b for detection window $m = 3$ months, 6 months, and 1 year are seen in figures 4.7, 4.8, and 4.9 respectively. The numerical results are seen in table 4.2. We make several observations about these results. First, the Bayesian changepoint algorithm of §4.3.1 is quite accurate. Considering a detection window of 1 year, the AUC is 0.8887, and if we are willing to accept a 50% chance of a false alarm within 10 years, we attain a detection rate of 89.0%. Second, the Naive changepoint of §4.3.2 is accurate but slightly underperforms compared to the Bayesian algorithm in terms of AUC and detection probability given false alarm chance of 50% across all detection windows considered (3 months, 6 months, 1 year). From the ROC curves, we observe the Bayesian approach performs at least as well as the Naive approach for nearly all fixed probabilities of false alarm. Third, the improvement in the Bayesian procedure over the Naive is greater for smaller detection windows. The Bayesian method induces a 3.2% relative improvement in AUC for 3 months detection window, but only a 0.15% relative improvement for 1 year detection window. This indicates the Bayesian method is faster to detect changes than the Naive method. Finally, both procedures are quite effective - the mean true BP at time the process signals was 140.6 for the Bayesian approach and

140.8 for the Naive approach for $m = 1$ year, indicating the process tends to signal near the desired threshold.

We note that the selection of initial BP of 135 mm Hg, quite close to the threshold of 140 mm Hg relative to the range of BP seen in patients, makes these performance results conservative to what we would see in practice. Users with lower true BP, for example 120 mm Hg, would produce test statistic S_t nearly always 0, resulting in very few false alarms. Similarly, users with significantly elevated BP, for example 155 mm Hg, would produce tail probabilities \hat{p}_t near to 1 and would result in rapid detection. An ancillary simulation study with the same parameters as above except user's initial BP sampled randomly from a data-driven distribution of population BP levels resulted in ROC values of 0.9836 and 0.9807 for the Bayesian and Naive algorithms, respectively. In addition, when false alarms do occur, the true VM tends to be close to the threshold - the average true BP when a false alarm was signaled was 137.8 mm Hg for the Bayesian algorithm. This is advantageous, since the threshold is not a firm cutoff - that is, there is likely to be benefit in recommending a patient with true BP close to but not exceeding the threshold to a physician for preventive care.

A baseline policy that signals the process is out of control when the weekly sample mean exceeds the threshold K resulted in $PH_0 = 0.9971, PH_1 = 1$. This indicates such a decision rule is extremely prone to type I errors : for example, when the true systolic BP is 135 mm Hg, the 7-day sample mean will exceed the threshold of 140 mm Hg with probability 0.2196, indicating a type I error occurs less than every 5 weeks on average. Such a policy's performance is unacceptable and would lead to increased burden on the healthcare system handling these false positives.

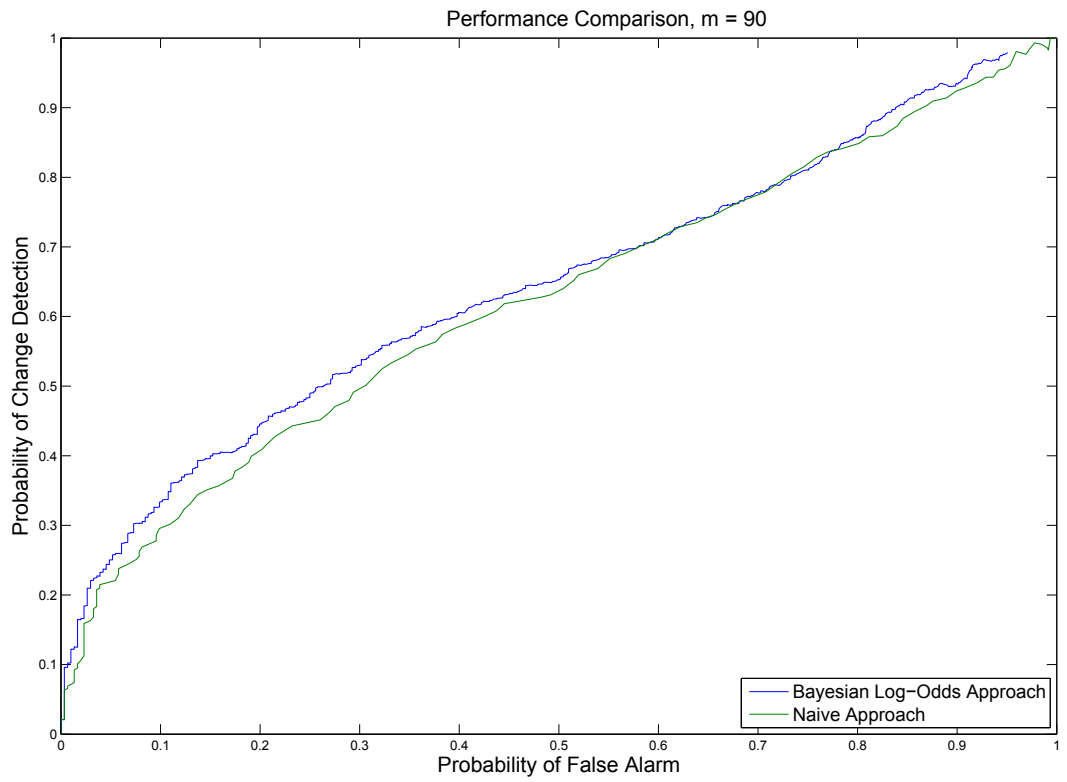


Figure 4.7: ROC Changepoint Detection Performance, $m = 90$

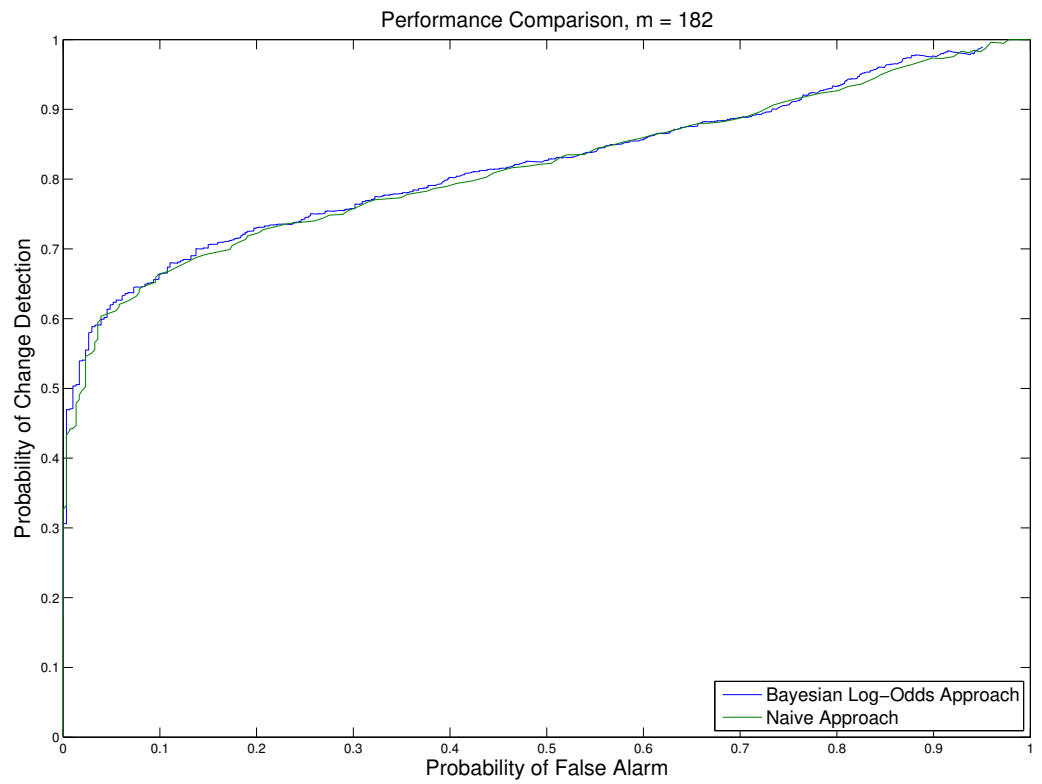


Figure 4.8: ROC Changepoint Detection Performance, $m = 182$

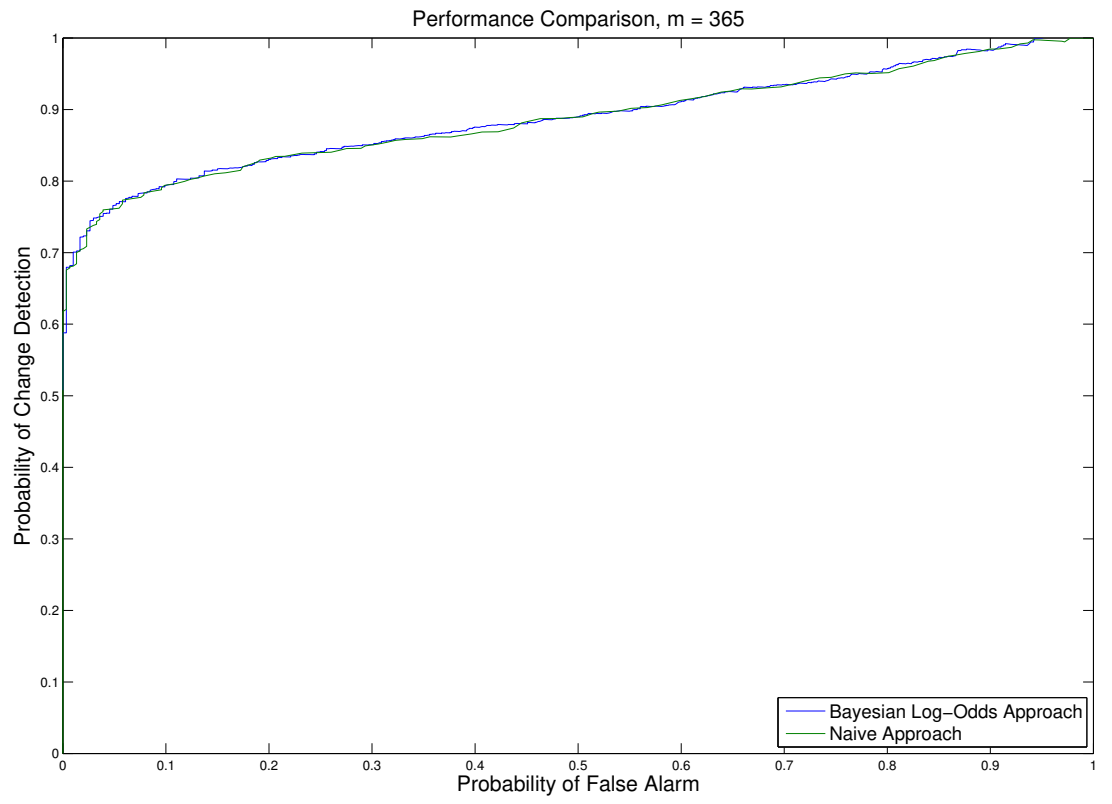


Figure 4.9: ROC Changepoint Detection Performance, $m = 365$

Table 4.2: BP Changepoint Detection Performance Statistics

	Bayesian Changepoint	Naive Changepoint
m = 90 days		
AUC	0.6444	0.6243
$PH_1 PH_0 = 0.5$	0.6525	0.6370
m = 182 days		
AUC	0.8203	0.8158
$PH_1 PH_0 = 0.5$	0.8266	0.8220
m = 365 days		
AUC	0.8887	0.8873
$PH_1 PH_0 = 0.5$	0.8901	0.8893

4.5 Discussion and Conclusion

In a recent review in the American Journal of Medicine, [184] lay out a vision reengineering health care delivery by 2020 to combat chronic disease. Among their recommendations, they are optimistic mHealth can positively affect healthy lifestyles and chronic disease management. The work in this chapter develops an analytics framework to statistically monitor vital measurements and indicate when the probability the measurement has exceeded some threshold is high. The changepoint detection algorithms presented in this study utilize the frequent observations from mHealth to signal the user when a sustained increase in the VM has occurred. These algorithms are applicable to a wide variety of VMs, such as cholesterol, glucose level, and heart rate.

The Bayesian changepoint algorithm of §4.3.1 was found to be highly accurate. The AUC of 0.8887 for one year detection window suggests this procedure can be effective for detecting shifts in the VM above the threshold and balancing risks of type I and type II error. The tradeoffs with this method are the added assumptions and computational effort required. The disease progression is assumed to be known and parameters fitted. Due to the correlation structure of the belief and test statistic, run length approximations are not easy to obtain in an analytical form. Therefore choos-

ing the decision threshold b to achieve some desired performance requires simulating the process, a computational and coding burden.

The naive changepoint algorithm of §4.3.2 overcomes some of these challenges at the cost of slightly decreased performance. The AUC of 0.8873 is slightly lower than the Bayesian AUC, and this difference increases for smaller detection windows. This approach is advantageous for several reasons: First, it is generalizable to any VM we are interested in tracking. Second, the approach requires minimal assumptions. No specific disease progression model was assumed. The only requirement is the assumption of observation noise being normally distributed with mean zero and known variance, but this is easily relaxed if the error follows some other known distribution or has a nonzero mean. If the variance is unknown, it can be estimated during some warm-up period before the process begins tracking the VM for changes. Finally, the algorithm is computationally simple and can be computed near-instantaneously with little formal coding.

We reiterate that the numerical results presented are conservative compared to what we would see in practice. The initial BP of 135 mm Hg is very close to the threshold of 140 mm Hg, resulting in increased type I errors. For example, a user with true BP of 120 mm Hg would almost never generate a false alarm. Similarly, a user with a highly elevated BP, for example 150 mm Hg, would almost certainly generate an out of control signal very rapidly. In our simulations, the mean true BP when a false signal was generated was 137.8 mm Hg, quite close to the threshold. In this context the threshold is a soft target, so recommending a user with BP quite close to the threshold consult their physician is still useful and not an egregious error.

Implementing these algorithms in practice will face additional challenges in trending and seasonality of the data. Blood pressure is known to follow a Circadian rhythm, being lowest at 3:00am, rising to its highest point mid-morning, then steadily decreasing throughout the remainder of the day [185]. In addition, BP varies based on season,

temperature, and hours of daylight [186]. Therefore the mHealth observations must be carefully considered with time stamps and adjusted with detrending methods. In addition, the mode of observation and associated stress levels must be considered. Even after accounting for time of day, it is reasonable to expect that, for example, data collected from car seat sensors driving in rush hour traffic would yield higher BP measurements due to stress than those obtained from a patient seated on the couch watching television. With proper detrending and normalizing, measurements from several sources could be aggregated to monitor the VM using all available data.

These results could be expanded to consider trends in individual's BP progression as well. Keeping within the changepoint detection framework, two monitoring statistics could be run side by side. The first is as described in this chapter, tracking when an individual's pressure has risen above the 140 mm Hg threshold. The second statistic would also be a changepoint detection statistic, but focused on the trend in pressure progression. That is, it would track how an individual's pressure was changing over time and signal if the trend deviated from the population level trend. That way, even if an individual's pressure was well below the threshold, say 120 mm Hg, but rising at an alarming rate, the individual would be notified to diagnose the problem and consider remedial steps. These side by side statistics could track both pressure level and change in pressure to give a more complete picture of an individual's BP.

A second approach, deviating from the changepoint detection approach of this chapter, is inspired by the prognostics literature for machine systems. Prognostics aims to predict the remaining useful life of a machine with noisy observations and historical data [187, 188]. For the BP problem, this would mean predicting when an individual is likely to cross the 140 mm Hg threshold from their noisy BP measurements. Such an approach is compatible with the framework of the mixture model for BP progression we have presented by capturing a Bayesian belief of progression distribution. For example, [189] proposes a method that updates the parameters of

the mixture components the observation is most likely to come from in a Bayesian fashion, and [190] proposes a sliding window approach to keep only the most recent observations in memory. One proposed method could incorporate the advantages of each approach. The first time seeing a patient, we would assume their BP progression follows population estimates. As we begin to gather observations, our predictions of their BP progression would incorporate these observations and forget the population level estimates. After we have gathered sufficiently many observations (dependent on the window size), the population estimates would have no impact and predictions would be based solely on the individual's observations. Such an approach would allow us to incorporate both estimates of true pressure and estimates of BP progression to estimate how long until an individual crosses the threshold.

CHAPTER 5

CONCLUSION

5.1 Summary

This thesis has developed tools from probability and stochastics, optimization, statistics, data science, and simulation in the operations research domain to explore issues in blood pressure management for reducing risk of cardiovascular disease, optimizing treatment decisions, and monitoring blood pressure from mobile health technologies.

In chapter II we improved cardiovascular disease risk prediction models by adding a novel predictor, antecedent blood pressure, into the model. These models were constructed and validated on the Framingham Offspring data set, the largest and longest running longitudinal study of blood pressure and cardiovascular disease. We demonstrated models with antecedent systolic pressure significantly outperformed models with current systolic pressure. When antecedent pressure was included in the model, adding current pressure did not improve the predictions, implying antecedent pressure alone was a better predictor than antecedent plus current pressure. We further demonstrated that addition of a categorical variable indicating antecedent hypertension did not improve a model with current pressure, demonstrating the importance of complete data records. These findings were robust against other measures of blood pressure and other baseline prediction dates. This work demonstrated the importance of a time integrated measure of blood pressure as a predictor of cardiovascular disease.

Motivated by the results of chapter II, chapter III developed a population level optimal policy for antihypertensive treatment decisions. The fundamental tradeoff was dictated by the J-curve effect, implying that over aggressive treatment can lower

blood pressure below optimal levels and increase risk. We used the Framingham Original cohort to fit a continuous time, continuous state stochastic process to model change in population blood pressure over time. We fit an estimate of cardiovascular disease hazard ratio of blood pressure from a large diverse population and the effects of antihypertensive treatment from a meta-analysis of randomized control trials. From these we derived an analytical expression of expectation and variance of T-year hazard ratio experienced by an individual initiating an antihypertension treatment. We used a mean-variance optimization model to pick the treatment option minimizing risk adjusted hazard ratio. We derived systolic and diastolic thresholds for initiation and intensification of various dosages of antihypertension treatment. In a large scale simulation model we demonstrated the improvement of our policy over existing clinical guidelines and predicted an estimated additional 15,100 premature deaths could be averted every year. Finally, we used radial basis functions to construct approximate confidence intervals on the experienced hazard ratio under different treatment options. These results suggest randomized control trials that could be run to examine treatment strategies and may be used in a decision support tool.

Chapter IV developed two changepoint detection algorithms for monitoring blood pressure from wearables and other mobile health technologies. The Bayesian method used knowledge of disease progression and maintained a belief of current pressure. The method was quite accurate, but faces parameter fitting and computational challenges in practice. To overcome these challenges, a Naive changepoint detection method was proposed that uses only the measurement error distribution. This method was simple to implement and calibrate, and still accurate but slightly less than the Bayesian approach. These methods demonstrate the value of measurements from mobile health technology in monitoring vital measurements such as cholesterol, glucose level, and pulse in the management of chronic disease.

REFERENCES

- [1] M. Heron, “Deaths: Leading causes for 2014”, *National Vital Statistics Report*, vol. 65, no. 5, pp. 1–94, 2016.
- [2] WHO, “Global status report on noncommunicable disease 2014”, *World Health Organization*, 2015.
- [3] D. Mozaffarian, E. J. Benjamin, A. S. Go, D. K. Arnett, M. J. Blaha, M. Cushman, S. R. Das, S. de Ferranti, J.-P. Després, H. J. Fullerton, *et al.*, “Executive summary: Heart disease and stroke statistics-2016 update: A report from the american heart association.”, *Circulation*, vol. 133, no. 4, p. 447, 2016.
- [4] World Health Organization, *Cardiovascular diseases (cvds)*, [Online; accessed 23-September-2016], 2016.
- [5] American Heart Association, *What is cardiovascular disease?*, [Online; accessed 23-September-2016], 2016.
- [6] B. J. Powers, M. K. Olsen, V. A. Smith, R. F. Woolson, H. B. Bosworth, and E. Z. Oddone, “Measuring blood pressure for decision making and quality reporting: Where and how many measures?”, *Annals of internal medicine*, vol. 154, no. 12, pp. 781–788, 2011.
- [7] US Preventive Services Task Force, “Screening for high blood pressure: US Preventive Services Task Force reaffirmation recommendation statement”, *Annals of Internal Medicine*, vol. 147, pp. 783–786, 2007.
- [8] Y. Jin, R. Bies, M. R. Gastonguay, N. Stockbridge, J. Gobburu, and R. Madabushi, “Misclassification and discordance of measured blood pressure from patient’s true blood pressure in current clinical practice: A clinical trial simulation case study”, *Journal of Pharmacokinetics and Pharmacodynamics*, vol. 39, no. 3, pp. 283–294, 2012.
- [9] J Hodgkinson, J Mant, U Martin, B Guo, F. Hobbs, J. Deeks, C Heneghan, N Roberts, and R. McManus, “Relative effectiveness of clinic and home blood pressure monitoring compared with ambulatory blood pressure monitoring in diagnosis of hypertension: Systematic review”, *BMJ*, vol. 342, p. d3621, 2011.
- [10] M. A. Piper, C. V. Evans, B. U. Burda, K. L. Margolis, E. O’Connor, and E. P. Whitlock, “Diagnostic and predictive accuracy of blood pressure screening methods with consideration of rescreening intervals: a systematic review for

- the US Preventive Services Task Force”, *Annals of Internal Medicine*, vol. 162, no. 3, pp. 192–204, 2015.
- [11] H. O. Dickinson, J. M. Mason, D. J. Nicolson, F. Campbell, F. R. Beyer, J. V. Cook, B. Williams, and G. A. Ford, “Lifestyle interventions to reduce raised blood pressure: A systematic review of randomized controlled trials”, *Journal of Hypertension*, vol. 24, no. 2, pp. 215–233, 2006.
- [12] L. J. Appel, C. M. Champagne, D. W. Harsha, L. S. Cooper, E. Obarzanek, P. J. Elmer, V. J. Stevens, W. M. Vollmer, P.-H. Lin, L. P. Svetkey, *et al.*, “Effects of comprehensive lifestyle modification on blood pressure control: main results of the PREMIER clinical trial”, *JAMA: Journal of the American Medical Association*, 2003.
- [13] H. B. Bosworth, M. K. Olsen, A. Neary, M. Orr, J. Grubber, L. Svetkey, M. Adams, and E. Z. Oddone, “Take Control of Your Blood Pressure (TCYB) study: a multifactorial tailored behavioral and educational intervention for achieving blood pressure control”, *Patient Education and Counseling*, vol. 70, no. 3, pp. 338–347, 2008.
- [14] A. Bitton and T. Gaziano, “The Framingham Heart Study’s impact on global risk assessment”, *Progress in Cardiovascular Diseases*, vol. 53.1, pp. 68–78, 2010.
- [15] W. B. Kannel, T. R. Dawber, A. Kagan, N. Revotskie, and J. Stokes, “Factors of risk in the development of coronary heart disease six-year follow-up experience: the Framingham Study”, *Annals of Internal Medicine*, vol. 55, no. 1, pp. 33–50, 1961.
- [16] J. Truett, J. Cornfield, and W. Kannel, “A multivariate analysis of the risk of coronary heart disease in Framingham”, *Journal of Chronic Diseases*, vol. 20, no. 7, pp. 511–524, 1967.
- [17] M Krikke, R. Hoogeveen, A. Hoepelman, F. Visseren, and J. Arends, “Cardiovascular risk prediction in HIV-infected patients: comparing the Framingham, atherosclerotic cardiovascular disease risk score (ASCVD), Systematic Coronary Risk Evaluation for the Netherlands (SCORE-NL) and Data Collection on Adverse Events of Anti-HIV Drugs (D: A: D) risk prediction models”, *HIV Medicine*, 2015.
- [18] N. S. Gale, M. M. Munnery, N. Chapman, D. J. Shale, and J. R. Cockcroft, “The Framingham risk score in chronic obstructive pulmonary disease (COPD)”, *Journal of the American Society of Hypertension*, vol. 9, no. 4, e30, 2015.

- [19] D. C. Goff, D. M. Lloyd-Jones, G. Bennett, S. Coady, R. B. D’Agostino, R. Gibbons, P. Greenland, D. T. Lackland, D. Levy, C. J. O’Donnell, *et al.*, “2013 ACC/AHA guideline on the assessment of cardiovascular risk: a report of the American College of Cardiology / American Heart Association Task Force on Practice Guidelines”, *Journal of the American College of Cardiology*, vol. 63, no. 25_PA, 2014.
- [20] Framingham Heart Study, *Original cohort*, [Online; accessed 5-September-2016], 2016.
- [21] Framingham Heart Study, *Offspring cohort*, [Online; accessed 5-September-2016], 2016.
- [22] W. B. Kannel, T. Gordon, and M. J. Schwartz, “Systolic versus diastolic blood pressure and risk of coronary heart disease: the Framingham study”, *The American Journal of Cardiology*, vol. 27.4, pp. 335–346, 1971.
- [23] I. M. G. Stewart, “Relation of reduction in pressure to first myocardial infarction in patients receiving treatment for severe hypertension”, *Lancet*, vol. 1979, pp. 861–5,
- [24] E. P. Tsika, L. Poulimenos, K. D. Boudoulas, and A. J. Manolis, “The J-curve in arterial hypertension: fact or fallacy?”, *Cardiology*, vol. 129, pp. 126–135, 2014.
- [25] F. Boutitie, F. Gueyffier, S. Pocock, R. Fagard, and J. P. Boissel, “J-shaped relationship between blood pressure and mortality in hypertensive patients: New insights from a meta-analysis of individual-patient data”, *Annals of Internal Medicine*, vol. 136, no. 6, pp. 438–448, 2002.
- [26] PROGRESS Collaborative Group, “Randomised trial of a perindopril-based blood-pressure-lowering regimen among 6105 individuals with previous stroke or transient ischaemic attack”, *The Lancet*, vol. 358, no. 9287, pp. 1033–1041, 2001.
- [27] G. Mancia and G. Grassi, “Aggressive blood pressure lowering is dangerous: the J-curve pro side of the argument”, *Hypertension*, vol. 63.1, pp. 29–36, 2014.
- [28] J. J. Sim, J. Shi, C. P. Kovesdy, K. Kalantar-Zadeh, and S. J. Jacobsen, “Impact of achieved blood pressures on mortality risk and end-stage renal disease among a large, diverse hypertension population”, *Journal of the American College of Cardiology*, vol. 64, no. 6, pp. 588–597, 2014.
- [29] P. Sleight, J. Redon, P. Verdecchia, G. Mancia, P. Gao, R. Fagard, H. Schumacher, M. Weber, M. Böhm, B. Williams, *et al.*, “Prognostic value of blood

- pressure in patients with high vascular risk in the Ongoing Telmisartan Alone and in combination with Ramipril Global Endpoint Trial study”, *Journal of Hypertension*, vol. 27, no. 7, pp. 1360–1369, 2009.
- [30] C. P. Kovesdy, A. J. Bleyer, M. Z. Molnar, J. Z. Ma, J. J. Sim, W. C. Cushman, L. D. Quarles, and K. Kalantar-Zadeh, “Blood pressure and mortality in US veterans with chronic kidney disease: a cohort study”, *Annals of Internal Medicine*, vol. 159, no. 4, pp. 233–242, 2013.
- [31] C. J. Pepine, E. M. Handberg, R. M. Cooper-DeHoff, R. G. Marks, P. Kowey, F. H. Messerli, G. Mancina, J. L. Cangiano, D. Garcia-Barreto, M. Keltai, *et al.*, “A calcium antagonist vs a non-calcium antagonist hypertension treatment strategy for patients with coronary artery disease: the International Verapamil-Trandolapril Study (INVEST): a randomized controlled trial”, *JAMA*, vol. 290, no. 21, pp. 2805–2816, 2003.
- [32] S. Bangalore, F. H. Messerli, C.-C. Wun, A. L. Zuckerman, D. DeMicco, J. B. Kostis, J. C. LaRosa, *et al.*, “J-curve revisited: an analysis of blood pressure and cardiovascular events in the Treating to New Targets (TNT) Trial”, *European Heart Journal*, ehq328, 2010.
- [33] E. M. Lonn, J. Bosch, P. López-Jaramillo, J. Zhu, L. Liu, P. Pais, R. Diaz, D. Xavier, K. Sliwa, A. Dans, *et al.*, “Blood-pressure lowering in intermediate-risk persons without cardiovascular disease”, *New England Journal of Medicine*, vol. 374, no. 21, pp. 2009–2020, 2016.
- [34] B. Divison-Garrote, J. R. Banegas, and J. J. De la Cruz, “Hypotension based on office and ambulatory monitoring blood pressure. prevalence and clinical profile among a cohort of 70,997 treated hypertensives”, *Journal of the American Society of Hypertension*, 2016.
- [35] J. J. Sim, J. Shi, C. P. Kovesdy, K. Kalantar-Zadeh, and S. J. Jacobsen, “Impact of achieved blood pressures on mortality risk and end-stage renal disease among a large, diverse hypertension population”, *Journal of the American College of Cardiology*, vol. 64, no. 6, pp. 588–597, 2014.
- [36] P. A. James, S. Oparil, B. L. Carter, W. C. Cushman, C. Dennison-Himmelfarb, J. Handler, D. T. Lackland, M. L. LeFevre, T. D. MacKenzie, O. Ogedegbe, *et al.*, “2014 evidence-based guideline for the management of high blood pressure in adults: report from the panel members appointed to the Eighth Joint National Committee (JNC 8)”, *JAMA*, vol. 311, no. 5, pp. 507–520, 2014.
- [37] G De Backer, E Ambrosioni, K Borch-Johnsen, C Brotons, R Cifkova, J Dal-longeville, S Ebrahim, O Faergeman, I Graham, G Mancina, *et al.*, “Third Joint Task Force of European and other Societies on Cardiovascular Disease

Prevention in Clinical Practice. European guidelines on cardiovascular disease prevention in clinical practice”, *European Heart Journal*, vol. 24, no. 17, pp. 1601–1610, 2003.

- [38] D. M. Cutler, G. Long, E. R. Berndt, J. Royer, A.-A. Fournier, A. Sasser, and P. Cremieux, “The value of antihypertensive drugs: A perspective on medical innovation”, *Health affairs*, vol. 26, no. 1, pp. 97–110, 2007.
- [39] N. K. Choudhry, A. R. Patrick, E. M. Antman, J. Avorn, and W. H. Shrank, “Cost-effectiveness of providing full drug coverage to increase medication adherence in post–myocardial infarction Medicare beneficiaries”, *Circulation*, vol. 117, no. 10, pp. 1261–1268, 2008.
- [40] A. E. Moran, M. C. Odden, A. Thanataveerat, K. Y. Tzong, P. W. Rasmussen, D. Guzman, L. Williams, K. Bibbins-Domingo, P. G. Coxson, and L. Goldman, “Cost-effectiveness of hypertension therapy according to 2014 guidelines”, *New England Journal of Medicine*, vol. 372, no. 5, pp. 447–455, 2015.
- [41] D. S. SHARMA, “Drugs used for the cure of high blood pressure (review)”, *International Journal of Scientific Research*, vol. 4, no. 8, 2016.
- [42] M. Law, N. Wald, J. Morris, and R. Jordan, “Value of low dose combination treatment with blood pressure lowering drugs: Analysis of 354 randomised trials”, *BMJ*, vol. 326, no. 7404, p. 1427, 2003.
- [43] M. Law, J. Morris, and N. Wald, “Use of blood pressure lowering drugs in the prevention of cardiovascular disease: Meta-analysis of 147 randomised trials in the context of expectations from prospective epidemiological studies”, *BMJ*, vol. 338, b1665, 2009.
- [44] P. Marinov, K. Georgiev, and M. Georgieva, “Some aspects of the modern antihypertensive drug therapy and most common side effects”, *Scripta Scientifica Pharmaceutica*, vol. 2, no. 1, pp. 7–14, 2015.
- [45] M. G. Myers, M. Godwin, M. Dawes, A. Kiss, S. W. Tobe, and J. Kaczorowski, “Measurement of blood pressure in the office”, *Hypertension*, vol. 55, no. 2, pp. 195–200, 2010.
- [46] E. M. Goldberg and P. D. Levy, “New approaches to evaluating and monitoring blood pressure”, *Current hypertension reports*, vol. 18, no. 6, pp. 1–7, 2016.
- [47] Consumer Technology Association, “Record year ahead: consumer enthusiasm for connectivity to propel tech industry to record-setting revenues, says CTA 2017”, 2017.

- [48] G. Strumolo, *Your car will take your blood pressure*, Ford, Ed., [Online; accessed 15-September-2016], 2013.
- [49] T. Smilkstein, M. Buenrostro, A. Kenyon, M. Lienemann, and G. Larson, “Heart rate monitoring using kinect and color amplification”, in *Healthcare Innovation Conference (HIC), 2014 IEEE*, IEEE, 2014, pp. 60–62.
- [50] D. Takahashi, *Omron Healthcare shows off wearable blood pressure monitor for your wrist*, VentureBeat, Ed., [Online; accessed 22-February-2018], 2018.
- [51] E. J. Topol, S. R. Steinhubl, and A. Torkamani, “Digital medical tools and sensors”, *Jama*, vol. 313, no. 4, pp. 353–354, 2015.
- [52] L. Piwek, D. A. Ellis, S. Andrews, and A. Joinson, “The rise of consumer health wearables: Promises and barriers”, *PLoS Med*, vol. 13, no. 2, e1001953, 2016.
- [53] SPRINT Research Group and others, “A randomized trial of intensive versus standard blood-pressure control”, *New England Journal of Medicine*, vol. 2015, no. 373, pp. 2103–2116, 2015.
- [54] D. Wood, G. De Backer, O. Faergeman, I. Graham, G. Mancia, and K. Pyörälä, “Prevention of coronary heart disease in clinical practice: Summary of recommendations of the Second Joint Task Force of European and other Societies on Coronary Prevention”, *The European Journal of General Practice*, vol. 5, no. 4, pp. 154–161, 1999.
- [55] R. B. D’Agostino, R. S. Vasan, M. J. Pencina, P. A. Wolf, M. Cobain, J. M. Massaro, and W. B. Kannel, “General cardiovascular risk profile for use in primary care: the Framingham Heart Study”, *Circulation*, vol. 117, no. 6, pp. 743–753, 2008.
- [56] H. Sasai, T. Sairenchi, F. Irie, E. Otaka, H. Iso, K. Tanaka, H. Ota, and T. Muto, “Long-term exposure to elevated blood pressure and mortality from cardiovascular disease in a Japanese population: the Ibaraki Prefectural Health Study”, *Hypertension Research*, vol. 34, no. 1, pp. 139–144, 2011.
- [57] N. Allen, J. D. Berry, H. Ning, L. Van Horn, A. Dyer, and D. M. Lloyd-Jones, “Impact of blood pressure and blood pressure change during middle age on the remaining lifetime risk for cardiovascular disease: The cardiovascular lifetime risk pooling project”, *Circulation*, vol. 125, no. 1, pp. 37–44, 2012.
- [58] R. S. Vasan, J. M. Massaro, P. W. Wilson, S. Seshadri, P. A. Wolf, D. Levy, and R. B. D’Agostino, “Antecedent blood pressure and risk of cardiovascular

- disease: The Framingham Heart Study”, *Circulation*, vol. 105, no. 1, pp. 48–53, 2002.
- [59] C. Höcht, F. M. Bertera, and C. A. Taira, “Importance of blood pressure variability in the assessment of cardiovascular risk and benefits of antihypertensive therapy”, *Expert Review of Clinical Pharmacology*, vol. 3, no. 5, pp. 617–621, 2010.
- [60] G. Parati, J. E. Ochoa, P. Salvi, C. Lombardi, and G. Bilo, “Prognostic value of blood pressure variability and average blood pressure levels in patients with hypertension and diabetes”, *Diabetes Care*, vol. 36, no. Supplement 2, S312–S324, 2013.
- [61] D. S. Lee, J. M. Massaro, T. J. Wang, W. B. Kannel, E. J. Benjamin, S. Kenchaiah, D. Levy, R. B. D’Agostino, and R. S. Vasan, “Antecedent blood pressure, body mass index, and the risk of incident heart failure in later life”, *Hypertension*, vol. 50, no. 5, pp. 869–876, 2007.
- [62] N. H. Lung and B. Institute, “Framingham Heart Study-Offspring Data Dictionary”, Tech. Rep.
- [63] D. Machin, Y. B. Cheung, and M. K. Parmar, “Cox’s proportional hazards model”, *Survival Analysis: A Practical Approach, Second Edition*, pp. 121–153, 2006.
- [64] M. J. Pencina and R. B. D’Agostino, “Overall C as a measure of discrimination in survival analysis: model specific population value and confidence interval estimation”, *Statistics in Medicine*, vol. 23, no. 13, pp. 2109–2123, 2004.
- [65] M. J. Pencina, R. B. D’Agostino, and R. S. Vasan, “Evaluating the added predictive ability of a new marker: from area under the ROC curve to reclassification and beyond”, *Statistics in Medicine*, vol. 27, no. 2, pp. 157–172, 2008.
- [66] S. S. Franklin, V. A. Lopez, N. D. Wong, G. F. Mitchell, M. G. Larson, R. S. Vasan, and D. Levy, “Single versus combined blood pressure components and risk for cardiovascular disease: the Framingham Heart Study”, *Circulation*, vol. 119, no. 2, pp. 243–250, 2009.
- [67] N. S. Beckett, R. Peters, A. E. Fletcher, J. A. Staessen, L. Liu, D. Dumitrascu, V. Stoyanovsky, R. L. Antikainen, Y. Nikitin, C. Anderson, *et al.*, “Treatment of hypertension in patients 80 years of age or older”, *New England Journal of Medicine*, vol. 358, no. 18, pp. 1887–1898, 2008.

- [68] T. Ayer, O. Alagoz, and N. K. Stout, “OR forum-a POMDP approach to personalize mammography screening decisions”, *Operations Research*, vol. 60, no. 5, pp. 1019–1034, 2012.
- [69] J. Zhang, B. T. Denton, H. Balasubramanian, N. D. Shah, and B. A. Inman, “Optimization of prostate biopsy referral decisions”, *Manufacturing & Service Operations Management*, vol. 14, no. 4, pp. 529–547, 2012.
- [70] G. J. Schell, W. J. Marrero, M. S. Lavieri, J. B. Sussman, and R. A. Hayward, “Data-driven markov decision process approximations for personalized hypertension treatment planning”, *MDM Policy & Practice*, vol. 1, no. 1, p. 2 381 468 316 674 214, 2016.
- [71] O. Alagoz, L. M. Maillart, A. J. Schaefer, and M. S. Roberts, “The optimal timing of living-donor liver transplantation”, *Management Science*, vol. 50, no. 10, pp. 1420–1430, 2004.
- [72] B. Sandıkçı, L. M. Maillart, A. J. Schaefer, O. Alagoz, and M. S. Roberts, “Estimating the patient’s price of privacy in liver transplantation”, *Operations Research*, vol. 56, no. 6, pp. 1393–1410, 2008.
- [73] B. T. Denton, M. Kurt, N. D. Shah, S. C. Bryant, and S. A. Smith, “Optimizing the start time of statin therapy for patients with diabetes”, *Medical Decision Making*, vol. 29, no. 3, pp. 351–367, 2009.
- [74] M. Kurt, B. T. Denton, A. J. Schaefer, N. D. Shah, and S. A. Smith, “The structure of optimal statin initiation policies for patients with type 2 diabetes”, *IIE Transactions on Healthcare Systems Engineering*, vol. 1, no. 1, pp. 49–65, 2011.
- [75] S. M. Shechter, M. D. Bailey, A. J. Schaefer, and M. S. Roberts, “The optimal time to initiate HIV therapy under ordered health states”, *Operations Research*, vol. 56, no. 1, pp. 20–33, 2008.
- [76] A. Tsoukalas, T. Albertson, and I. Tagkopoulos, “From data to optimal decision making: A data-driven, probabilistic machine learning approach to decision support for patients with sepsis”, *JMIR medical informatics*, vol. 3, no. 1, e11, 2015.
- [77] J. Chhatwal, O. Alagoz, and E. S. Burnside, “Optimal breast biopsy decision-making based on mammographic features and demographic factors”, *Operations Research*, vol. 58, no. 6, pp. 1577–1591, 2010.

- [78] H. D. Sesso, R. S. Chen, J. Gilbert, P. Lapuerta, W. C. Lee, and R. J. Glynn, “Blood pressure lowering and life expectancy based on a Markov model of cardiovascular events”, *Hypertension*, vol. 42, no. 5, pp. 885–890, 2003.
- [79] V. Fontil, K. Bibbins-Domingo, D. S. Kazi, S. Sidney, P. G. Coxson, R. Khanna, R. G. Victor, and M. J. Pletcher, “Simulating strategies for improving control of hypertension among patients with usual source of care in the United States: the blood pressure control model”, *Journal of General Internal Medicine*, vol. 30, no. 8, pp. 1147–1155, 2015.
- [80] K. Lovibond, S. Jowett, P. Barton, M. Caulfield, C. Heneghan, F. R. Hobbs, J. Hodgkinson, J. Mant, U. Martin, B. Williams, *et al.*, “Cost-effectiveness of options for the diagnosis of high blood pressure in primary care: A modelling study”, *The Lancet*, vol. 378, no. 9798, pp. 1219–1230, 2011.
- [81] M. C. Weinstein, P. G. Coxson, L. W. Williams, T. M. Pass, W. B. Stason, and L. Goldman, “Forecasting coronary heart disease incidence, mortality, and cost: the Coronary Heart Disease Policy Model”, *American Journal of Public Health*, vol. 77, no. 11, pp. 1417–1426, 1987.
- [82] J. E. Mason, B. T. Denton, N. D. Shah, and S. A. Smith, “Optimizing the simultaneous management of blood pressure and cholesterol for type 2 diabetes patients”, *European Journal of Operational Research*, vol. 233, no. 3, pp. 727–738, 2014.
- [83] R. Ibrahim, B. Kucukyazici, V. Verter, M. Gendreau, and M. Blostein, “Designing personalized treatment: An application to anticoagulation therapy”, *Production and Operations Management*, vol. doi 10.1111/poms.12514, 2015.
- [84] M Zargoush, M Gumus, V Verter, and S Daskalopoulou, “Designing individualized therapy for patients with hypertension”, 2016.
- [85] C. C. L. Epstein, “An analytics approach to hypertension treatment”, PhD thesis, Massachusetts Institute of Technology, 2014.
- [86] A. K. Wills, D. A. Lawlor, F. E. Matthews, A. A. Sayer, E. Bakra, Y. Ben-Shlomo, M. Benzeval, E. Brunner, R. Cooper, M. Kivimaki, *et al.*, “Life course trajectories of systolic blood pressure using longitudinal data from eight UK cohorts”, *PLoS Med*, vol. 8, no. 6, e1000440, 2011.
- [87] G. J. Schell, “Personalized medicine in chronic disease management”, PhD thesis, University of Michigan, 2015.

- [88] H. Garnier and P. C. Young, “The advantages of directly identifying continuous-time transfer function models in practical applications”, *International Journal of Control*, vol. 87, no. 7, pp. 1319–1338, 2014.
- [89] B. A. Craig and P. P. Sendi, “Estimation of the transition matrix of a discrete-time markov chain”, *Health Economics*, vol. 11.1, pp. 33–42, 2002.
- [90] L. Ljung, “Experiments with identification of continuous time models”, *IFAC Proceedings Volumes*, vol. 42, no. 10, pp. 1175–1180, 2009.
- [91] D. Bertsimas, A. O’Hair, S. Relyea, and J. Silberholz, “An analytics approach to designing combination chemotherapy regimens for cancer”, *Management Science*, vol. 62, no. 5, pp. 1511–1531, 2016.
- [92] D. M. Negoescu, K. Bimpikis, M. L. Brandeau, D. A. Iancu, *et al.*, “Dynamic learning of patient response types: An application to treating chronic diseases”, 2017.
- [93] T. Rolski, H. Schmidli, V. Schmidt, and J. Teugels, *Stochastic processes for insurance and finance*. John Wiley & Sons, 2009, vol. 505.
- [94] J.-P. Bouchaud and D. Sornette, “The Black-Scholes option pricing problem in mathematical finance: generalization and extensions for a large class of stochastic processes”, *Journal de Physique I*, vol. 4.6, pp. 863–881, 1994.
- [95] D. Lamberton and B. Lapeyre, *Introduction to stochastic calculus applied to finance*. CRC press, 2007.
- [96] S. E. Shreve, *Stochastic calculus for finance II: Continuous-time models*. Science & Business Media: Springer, 2004, vol. 11.
- [97] J. E. Helm, M. S. Lavieri, M. P. Van Oyen, J. D. Stein, and D. C. Musch, “Dynamic forecasting and control algorithms of glaucoma progression for clinician decision support”, *Operations Research*, vol. 63, no. 5, pp. 979–999, 2015.
- [98] P. Kazemian, J. E. Helm, M. S. Lavieri, J. Stein, and M. P. Van Oyen, “Dynamic monitoring and control of irreversible chronic diseases with application to glaucoma”, *Available at SSRN*, 2016.
- [99] A. Sabouri, W. T. Huh, and S. M. Shechter, “Screening strategies for patients on the kidney transplant waiting list”, *Operations Research*, 2017.
- [100] Q. Cao, E. Buskens, T. Feenstra, T. Jaarsma, H. Hillege, and D. Postmus, “Continuous-time semi-Markov models in health economic decision making:

- An illustrative example in heart failure disease management”, *Medical Decision Making*, vol. 36, no. 1, pp. 59–71, 2016.
- [101] Y. Wang and J. M. G. Taylor, “Jointly modeling longitudinal and event time data with application to acquired immunodeficiency syndrome”, *Journal of the American Statistical Association*, vol. 96, no. 455, pp. 895–905, 2001.
- [102] J Jonasson, S Deo, S Deo, C. C, S. P, and L. A, “Deployment guidelines for community health workers in sub-Saharan Africa”, Working paper, 2017.
- [103] H Bastani and M Bayati, “Online decision-making with high-dimensional covariates”, Working paper, 2017.
- [104] R. Hentati-Kaffel and J. I. Prigent, “Optimal positioning in financial derivatives under mixture distributions”, *Economic Modelling*, vol. 52, pp. 115–124, 2016.
- [105] R. Katz and M. Parlange, “Mixtures of stochastic processes: Application to statistical downscaling”, *Climate Research*, vol. 7, no. 2, pp. 185–193, 1996.
- [106] S. S. Yoon, Q. Gu, T. Nwankwo, J. D. Wright, Y. Hong, and V. Burt, “Trends in blood pressure among adults with hypertension”, *Hypertension*, HYPERTENSIONAHA-114, 2014.
- [107] L. C. G. Rogers and D. Williams, *Diffusions, Markov processes and martingales: Volume 2, Itô calculus*. Cambridge university press, 2000, vol. 2.
- [108] D. Reynolds, “Gaussian mixture models”, in *Encyclopedia of Biometrics*, U. S. Springer, Ed., 2009, pp. 659–663.
- [109] T. G. Andersen, T. Bollerslev, F. X. Diebold, and P. Labys, “Modeling and forecasting realized volatility”, *Econometrica*, vol. 71, no. 2, pp. 579–625, 2003.
- [110] D. A. Reynolds, T. F. Quatieri, and R. B. Dunn, “Speaker verification using adapted gaussian mixture models”, *Digital Signal Processing*, vol. 10.1, pp. 19–41, 2000.
- [111] R. A. Redner and H. F. Walker, “Mixture densities, maximum likelihood and the EM algorithm”, *SIAM Review*, vol. 26.2, pp. 195–239, 1984.
- [112] M. Law, J. Morris, and N. Wald, “Use of blood pressure lowering drugs in the prevention of cardiovascular disease: Meta-analysis of 147 randomised trials in the context of expectations from prospective epidemiological studies”, *BMJ*, vol. 338, b1665, 2009.

- [113] S. L. Spruance, J. E. Reid, M. Grace, and M. Samore, “Hazard ratio in clinical trials”, *Antimicrobial Agents and Chemotherapy*, vol. 48, no. 8, pp. 2787–2792, 2004.
- [114] S. J. Denardo, Y. Gong, W. W. Nichols, F. H. Messerli, A. A. Bavry, R. M. Cooper-DeHoff, E. M. Handberg, A. Champion, and C. J. Pepine, “Blood pressure and outcomes in very old hypertensive coronary artery disease patients: an INVEST substudy”, *The American Journal of Medicine*, vol. 123, no. 8, pp. 719–726, 2010.
- [115] T. Björk, A. Murgoci, and X. Y. Zhou, “Mean–variance portfolio optimization with state-dependent risk aversion”, *Mathematical Finance*, vol. 24, no. 1, pp. 1–24, 2014.
- [116] S. Basak and G. Chabakauri, “Dynamic mean-variance asset allocation”, *Review of financial Studies*, vol. 23, no. 8, pp. 2970–3016, 2010.
- [117] M. C. Chiu and D. Li, “Asset and liability management under a continuous-time mean–variance optimization framework”, *Insurance: Mathematics and Economics*, vol. 39, no. 3, pp. 330–355, 2006.
- [118] A. Castaño-Martínez and F. López-Blázquez, “Distribution of a sum of weighted central chi-square variables”, *Communications in Statistics—Theory and Methods*, vol. 34, no. 3, pp. 515–524, 2005.
- [119] M. D. Buhmann, “Radial basis functions”, *Acta Numerica*, vol. 2000, no. 9, pp. 1–38, 2000.
- [120] S. Zhu, “Compactly supported radial basis functions: How and why?”, *SIAM Review*, 2012.
- [121] H. Wendland, “Error estimates for interpolation by compactly supported radial basis functions of minimal degree”, *Journal of Approximation Theory*, vol. 93.2, pp. 258–272, 1998.
- [122] A. G. Zauber, I. Lansdorp-Vogelaar, A. B. Knudsen, J. Wilschut, M. van Ballegooijen, and K. M. Kuntz, “Evaluating test strategies for colorectal cancer screening: A decision analysis for the US Preventive Services Task Force”, *Annals of internal medicine*, vol. 149, no. 9, pp. 659–669, 2008.
- [123] M. Haby, T. Vos, R. Carter, M. Moodie, A. Markwick, A. Magnus, K. Tay-Teo, and B. Swinburn, “A new approach to assessing the health benefit from obesity interventions in children and adolescents: The assessing cost-effectiveness in obesity project”, *International journal of obesity*, vol. 30, no. 10, pp. 1463–1475, 2006.

- [124] G. Bennett, C. J. O'Donnell, S. Coady, J. Robinson, F. R. B. D'Agostino Sr, F. J. S. Schwartz, R. Gibbons, F. S. T. Shero, P. Greenland, F. S. C. Smith Jr, *et al.*, "2013 ACC/AHA guideline on the assessment of cardiovascular risk", 2013.
- [125] R. Khatib, J.-D. Schwalm, S. Yusuf, R. B. Haynes, M. McKee, M. Khan, and R. Nieuwlaat, "Patient and healthcare provider barriers to hypertension awareness, treatment and follow up: A systematic review and meta-analysis of qualitative and quantitative studies", *PLoS One*, vol. 9, no. 1, e84238, 2014.
- [126] C. P. Kovesdy, A. J. Bleyer, M. Z. Molnar, J. Z. Ma, J. J. Sim, W. C.ushman, L. D. Quarles, and K. Kalantar-Zadeh, "Blood pressure and mortality in US veterans with chronic kidney disease: a cohort study", *Annals of Internal Medicine*, vol. 159, no. 4, pp. 233–242, 2013.
- [127] C. A. Peralta, M. G. Shlipak, C. Wassel-Fyr, H. Bosworth, B. Hoffman, S. Martins, E. Oddone, and M. K. Goldstein, "Association of antihypertensive therapy and diastolic hypotension in chronic kidney disease", *Hypertension*, vol. 50, no. 3, pp. 474–480, 2007.
- [128] T. Ohkubo, M. Kikuya, H. Metoki, K. Asayama, T. Obara, J. Hashimoto, K. Totsune, H. Hoshi, H. Satoh, and Y. Imai, "Prognosis of masked hypertension and white-coat hypertension detected by 24-h ambulatory blood pressure monitoring: 10-year follow-up from the ohasama study", *Journal of the American College of Cardiology*, vol. 46, no. 3, pp. 508–515, 2005.
- [129] A. S. Go, M. A. Bauman, S. M. C. King, G. C. Fonarow, W. Lawrence, K. A. Williams, and E. Sanchez, "An effective approach to high blood pressure control: a science advisory from the American Heart Association, the American College of Cardiology, and the Centers for Disease Control and Prevention", *Journal of the American College of Cardiology*, vol. 63, no. 12, pp. 1230–1238, 2014.
- [130] P. K. Whelton, R. M. Carey, W. S. Aronow, D. E. Casey, K. J. Collins, C. D. Himmelfarb, S. M. DePalma, S. Gidding, K. A. Jamerson, D. W. Jones, *et al.*, "2017 ACC/AHA/AAPA/ABC/ACPM/AGS/APhA/ASH/ASPC/NMA/PCNA guideline for the prevention, detection, evaluation, and management of high blood pressure in adults: A report of the American College of Cardiology/American Heart Association Task Force on Clinical Practice Guidelines", *Journal of the American College of Cardiology*, p. 24 430, 2017.
- [131] G. Corrao, P. Mazzola, M. M. Compagnoni, F. Rea, L. Merlino, G. Annoni, and G. Mancia, "Antihypertensive medications, loop diuretics, and risk of hip fracture in the elderly: A population-based cohort study of 81,617 italian

- patients newly treated between 2005 and 2009”, *Drugs & aging*, vol. 32, no. 11, pp. 927–936, 2015.
- [132] A. J. Zillich, J. Garg, S. Basu, G. L. Bakris, and B. L. Carter, “Thiazide diuretics, potassium, and the development of diabetes”, *Hypertension*, vol. 48, no. 2, pp. 219–224, 2006.
- [133] D. F. Hayes, H. S. Markus, R. D. Leslie, and E. J. Topol, “Personalized medicine: Risk prediction, targeted therapies and mobile health technology”, *BMC Medicine*, vol. 12, no. 1, p. 37, 2014.
- [134] N. J. Schork, “Personalized medicine: Time for one-person trials”, *Nature*, vol. 520, no. 7549, pp. 609–11, 2015.
- [135] J. E. Radder, S. D. Shapiro, and A. Berndt, “Personalized medicine for chronic, complex diseases: Chronic obstructive pulmonary disease as an example”, *Personalized Medicine*, vol. 11, no. 7, pp. 669–679, 2014.
- [136] A. S. Lok, “Personalized treatment of hepatitis B”, *Clinical Molecular Hepatology*, vol. 21, no. 1, pp. 1–6, 2015.
- [137] World Health Organization: Geneva, “Global status report on noncommunicable diseases”, 2011.
- [138] Z. J. Eapen, M. P. Turakhia, M. V. McConnell, G. Graham, P. Dunn, C. Tiner, C. Rich, R. A. Harrington, E. D. Peterson, and P. Wayte, “Defining a mobile health roadmap for cardiovascular health and disease”, *Journal of the American Heart Association*, vol. 5, no. 7, e003119, 2016.
- [139] M. Ruzicka, A. Akbari, E. Bruketa, J. F. Kayibanda, C. Baril, and S. Hiremath, “How accurate are home blood pressure devices in use? a cross-sectional study”, *PloS one*, vol. 11, no. 6, e0155677, 2016.
- [140] T. B. Plante, B. Urrea, Z. T. MacFarlane, R. S. Blumenthal, E. R. Miller, L. J. Appel, and S. S. Martin, “Validation of the instant blood pressure smartphone app”, *JAMA internal medicine*, vol. 176, no. 5, pp. 700–702, 2016.
- [141] E. Chiauzzi, C. Rodarte, and P. DasMahapatra, “Patient-centered activity monitoring in the self-management of chronic health conditions”, *BMC medicine*, vol. 13, no. 1, p. 77, 2015.
- [142] R. V. Milani, R. M. Bober, and C. J. Lavie, “The role of technology in chronic disease care”, *Progress in cardiovascular diseases*, vol. 58, no. 6, pp. 579–583, 2016.

- [143] L. Shamma, T. Zentek, B. von Haaren, S. Schlesinger, S. Hey, and A. Rashid, “Home-based system for physical activity monitoring in patients with multiple sclerosis (pilot study)”, *Biomedical engineering online*, vol. 13, no. 1, p. 10, 2014.
- [144] S. Patel, H. Park, P. Bonato, L. Chan, and M. Rodgers, “A review of wearable sensors and systems with application in rehabilitation”, *Journal of neuroengineering and rehabilitation*, vol. 9, no. 1, p. 21, 2012.
- [145] D. M. Hoelscher, N. Ranjit, and A. Pérez, “Surveillance systems to track and evaluate obesity prevention efforts”, *Annual Review of Public Health*, no. 0, 2017.
- [146] M. Alharbi, N. Straiton, and R. Gallagher, “Harnessing the potential of wearable activity trackers for heart failure self-care”, *Current Heart Failure Reports*, pp. 1–7, 2017.
- [147] L. E. Burke, J. Ma, K. M. Azar, G. G. Bennett, E. D. Peterson, Y. Zheng, W. Riley, J. Stephens, S. H. Shah, B. Suffoletto, *et al.*, “Current science on consumer use of mobile health for cardiovascular disease prevention”, *Circulation*, CIR–0 000 000 000 000 232, 2015.
- [148] L. H. Schwamm, N. Chumbler, E. Brown, G. C. Fonarow, D. Berube, K. Nystrom, R. Suter, M. Zavala, D. Polsky, K. Radhakrishnan, *et al.*, “Recommendations for the implementation of telehealth in cardiovascular and stroke care: A policy statement from the american heart association”, *Circulation*, CIR–0 000 000 000 000 475, 2016.
- [149] H. M. Kelli, B. Witbrodt, and A. Shah, “The future of mobile health applications and devices in cardiovascular health”, *European medical journal. Innovations*, vol. 2017, p. 92, 2017.
- [150] R. S. Vasan and E. J. Benjamin, “The future of cardiovascular epidemiology”, *Circulation*, vol. 133, no. 25, pp. 2626–2633, 2016.
- [151] Y. Watanabe, F. Halberg, K. Otsuka, and G. Cornelissen, “Toward a personalized chronotherapy of high blood pressure and a circadian overswing”, *Clinical and Experimental Hypertension*, vol. 35, no. 4, pp. 257–266, 2013.
- [152] J. Sun, C. D. McNaughton, P. Zhang, A. Perer, A. Gkoulalas-Divanis, J. C. Denny, J. Kirby, T. Lasko, A. Saip, and B. A. Malin, “Predicting changes in hypertension control using electronic health records from a chronic disease management program”, *Journal of the American Medical Informatics Association*, vol. 21, no. 2, pp. 337–344, 2014.

- [153] J. van der Leeuw, P. M. Ridker, Y. van der Graaf, and F. L. Visseren, “Personalized cardiovascular disease prevention by applying individualized prediction of treatment effects”, *European Heart Journal*, ehu004, 2014.
- [154] G. J. Schell, “Personalized medicine in chronic disease management”, PhD thesis, The University of Michigan, 2015.
- [155] C. C. L. Epstein, “An analytics approach to hypertension treatment”, PhD thesis, Massachusetts Institute of Technology, 2014.
- [156] L. Chin, J. N. Andersen, and P. A. Futreal, “Cancer genomics: From discovery science to personalized medicine”, *Nature Medicine*, vol. 17, no. 3, pp. 297–303, 2011.
- [157] F. Meric-Bernstam, C. Farhangfar, J. Mendelsohn, and G. B. Mills, “Building a personalized medicine infrastructure at a major cancer center”, *Journal of Clinical Oncology*, vol. 31, no. 15, pp. 1849–1857, 2013.
- [158] T. Ayer, O. Alagoz, and N. K. Stout, “OR forum—a POMDP approach to personalize mammography screening decisions”, *Operations Research*, vol. 60, no. 5, pp. 1019–1034, 2012.
- [159] A.-M. Tsimberidou, N. G. Iskander, D. S. Hong, J. J. Wheeler, G. S. Falchook, S. Fu, S. Piha-Paul, A. Naing, F. Janku, R. Luthra, *et al.*, “Personalized medicine in a phase I clinical trials program: the MD Anderson Cancer Center initiative”, *Clinical Cancer Research*, vol. 18, no. 22, pp. 6373–6383, 2012.
- [160] J. E. Helm, M. S. Lavieri, M. P. Van Oyen, J. D. Stein, and D. C. Musch, “Dynamic forecasting and control algorithms of glaucoma progression for clinician decision support”, *Operations Research*, vol. 63, no. 5, pp. 979–999, 2015.
- [161] A. Gelman, J. B. Carlin, H. S. Stern, and D. B. Rubin, *Bayesian data analysis*. Chapman & Hall/CRC Boca Raton, FL, USA, 2014, vol. 2.
- [162] J. O. Berger, *Statistical decision theory and Bayesian analysis*. Springer Science & Business Media, 2013.
- [163] J. Parslow, N. Cressie, E. P. Campbell, E. Jones, and L. Murray, “Bayesian learning and predictability in a stochastic nonlinear dynamical model”, *Ecological applications*, vol. 23, no. 4, pp. 679–698, 2013.
- [164] S. T. Rachev, J. S. Hsu, B. S. Bagasheva, and F. J. Fabozzi, *Bayesian methods in finance*. John Wiley & Sons, 2008, vol. 153.

- [165] C. S. Jones, “Bayesian estimation of continuous-time finance models”, *manuscript University of Rochester*, 1998.
- [166] G. Baio, *Bayesian methods in health economics*. CRC Press, 2012.
- [167] A. R. Willan, “Bayesian methods for the design, analysis and interpretation of clinical studies”, *Important Considerations for Clinical Trial Methodologies. Future Medicine London*, 2013.
- [168] D. M. Sobieraj, J. C. Cappelleri, W. L. Baker, O. J. Phung, C. M. White, and C. I. Coleman, “Methods used to conduct and report bayesian mixed treatment comparisons published in the medical literature: A systematic review”, *BMJ open*, vol. 3, no. 7, e003111, 2013.
- [169] R. Y. Coley, A. J. Fisher, M. Mamawala, H. B. Carter, K. J. Pienta, and S. L. Zeger, “A bayesian hierarchical model for prediction of latent health states from multiple data sources with application to active surveillance of prostate cancer”, *Biometrics*, 2016.
- [170] M. B. Sesen, A. E. Nicholson, R. Banares-Alcantara, T. Kadir, and M. Brady, “Bayesian networks for clinical decision support in lung cancer care”, *PLoS one*, vol. 8, no. 12, e82349, 2013.
- [171] C. B. Schechter, “Sequential analysis in a bayesian model of diastolic blood pressure measurement”, *Medical Decision Making*, vol. 8, no. 3, pp. 191–196, 1988.
- [172] J. Mar, R. Pastor, R. Abasolo, and R. R. De Gauna, “Ambulatory blood pressure monitoring and diagnostic errors in hypertension a bayesian approach”, *Medical decision making*, vol. 18, no. 4, pp. 429–435, 1998.
- [173] A. Blinowska, G. Chatellier, J. Bernier, and M. Lavril, “Bayesian statistics as applied to hypertension diagnosis”, *IEEE transactions on biomedical engineering*, vol. 38, no. 7, pp. 699–706, 1991.
- [174] A. Tartakovsky, I. Nikiforov, and M. Basseville, *Sequential analysis: Hypothesis testing and changepoint detection*. CRC Press, 2014.
- [175] A. G. Tartakovsky, A. S. Polunchenko, and G. Sokolov, “Efficient computer network anomaly detection by changepoint detection methods”, *IEEE Journal of Selected Topics in Signal Processing*, vol. 7, no. 1, pp. 4–11, 2013.
- [176] J. Reeves, J. Chen, X. L. Wang, R. Lund, and Q. Q. Lu, “A review and comparison of changepoint detection techniques for climate data”, *Journal of Applied Meteorology and Climatology*, vol. 46, no. 6, pp. 900–915, 2007.

- [177] A. Ranganathan, “Pliss: Labeling places using online changepoint detection”, *Autonomous Robots*, vol. 32, no. 4, pp. 351–368, 2012.
- [178] C. Sonesson and D. Bock, “A review and discussion of prospective statistical surveillance in public health”, *Journal of the Royal Statistical Society: Series A (Statistics in Society)*, vol. 166, no. 1, pp. 5–21, 2003.
- [179] R. Cmejla, J. Rusz, P. Bergl, and J. Vokral, “Bayesian changepoint detection for the automatic assessment of fluency and articulatory disorders”, *Speech Communication*, vol. 55, no. 1, pp. 178–189, 2013.
- [180] H. Assareh, I. Smith, and K. Mengersen, “Bayesian change point detection in monitoring cardiac surgery outcomes”, *Quality Management in Healthcare*, vol. 20, no. 3, pp. 207–222, 2011.
- [181] D. B. Owen, “Tables for computing bivariate normal probabilities”, *The Annals of Mathematical Statistics*, vol. 27, no. 4, pp. 1075–1090, 1956.
- [182] D. C. Montgomery, *Statistical quality control*. Wiley New York, 2009, vol. 7.
- [183] A. Tartakovsky, “Asymptotic performance of a multichart cusum test under false alarm probability constraint”, in *Decision and Control, 2005 and 2005 European Control Conference. CDC-ECC’05. 44th IEEE Conference on*, IEEE, 2005, pp. 320–325.
- [184] R. V. Milani and C. J. Lavie, “Health care 2020: Reengineering health care delivery to combat chronic disease”, *The American journal of medicine*, vol. 128, no. 4, pp. 337–343, 2015.
- [185] M. Millar-Craig, C. Bishop, and E. Raftery, “Circadian variation of blood pressure”, *The Lancet*, vol. 311, no. 8068, pp. 795–797, 1978.
- [186] P. A. Modesti, “Season, temperature and blood pressure: A complex interaction”, *European journal of internal medicine*, vol. 24, no. 7, pp. 604–607, 2013.
- [187] A. K. Jardine, D. Lin, and D. Banjevic, “A review on machinery diagnostics and prognostics implementing condition-based maintenance”, *Mechanical systems and signal processing*, vol. 20, no. 7, pp. 1483–1510, 2006.
- [188] J. Lee, F. Wu, W. Zhao, M. Ghaffari, L. Liao, and D. Siegel, “Prognostics and health management design for rotary machinery systems - reviews, methodology and applications”, *Mechanical systems and signal processing*, vol. 42, no. 1-2, pp. 314–334, 2014.

- [189] T. Qiu, F. Shen, and J. Zhao, “Local adaptive and incremental gaussian mixture for online density estimation”, in *Pacific-Asia Conference on Knowledge Discovery and Data Mining*, Springer, 2015, pp. 418–428.
- [190] X. Xie and H. Shi, “Dynamic multimode process modeling and monitoring using adaptive gaussian mixture models”, *Industrial & Engineering Chemistry Research*, vol. 51, no. 15, pp. 5497–5505, 2012.

VITA

Anthony Joseph Bonifonte was born in Allentown, Pennsylvania, and raised in Wilkes-Barre Pennsylvania, a town he is still learning to pronounce correctly. His love of math was established as an adolescent by solving algebra equations to optimize video game choices and beat his friends at board games. Attending John's Hopkins Center for Talented Youth summer classes opened him to a world of academic possibilities, all generously paid for by scholarship. In high school he was nicknamed 'TI', intended in a gibing way, which he adopted with pride. In 2007 he attended Oberlin College, where he majored in math, caught crayfish over the summer for (supposed) research purposes, and led a team to victory in Obiegame, Oberlin's premier week long immersive puzzle experience. His future career in teaching was ordained when he taught a 1 credit course on Calvin and Hobbes, and designed another on the History of Piracy, which included a historical pirate shanty sing-a-long. The first day of Optimization class playing with Legos to illustrate linear programming inspired him to pursue a Ph.D. in operations research. In 2011 he attended Georgia Institute of Technology, earning an M.S. in 2015 and Ph.D. in 2018. Fascinated by the real world impacts and intellectual alchemy of producing something from nothing in the organ allocation problem, his research focused on medical decision making. He also served as graduate assistant in the Center for the Enhancement of Teaching and Learning, studying rubric design and helping implement a new course evaluation system. In August 2017 he began as the inaugural faculty hire in the Data Analytics department at Denison University. There he teaches data analytics skills to undergraduate students in diverse application areas such as biology, political science, and literature. He currently resides in Granville, Ohio with his wife Ondrea, his cats Nona and Mika, and several turtles and snakes who are glad to have returned to their Ohio birthplace.